

***Self-consistent Green's function in
Finite Nuclei and related things...***

-

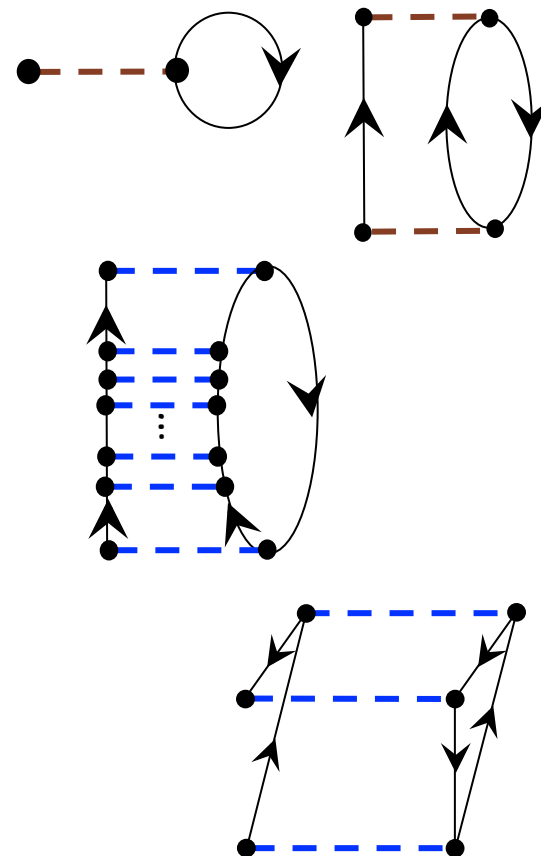
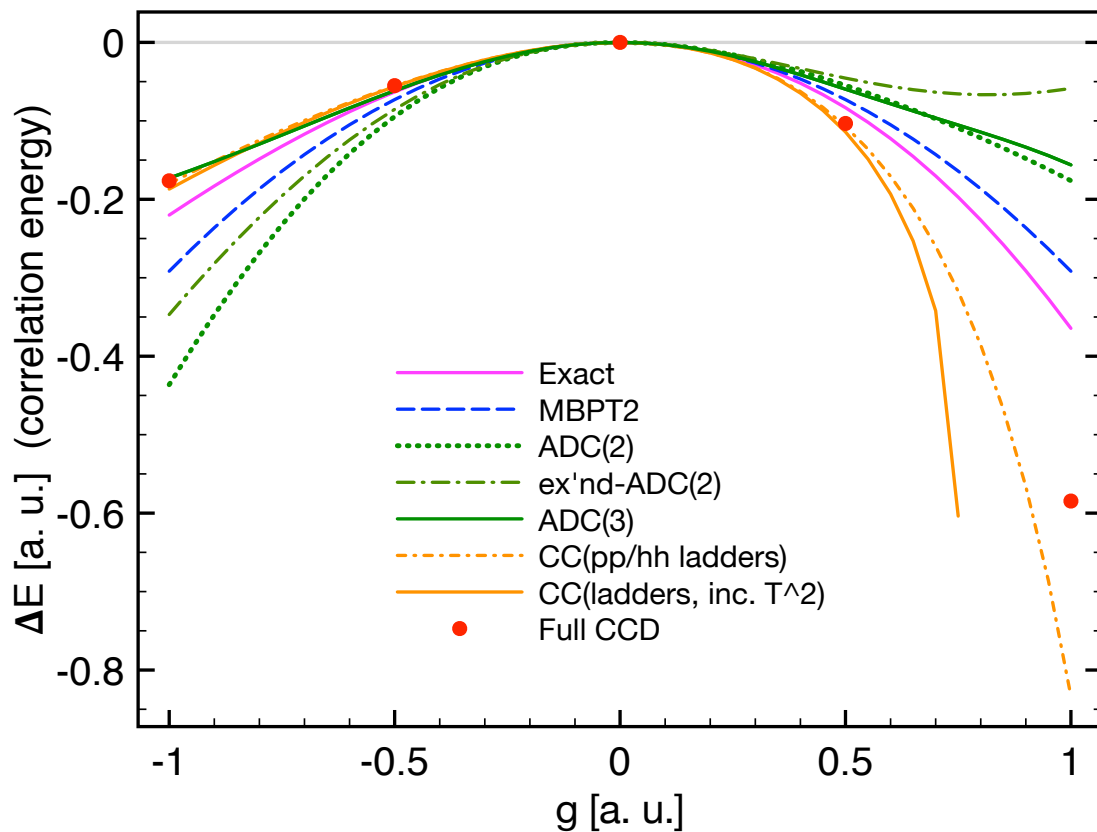
Lectures IV and V

***RPA, other approximation to the self-energy: GW,
FRPA, adding 3NF and applications to finite nuclei***



Results for the pairing model

Correlation energy for the 4-level and 4-fermions pairing model



$$\langle \Phi_k; 1h | H_1 | \Phi_{k_1, k_2}^n; 2h1p \rangle = \langle \begin{array}{c} \text{--- } E_E \text{ ---} \\ \text{---} \\ \text{---} \\ \text{---} \\ \text{---} \\ \text{---} \\ \text{---} \\ \text{---} \\ \text{---} \\ \text{---} \end{array} \left| \sum_{p \cdot q} P_p^\dagger P_q \right| \begin{array}{c} \text{---} \\ \text{---} \\ \text{---} \\ \text{---} \\ \text{---} \\ \text{---} \\ \text{---} \\ \text{---} \\ \text{---} \\ \text{---} \end{array} E_F \rangle = 0$$

Nuclear matter project with Green's function and coupled cluster

This week we will start looking into how to calculate nuclear matter with the same methods introduced last week. Some short comments on this:

- We will discretize the continuous momentum space by using a box with periodic boundary conditions (PBC). This will be discussed in much detail by Gaute in the next lecture.
- The setup of the basis and the calculation of the reference HF state is the same for all methods (MBPT, CCM, SCGF...) and so next talk will apply to all projects.
- So set up you code with a general basis infrastructure, that will be separate from the solver...
- Some more comments specific to GF:
 - Once the HF is set up, we will need to build bases for pp and hh configurations (as for CC) but also 2p1h and 2h1p. These are all built very similarly.
 - We will use the ADC(2) approach and later move to extended ADC(2), which requires a relatively small extra effort.
 - The self-energy is diagonal in k-space, which is a great simplification: for each value of momentum, we can diagonalize a part of the Dyson equations independently.
 - The approach is very similar to last week pairing model. However, we will have to deal with technical complications (the more sophisticated basis to handle, with more quantum numbers, the dimension of the Dyson sub-matrices, ecc...). All of this will be discussed little by little.



Principal Many-body Green's functions

Quasiparticle and phonon excitations can be described with many-body Green's functions:

$$g_{\alpha\beta}(\omega) = \langle \Psi_0^A | c_\alpha \frac{1}{\omega - H + i\eta} c_\beta^\dagger | \Psi_0^A \rangle + \dots \quad \text{one-body propagator}$$

$$G_{\alpha\beta, \gamma\delta}^{\text{II}}(\omega) = \langle \Psi_0^A | c_\alpha c_\beta \frac{1}{\omega - H + i\eta} c_\delta^\dagger c_\gamma^\dagger | \Psi_0^A \rangle + \dots \quad \text{two-body propagator}$$

$$\Pi_{\alpha\beta, \gamma\delta}(\omega) = \langle \Psi_0^A | c_\alpha^\dagger c_\beta \frac{1}{\omega - H + i\eta} c_\delta^\dagger c_\gamma | \Psi_0^A \rangle + \dots \quad \begin{array}{l} \text{polarization (ph)} \\ \text{propagator} \end{array}$$

Principal Many-body Green's functions

Quasiparticle and phonon excitations can be described with many-body Green's functions:

$g_{\alpha\beta}(\omega)$ addition removal of *one* particle, spectra of $A\pm 1$ particle systems, one-body density, optical potential.

$G_{\alpha\beta, \gamma\delta}^{\text{II}}(\omega)$ addition removal of *two* particles, spectra of $A\pm 2$ particle systems, two-body density

$\Pi_{\alpha\beta, \gamma\delta}(\omega)$ spectrum of the A particle systems, one-body response

→ linked to a lot of exp. information

→ "efficiency" with information, only transition amplitudes are generated

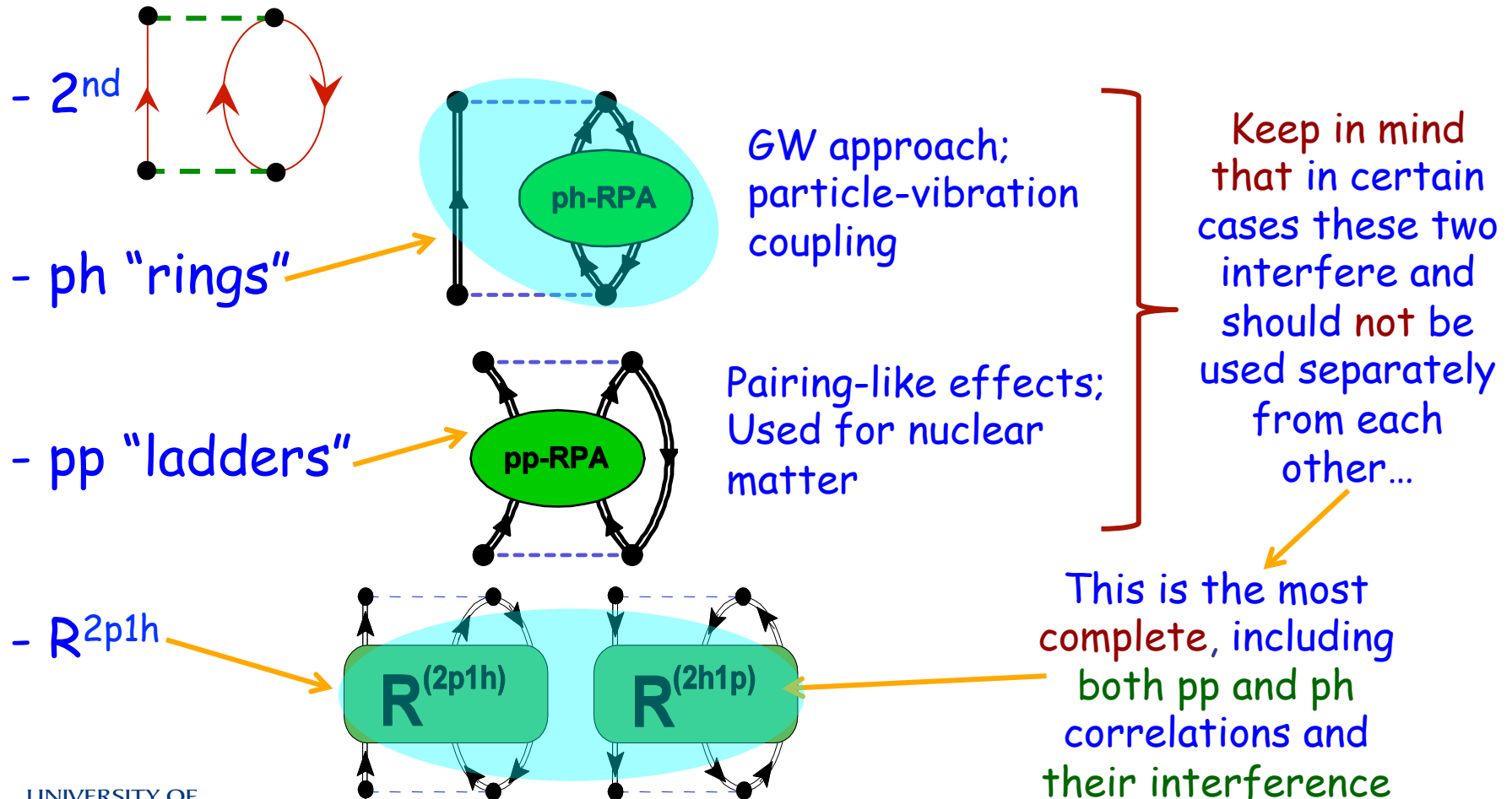


Approximations for the self-energy

- GW approximation
- Faddeev Random Phase Approximation (FRPA)

Approximations for the Self-energy

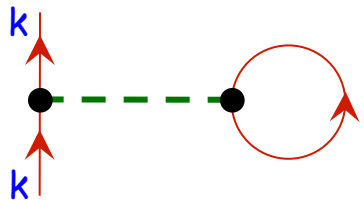
Diagrams of some common approximations for the self-energy:



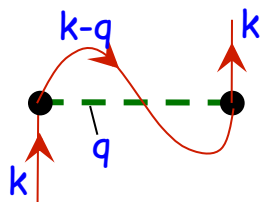
The GW method

Consider the self-energy of the uniform electron gas and use only direct matrix elements of V (i.e. not antisymmetrized).

The Hartree term is


$$= \Sigma^{Hartree}(\mathbf{k}, \omega) \sim \tilde{v}(\mathbf{q}=0) \rho$$

The Fock contribution

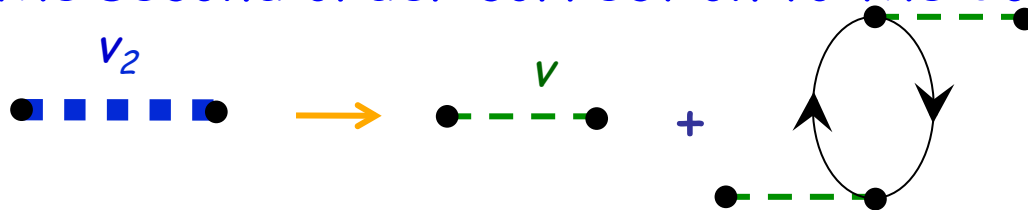

$$= \Sigma^{Fock}(\mathbf{k}, \omega) = i \int \frac{d\mathbf{q}}{(2\pi)^3} \tilde{v}(\mathbf{q}) g(\mathbf{k} - \mathbf{q}, \omega)$$

→ The Hartree correlations simply give the electrostatic repulsion which is a constant term, so we only consider the Fock part...

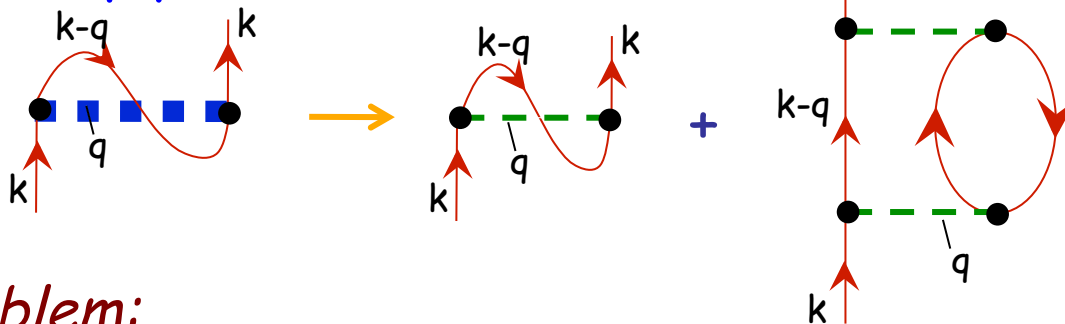
The GW method

Want to correct the interaction for the effects of the medium.

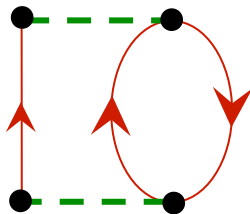
Take the second order correction to the Coulomb force:



This imply:



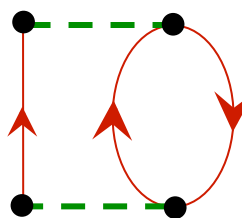
Problem:



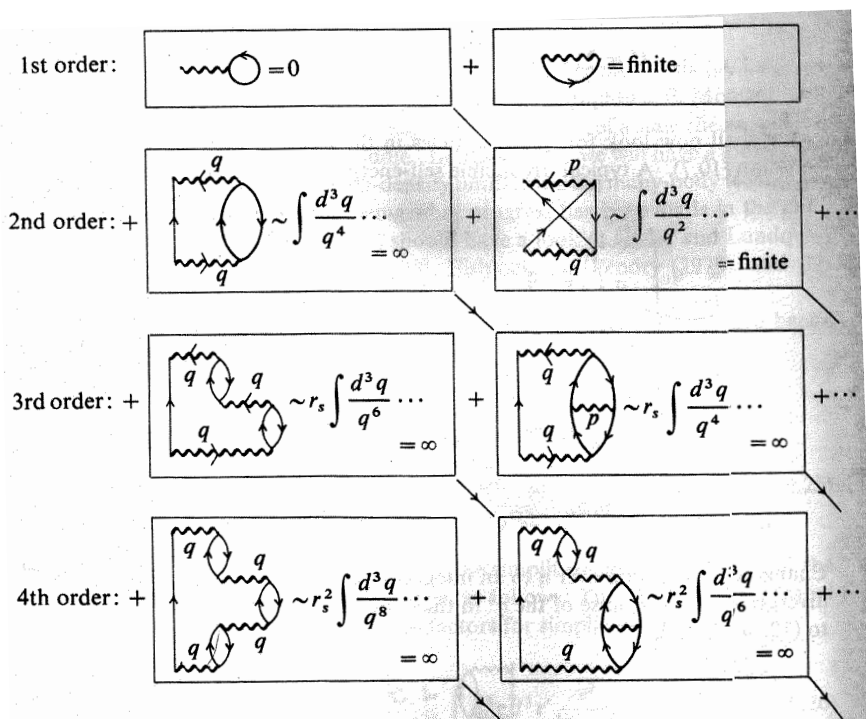
← This term **diverges**, and the divergence become **worse** going to higher orders...

The GW method

The divergence is due to the long-range part of the Coulomb interaction:



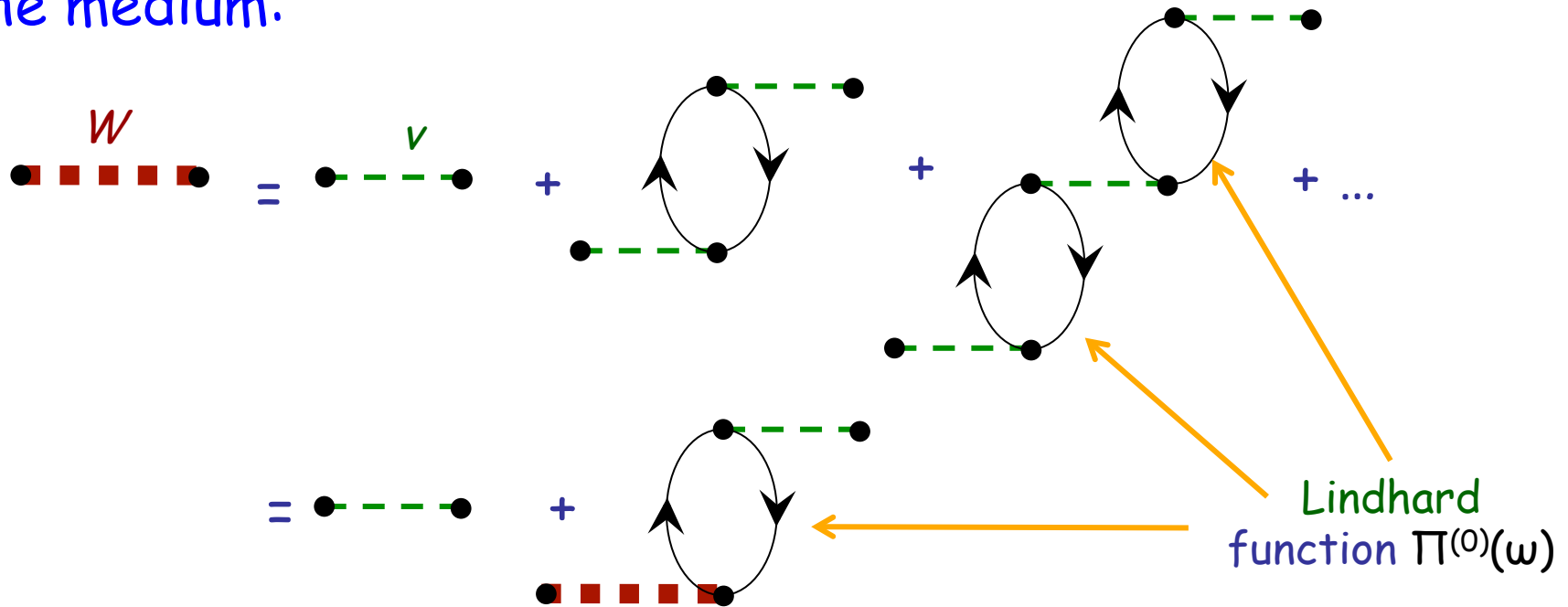
$$= \Sigma^{2nd}(\mathbf{k}, \omega) = i \int \frac{d\mathbf{q}}{(2\pi)^3} \tilde{v}(\mathbf{q}) g(\mathbf{k} - \mathbf{q}, \omega) \Pi^{(0)}(\mathbf{q}, \omega) \tilde{v}(\mathbf{q})$$



[Picture from Mattuck]

RPA approx. for the pol. prop.

Use RPA to evaluate the electron-electron interaction in the medium:



Then:

$$W_{\alpha\beta,\gamma\delta}(\omega) = v_{\alpha\delta,\beta\gamma} + v_{\alpha\nu,\beta\mu} \Pi_{\mu\nu,\rho\zeta}^{(0)}(\omega) W_{\rho\zeta,\gamma\delta}(\omega)$$

the in-medium
interaction
depends on energy!

RPA approx. for the pol. prop.

Use RPA to evaluate the electron-electron interaction in the medium:

The bare interaction is:

$$\langle \mathbf{p}_1, \mathbf{p}_2 | \hat{V}^{Coulomb} | \mathbf{p}_3, \mathbf{p}_4 \rangle = \delta(\mathbf{p}_1 + \mathbf{p}_2 - \mathbf{p}_3 - \mathbf{p}_4) \tilde{v}(\mathbf{p}_1 - \mathbf{p}_3)$$

with: $\tilde{v}(\mathbf{q}) = +\frac{4\pi e^2}{q^2}$ ← In this case, this is **NOT antisymmetrized**—it depends only on the momentum transferred in the “t” channel.

The Lindhard function is:

$$\text{Re } \Pi^{(0)}(\mathbf{q}, \omega) \longrightarrow \frac{mk_F}{4\pi^2} \frac{4}{3} \frac{q^2 k_F^2}{m^2 \omega^2} \quad \mathbf{q} \rightarrow 0$$

RPA eq.:

$$W(\mathbf{q}, \omega) = v(\mathbf{q}) + v(\mathbf{q}) \Pi^{(0)}(\mathbf{q}, \omega) W(\mathbf{q}, \omega) \Rightarrow W(\mathbf{q}, \omega) = \frac{v(\mathbf{q})}{1 - v(\mathbf{q}) \Pi^{(0)}(\mathbf{q}, \omega)}$$

And in the limit of small momenta:

$$W(\mathbf{q}, \omega) \longrightarrow \frac{4\pi e^2}{q^2 + K} \quad \mathbf{q} \rightarrow 0$$

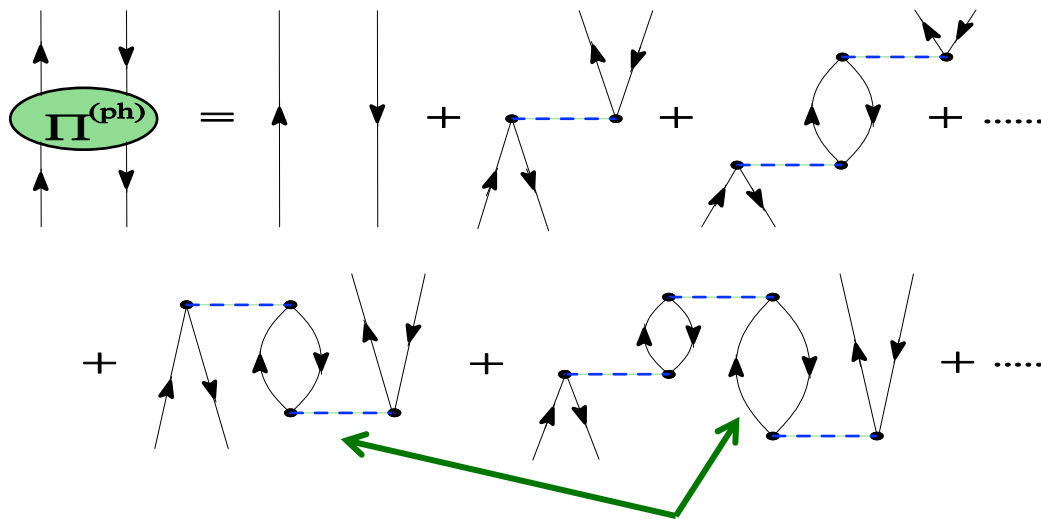
← The coulomb interaction in the electron gas is screened at long distances and behave like a Yukawa force!!!

Approximations for the polarization propagator

Ring expansion of RPA

$$\Pi_{\alpha\beta,\gamma\delta}(\omega) = \Pi_{\alpha\beta,\gamma\delta}^{(0)}(\omega) + \left\{ \frac{f_{\alpha\beta,\mu\nu}^{(0)}}{\hbar\omega - E_x^n + i\eta} - \frac{f_{\nu\mu,\beta\alpha}^{(0)}}{\hbar\omega + E_x^n - i\eta} \right\} v_{\mu\lambda,\nu\kappa} \Pi_{\kappa\lambda,\gamma\delta}(\omega)$$

The RPA equations correspond to the following series of diagrams:



to the following

TDA

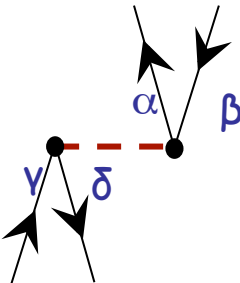
RPA

Pauli correlations are partially neglected, but one assumes (=hopes) that the missing corrections cancel each other "randomly" (→RPA)

Approximations for the polarization propagator

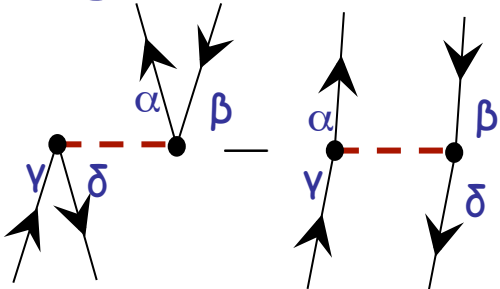
Beware: there are **two** definitions of RPA! —

1) V contains only the direct term:

$$K_{\alpha\beta,\gamma\delta}^{ph,RPA} = \tilde{v}_{\alpha\delta,\beta\gamma} = \frac{i \delta \Sigma_{\alpha\beta}^H}{\hbar \delta g_{\gamma\delta}}$$


Hartree potential

2) V has both direct and exchange terms:

$$K_{\alpha\beta,\gamma\delta}^{ph,GRPA} = v_{\alpha\delta,\beta\gamma} = \tilde{v}_{\alpha\delta,\beta\gamma} - \tilde{v}_{\alpha\delta,\gamma\beta} = \frac{i \delta \Sigma_{\alpha\beta}^{HF}}{\hbar \delta g_{\gamma\delta}}$$


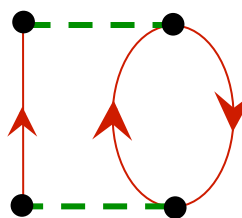
Hartree-Fock potential

N.B.: This is sometimes called "Generalized RPA" (GRPA), e.g. in atomic physics, and other times simply "RPA" (in nuclear physics).

$$\tilde{v}_{\alpha\beta,\gamma\delta} = \int d\mathbf{r}_1 \int d\mathbf{r}_2 u_{\alpha}^*(\mathbf{r}_1) u_{\beta}^*(\mathbf{r}_2) V(\mathbf{r}_1, \mathbf{r}_2) u_{\gamma}(\mathbf{r}_1) u_{\delta}(\mathbf{r}_2)$$

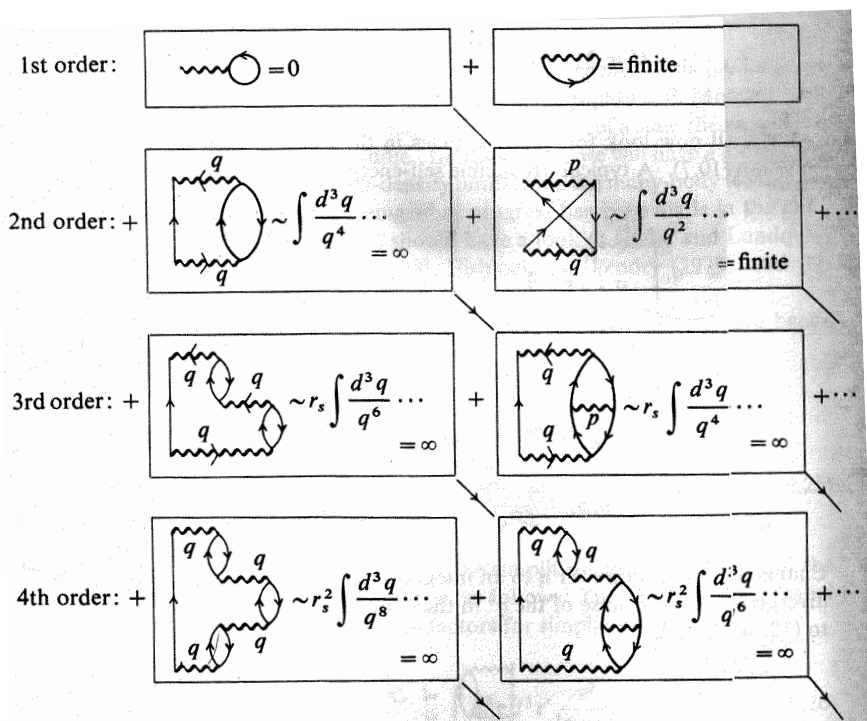
The GW method

The divergence is due to the long-range part of the Coulomb interaction:



$$= \Sigma^{2nd}(\mathbf{k}, \omega) = i \int \frac{d\mathbf{q}}{(2\pi)^3} \tilde{v}(\mathbf{q}) g(\mathbf{k} - \mathbf{q}, \omega) \Pi^{(0)}(\mathbf{q}, \omega) \tilde{v}(\mathbf{q})$$

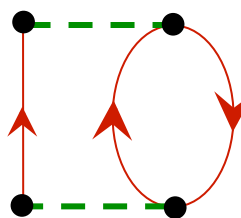
q^{-2}



[Picture from Mattuck]

The GW method

The divergence is due to the long-range part of the Coulomb interaction:



$$= \Sigma^{2nd}(\mathbf{k}, \omega) = i \int \frac{d\mathbf{q}}{(2\pi)^3} \tilde{v}(\mathbf{q}) g(\mathbf{k} - \mathbf{q}, \omega) \Pi^{(0)}(\mathbf{q}, \omega) \tilde{v}(\mathbf{q})$$

$$\tilde{v}(\mathbf{q}) = + \frac{4\pi e^2}{q^2}$$

Need to resum the full RPA series:

$$W^{(0)}(\mathbf{q}, \omega) = \frac{v(\mathbf{q})}{1 - v(\mathbf{q}) \Pi^{(0)}(\mathbf{q}, \omega)} \longrightarrow \frac{4\pi e^2}{q^2 + K} \quad \mathbf{q} \rightarrow 0$$

The screening from RPA avoids the infrared divergence!

The GW method

The GW self-energy is:

$$\Sigma^{G^0W^0}(\mathbf{k}, \omega) = i \int \frac{d\omega_1}{2\pi} \int \frac{d\mathbf{q}}{(2\pi)^3} W^{(0)}(\mathbf{q}, \omega_1) g^{(0)}(\mathbf{k} - \mathbf{q}, \omega - \omega_1)$$

This is named in different ways, according to whether the propagator $g(\omega)$ and the one used calculating the in-medium interaction ($\Pi^{(0)}$ or Π^f) are unperturbed or self-consistent:

$$G^0W^0 = \text{Diagram: A red arrow line with two black dots. A dashed green arc connects the two dots above the line.$$

$$GW^0 = \text{Diagram: Two parallel red arrow lines. Two black dots are on the top line. A dashed green arc connects the two dots above the top line.$$

$$GW = \text{Diagram: Two parallel red arrow lines. Two black dots are on the top line. A solid green arc connects the two dots above the top line.$$

The GW method for the electron gas

Self-consistent GW calculations electron gas were achieved only in the last years, see:

- B. Holm and U. von Barth, Phys. Rev. B57, 2108 (1998).
- B. Holm, Phys. Rev. Lett. 83, 788 (1999).
- P. García-González and R. W. Godby, Phys. Rev B63, 075112 (2001).
- Y. Dewulf, D. Van Neck, and M. Waroquier, Phys. Rev. B245122 (05).

The GW method for the electron gas

Numerical implementation (Holm and von Barth).

Write the single-particle propagator in terms of its spectral function,

$$g_{\alpha\beta}(\omega) = \int d\omega' \frac{S_{\alpha\beta}^p(\omega')}{\omega - \omega' + i\eta} + \int d\omega' \frac{S_{\alpha\beta}^h(\omega')}{\omega - \omega' - i\eta}$$

and expand in a sum of Gaussians:

$$S(\mathbf{k}, \omega) = \sum_{\nu} \frac{W_{\nu}(\mathbf{k})}{\sqrt{2\pi}\Gamma_{\nu}(\mathbf{k})} \exp\left[-\frac{[\omega - E_{\nu}(\mathbf{k})]^2}{2\Gamma_{\nu}^2(\mathbf{k})}\right]$$

[B. Holm and U. von Barth, Phys. Rev. B57, 2108 (1998)]

The GW method for the electron gas

Results for G^0W^0 to GW

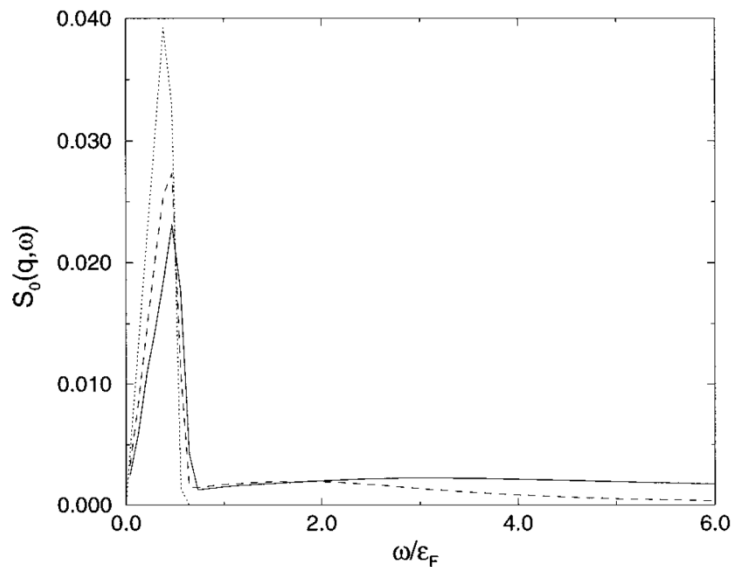


FIG. 2. The spectral function $\Pi(\mathbf{q}, \omega)$ of the irreducible “polarizability” at full self-consistency [$r_s=2$ (dashed) and $r_s=4$ (solid)] is compared to the corresponding quantity for noninteracting electrons (dotted). The latter is independent of r_s in the reduced units defined under Fig. 1 and used throughout. Notice the much more extended tail in the more strongly interacting case ($r_s=4$). Here, $|\mathbf{q}|=0.25$.

Note: r_s is the radius of the mean volume occupied by each electron (in Bohr's radii): $\frac{4\pi}{3}(r_s a_0)^3 \rho = 1$, $\rho \equiv \frac{N}{V}$

In practice, it is used to label the density.

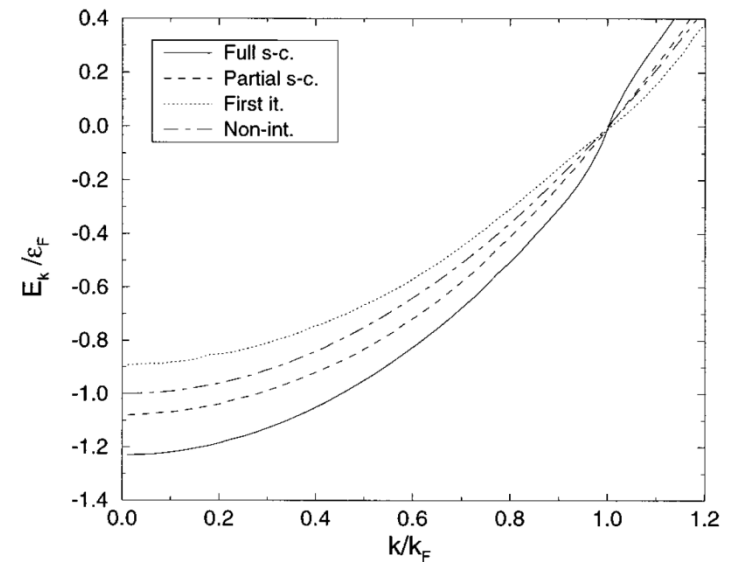


FIG. 9. The dispersion $E_{\mathbf{k}}$ of the quasiparticles is compared to a free-electron parabola (small dots) for the cases G_0W_0 (dotted), GW_0 (dash-dotted), and GW (solid). Only the simplest G_0W_0 shows the desired band narrowing and the GW result is the worst. Here, $r_s=4$.

The *GW* method for the electron gas

Correlation energies (= $\text{tot. energy} - \text{HF}$) of the electron gas from quantum Monte Carlo and *GW* approaches

TABLE I. Minus XC energies per particle (in Hartrees) for the spin-unpolarized phase of the 3D homogeneous electron gas obtained through several *GW* schemes. The second row in the *GW* entry corresponds to Ref. 6. Also shown are the RPA results, and the QMC values from Ref. 23 (first row) and Ref. 24 (second row). Parentheses indicate the numerical uncertainty in the last significant figure. For reference, the exchange energy per particle ε_X is included.

r_s	1	2	4	5	10	20
QMC	0.5180	0.2742	0.1464	0.1197	0.0644	0.0344
	0.5127	0.2713		0.1201		0.0344
<i>GW</i>	0.5160(2)	0.2727(5)	0.1450(5)	0.1185(5)	0.0620(9)	0.032(1)
		0.2741	0.1465			
GW_0	0.5218(1)	0.2736(1)	0.1428(1)	0.1158(1)	0.0605(4)	0.030(1)
G_0W_0	0.5272(1)	0.2821(1)	0.1523(1)	0.1247(1)	0.0665(2)	0.0363(5)
RPA	0.5370	0.2909	0.1613	0.1340	0.0764	0.0543
$-\varepsilon_X$	0.4582	0.2291	0.1145	0.0916	0.0458	0.0229

Two words on GW vs DFT...

Ionization energies for atoms:

[S. Verdonck, et al., Phys. Rev A74, 062503 (2006)]

TABLE IV. First ionization energies (a.u.), obtained with different self-energies: second-order non-self-consistently [$\Sigma^{(2)}(G_{\text{HF}})$], self-consistently [$\Sigma^{(2)}(G)$], and G_0W_0 . Extrapolation bounds are given between brackets. The column labeled (Expt.) contains the estimated nonrelativistic ionization energies from Ref. [48] for the atoms He through Ar; values for Ca through Kr are taken from Ref. [49].

	HF	$\Sigma^{(2)}(G_{\text{HF}})$	$\Sigma^{(2)}(G)$ [28]	G_0W_0	GG_0W_0	Expt.
He	0.918	0.905	0.906	0.9089 [0.9096,0.9100]	0.878	0.9037
Be	0.309	0.330	0.320	0.3367 [0.3378,0.3383]	/	0.3426
Ne	0.850	0.745	0.763	0.801 [0.805,0.807]	0.714	0.7946
Mg	0.253	0.276	0.274	0.281 [0.282,0.283]	(0.412)	0.2808
Ar	0.590	0.578	0.585	0.595 [0.598,0.599]	0.609	0.583
Ca	0.195	0.224		0.224	/	0.2247
Zn	0.291	0.329		0.331	(0.484)	0.3452
Kr	0.524	0.526	0.560	0.536	0.548	0.5145

2nd order unperturbed

2nd order self-consistent

GGW=="generalized GW" contains the Pauli exchange term of the interaction in the calculation of W (GRPA)... → it is the most complete but it gives poor results...

The GW method for the electron gas

Density functional theory (DFT) summarized in two words

→ For confined systems (e.g. electrons in an atom or crystal) there exist a universal (==the same for any system!) energy functional of the density $E[\rho]$: if one knows the exact density, it is immediate to extract the energy.

→ in the Kohn-Sham formulation of DFT the density is expanded in a Slater determinant; this leads to a one-body Schroedinger-like equation, no matter the number of particles N . It can therefore be solved very easily.

→ The $E[\rho]$ functional is proven to exist but it is not known. If it was known, it would be possible to calculate for any system the exact energy, density and first ionization potential (and only the first!!!).

→ In practice, one uses a phenomenological potential. Results for the energies are usually very good, first ionizations and cases with substantial long-range correlations (e.g. Van der Waals) can be poor.

[W. Kohn and L. J. Sham, Phys. Rev. 140, A1133 (1965).
P. Hohenberg and W. Kohn, Phys. Rev. 136, B864 (1964)]

Two words on GW vs DFT...

For a comparison between Green's function and DFT see the review of Onida et al., [Rev. Mod. Phys. 74, 601 (2002)]

For the single-particle spectrum:

DFT

It is *fast* to solve

Kohn-Sham orbitals and energies do not have a physical meaning associated (except the first ionization)

Kohn-Sham orbitals and energies usually give a *good input* for G^0W^0 calculations.

Band gaps in insulators and semiconductors are usually underestimated.

GW

Calculations are more cumbersome

Single-particle properties are directly related to experimental quantities

G^0W^0 can give quite accurate s-p spectra.

The more elaborated GW does better on energies but ruins the s-p spectra—Note that GW is **NOT** a conserving approx. (Baym-Kadanoff)

Two words on GW vs DFT...

Example of band calculation for copper

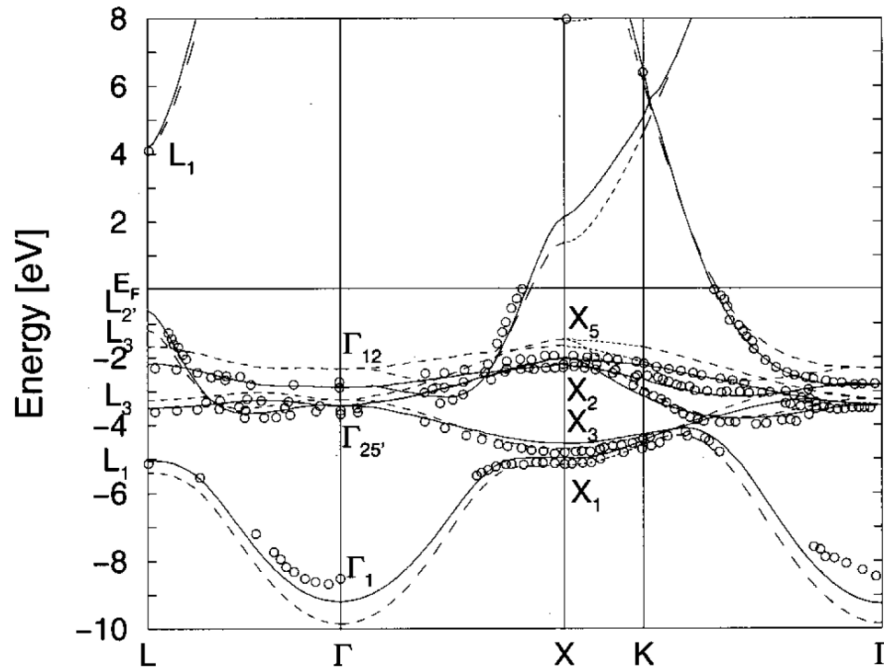


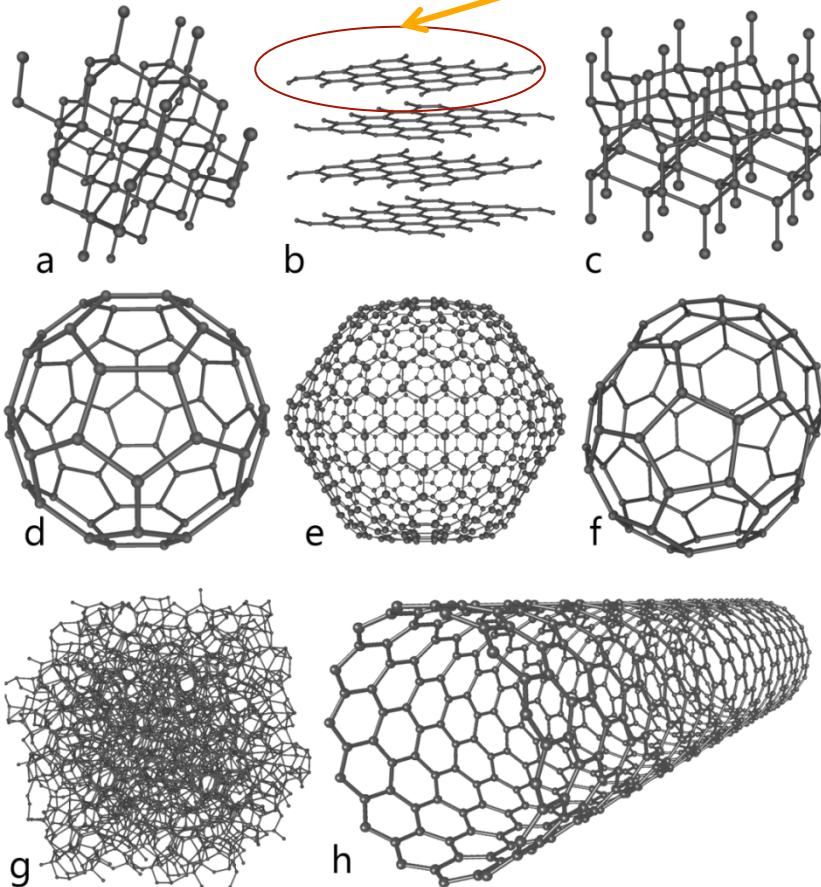
FIG. 2. Comparison of the calculated and experimental band structures for copper: solid line, *GW* quasiparticle excitation energies (Marini *et al.*, 2002); dashed line, DFT-LDA eigenvalues; \circ , experimental data compiled by Courths and Hüfner (1984). A comparison to more recent experimental data (Stroscov *et al.*, 1998, 2001) yields the same agreement.

[Onida *et al.*, *Rev. Mod. Phys.* 74, 601 (2002)]

Graphite → graphene and graphane

Some allotropes of carbon:

Graphene is a one-atom thick sheet of Graphite
[K.S.Novoselof, et al., Science 306, 666 (2004).]



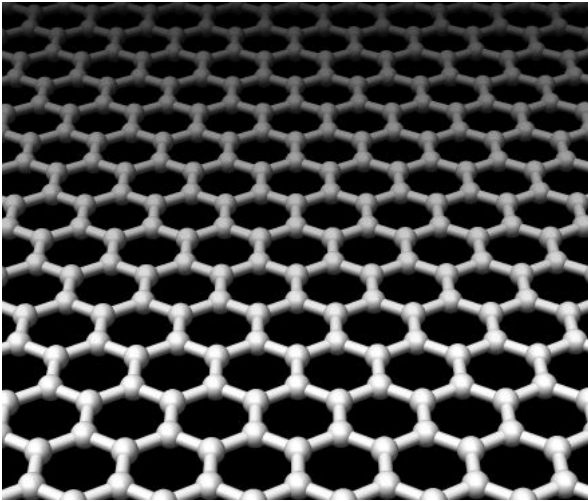
a) diamond;
b) graphene;
c) lonsdaleite;
d-f) fullerenes (C₆₀, C₅₄₀, C₇₀);
g) amorphous carbon;
h) carbon nanotube.

[Picture from Wikipedia]

Graphite → graphene and graphane

Graphene is a good candidate material for constructing future electronics components

→ one wish to turn it into a semiconductor, while keeping it two-dimensional



[Source: Wikipedia]

Graphene is a one-atom-thick planar sheet of sp^2 -bonded carbon atoms that are densely packed in a honeycomb crystal lattice.

The carbon-carbon bond length in graphene is approximately 0.142 nm.

Graphene is the basic structural element of some carbon allotropes including graphite, carbon nanotubes and fullerenes.

Measurements have shown that graphene has a breaking strength 200 times greater than steel, making it the strongest material ever tested.

It is a good conductor of heat and electricity.

.

Graphite → graphene and graphane

Graphane is Hydrogenated graphene.

It was:

1) predicted theoretically
based on DFT-GGA calculations

[J. O. Sofo, et al. Rev. B 75, 153401 (2007).

D. W. Boukhvalov, et al., Phys. Rev. B 77, 035427 (2008).]

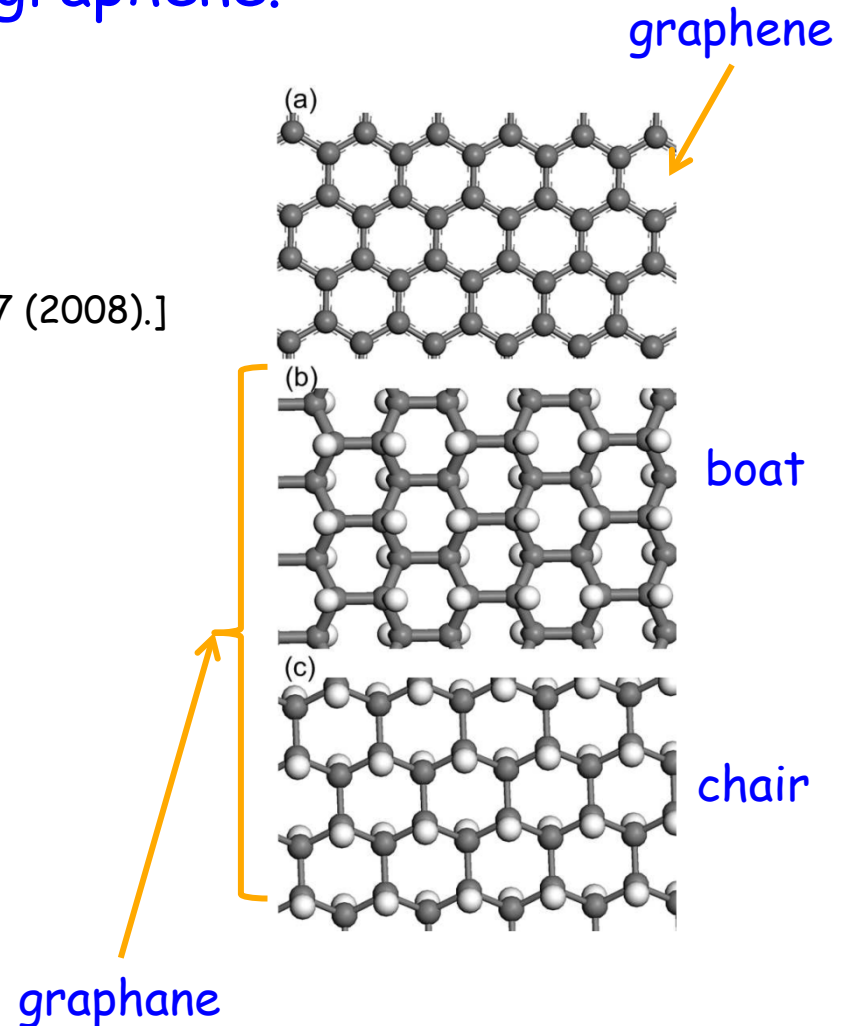
2) Recently synthesized

[D.C.Elias, et al. Science 323, 320 (2009)]

3) The band-gap is not known
but it is predicted by DFT-GGA
to be a semiconductor...

4) GW calculations instead suggest
that it is an insulator!

[Phys. Rev. B 79, 245117 (2009)]



[Picture: arXiv:0903.0278v1]

Graphite \rightarrow graphene and graphane

Graphane is predicted to be:

- a semiconductor by DFT-GGA calculations.
- an insulator in GW

TABLE I: Values in eV of the transition energies of graphane at some high-symmetry points of the Brillouin zone for both conformers (chair or boat). The minimum band gap occurs at the Γ point. The last two lines refer to calculations performed with a 2×2 supercell, in which either an hydroxyl group (OH) or a H vacancy was introduced.

Conformation	Transition	GGA value (eV)	GW value (eV)
Chair	$\Gamma_v \rightarrow \Gamma_c$	3.5	5.4
	$M_v \rightarrow M_c$	10.8	13.7
	$K_v \rightarrow K_c$	12.2	15.9
Boat	$\Gamma_v \rightarrow \Gamma_c$	3.3	5.1
	$X_v \rightarrow X_c$	7.0	9.0
	$S_v \rightarrow S_c$	10.7	13.9
	$Y_v \rightarrow Y_c$	9.4	12.6
Chair+ OH	$\Gamma_v \rightarrow \Gamma_c$	3.3	5.0
Chair+ H vacancy	$\Gamma_v \rightarrow \Gamma_c$	3.7	5.4

[Phys. Rev. B79, 245117 (2009)]

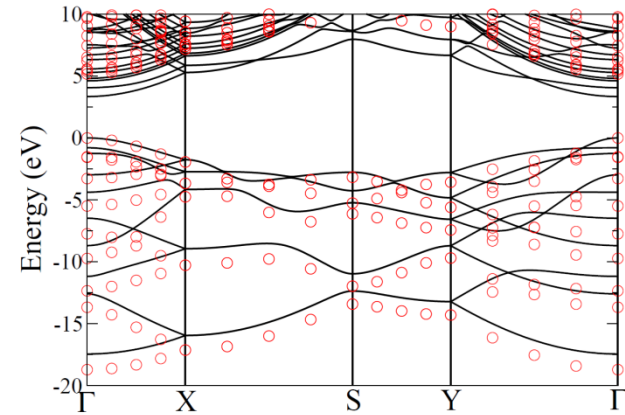


FIG. 3: (Color online) The GGA bandstructure (full lines) and the GW bandstructure (red dots) of graphane in the boat conformation. The top of the valence bands is chosen as the zero energy.

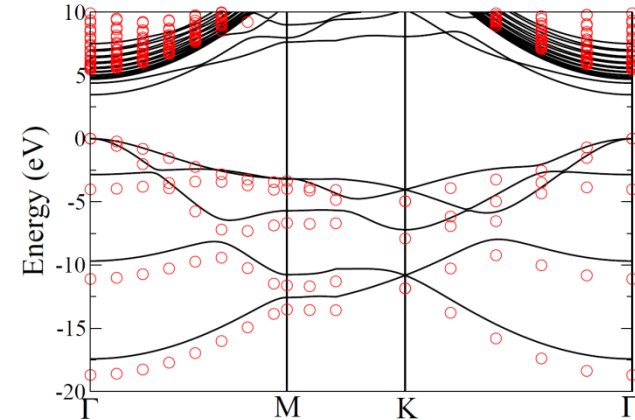
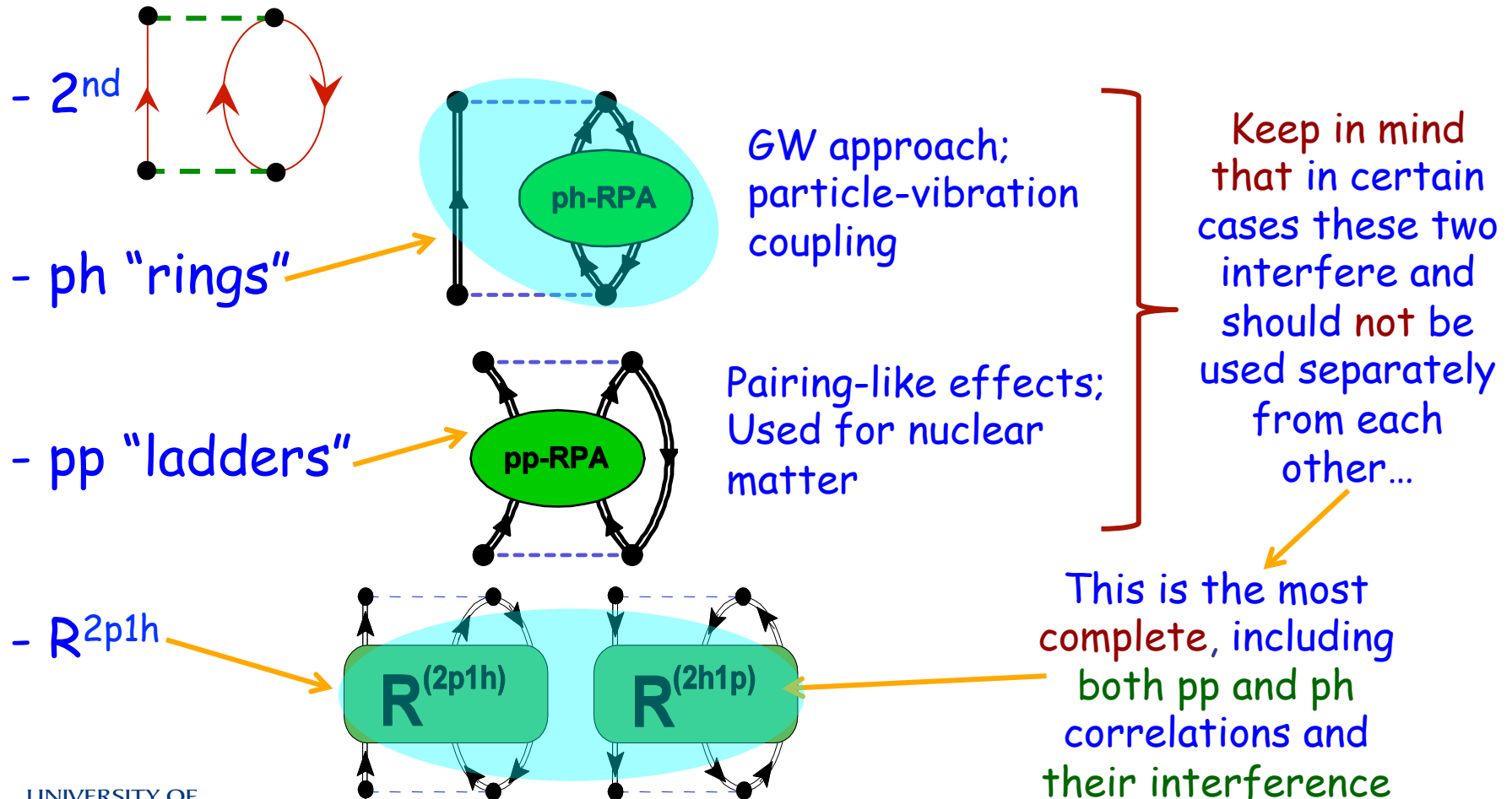


FIG. 2: (Color online) The GGA bandstructure (full lines) and the GW bandstructure (red dots) of graphane in the chair conformation. The top of the valence bands is chosen as the zero energy.



Approximations for the Self-energy

Diagrams of some common approximations for the self-energy:



Self-energy and 2p1h/2h1p propagator

Using the EOM of both t and t' , one finds again the Dyson equation with self-energy given (in a symmetric form) by

$$\Sigma_{\alpha\beta}^*(t - t') = \Sigma_{\alpha\beta}^{HF} + v_{\alpha\lambda,\mu\nu} R_{\mu\nu\lambda,\gamma\delta\zeta}(t, t') v_{\gamma\delta,\beta\zeta},$$

where:

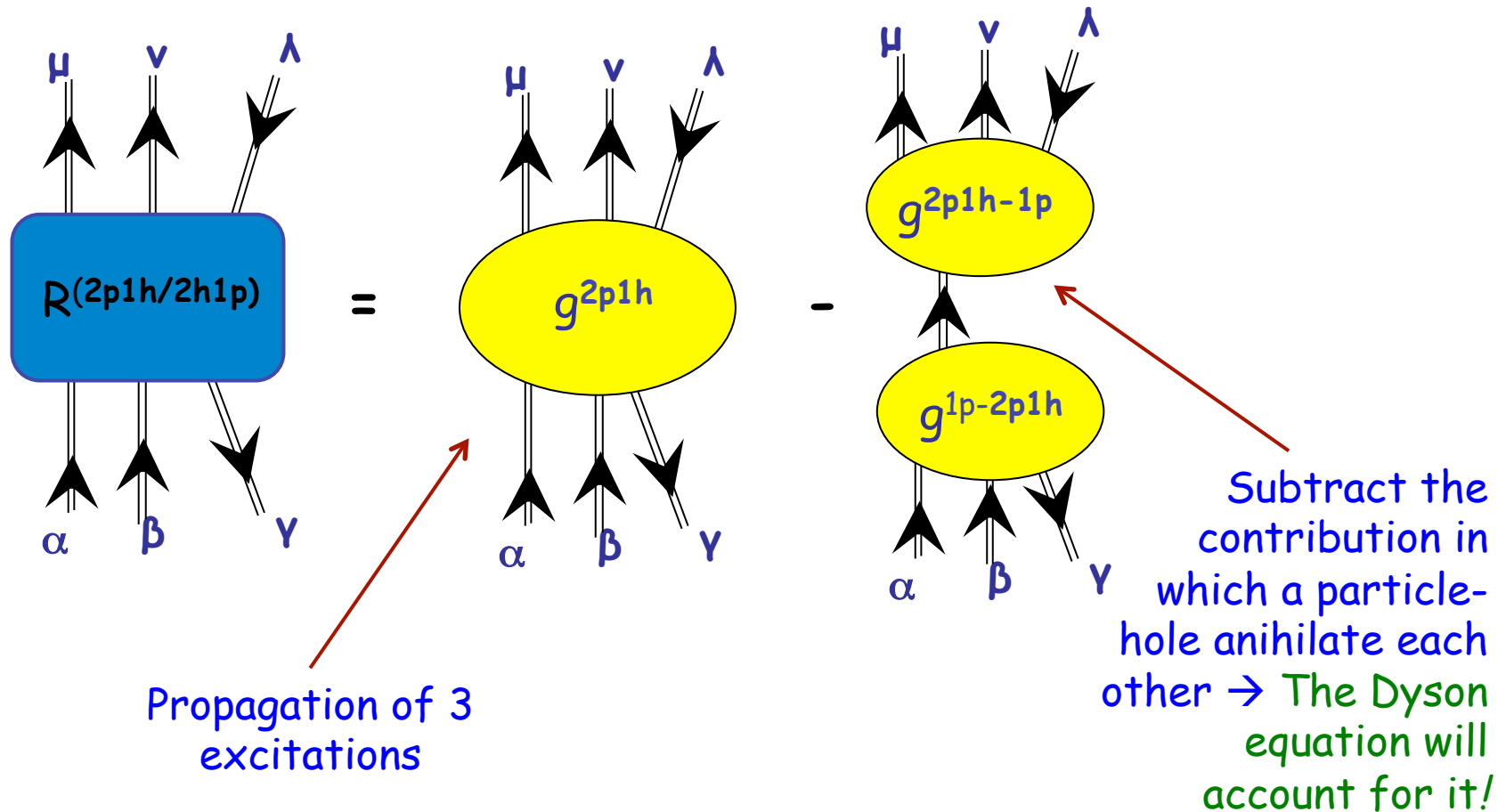
$$R_{\mu\nu\lambda,\alpha\beta\gamma}(t; t') \equiv g_{\mu\nu\lambda,\alpha\beta\gamma}^{2p1h}(t; t') - g_{\mu\nu\lambda,\eta}^{2p1h-1p}(t, t_1) g_{\eta\sigma}^{-1}(t_1 - t_2) g_{\sigma,\alpha\beta\gamma}^{1p-2p1h}(t_2, t')$$

Irreducible
2p1h/2h1p
propagator

$$g_{\alpha,\mu\nu\lambda}^{1p-2p1h}(t - t') \equiv -\frac{i}{\hbar} \langle \Psi_0^N | T[c_\alpha(t) c_\mu^\dagger(t') c_\nu^\dagger(t') c_\lambda(t')] | \Psi_0^N \rangle$$

Self-energy and 2p1h/2h1p propagator

Graphic representation of the 2p1h/2h1p irreducible propagator $R(\omega)$:



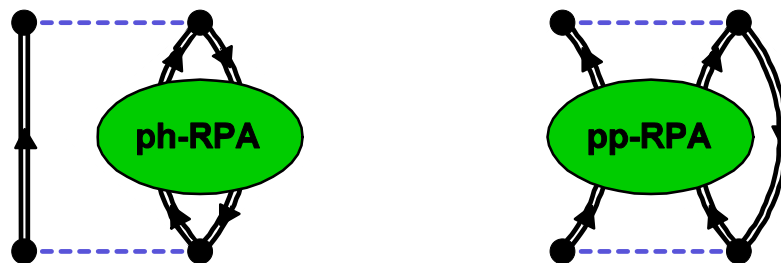
Propagation of 3 excitations

Subtract the contribution in which a particle-hole annihilate each other \rightarrow The Dyson equation will account for it!

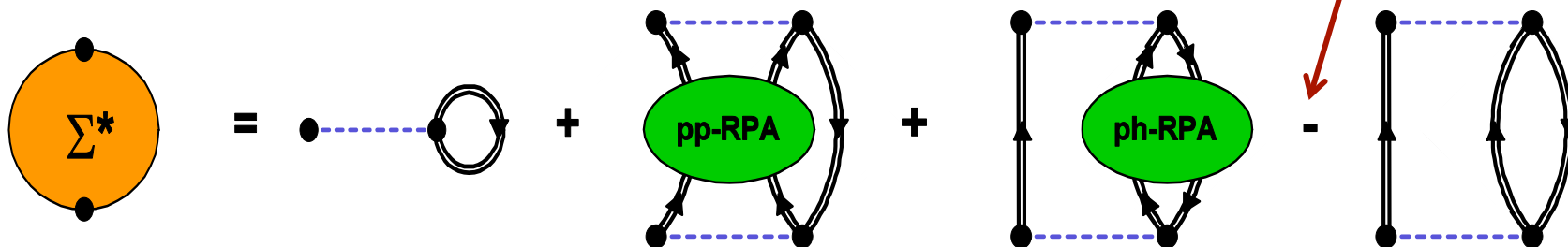
Faddeev RPA method

The following two diagrams can be equally important. However summing them would not work well:

- They both contain $\Sigma_{\alpha\beta}^{2nd}(\omega)$, which would be over counted
- They would not interfere...

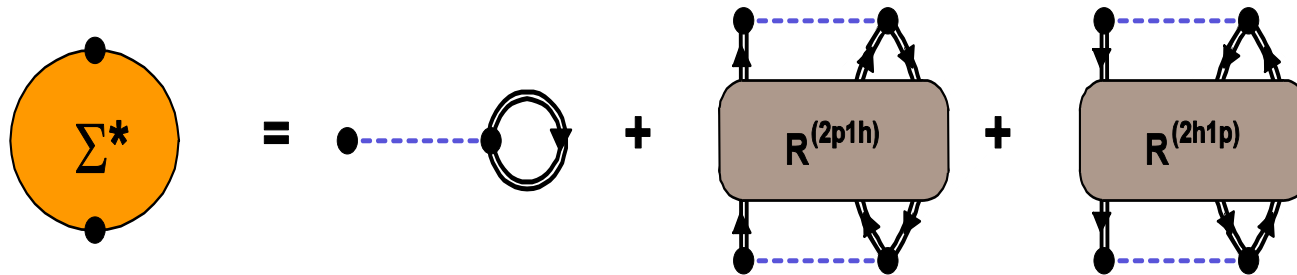


So, the following is **NOT** good:

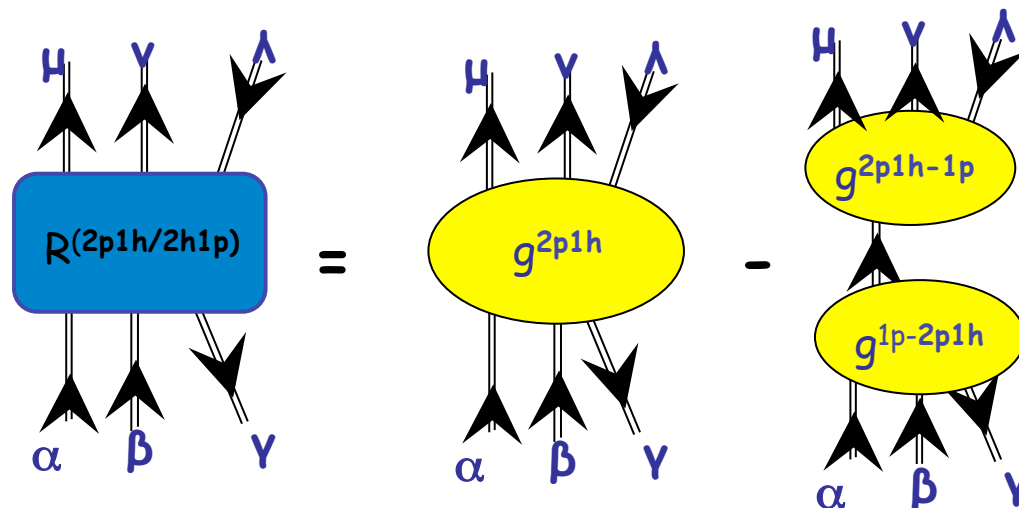


Faddeev RPA method

Thus, to include both "ladder" and "ring" correlations one **must** calculate the full **2p1h/2h1p** propagator

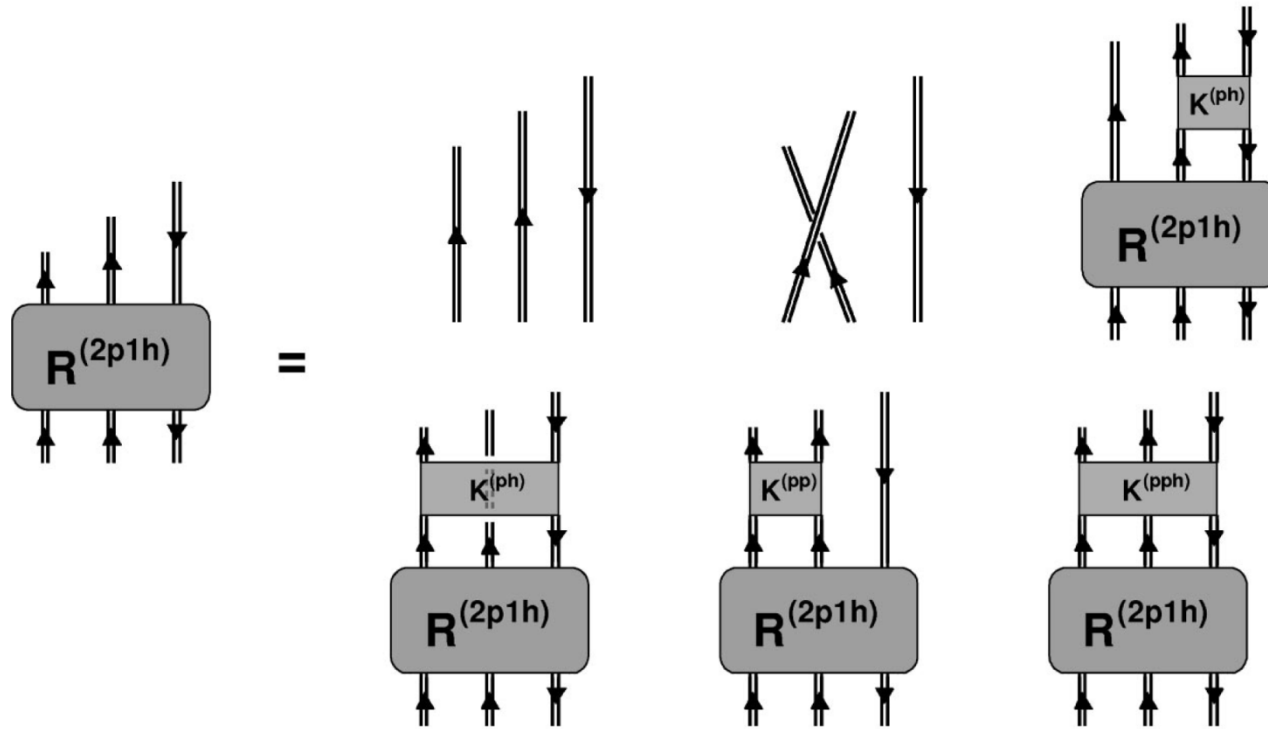


In general this is **exact** if one can calculate the full 6-points Green's function (see lecture of Apr. 13th):



Faddeev RPA method

The full $2p1h/2h1p$ polarization propagator also satisfies a Bethe-Salpeter-like equation:



However, this depends on 4-times (3 frequencies) and it is much more complicated than the p-h Bethe-Salpeter.

Faddeev RPA method

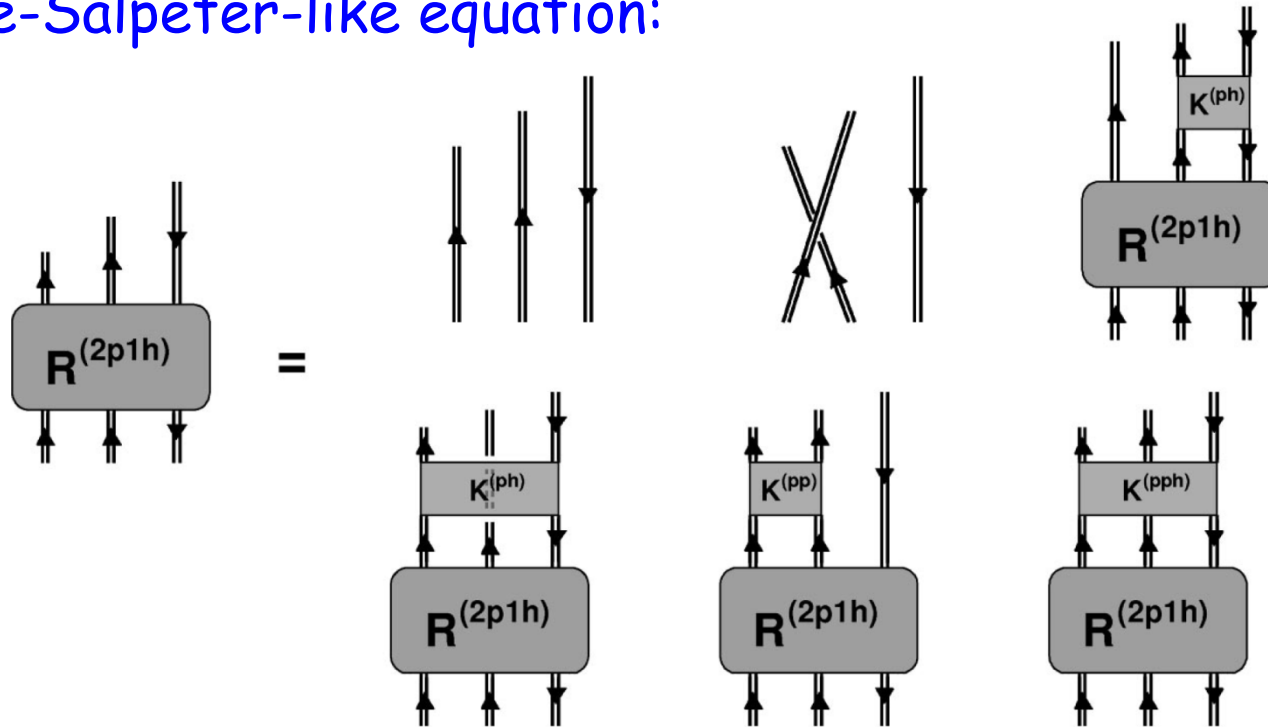
The full 2p1h/2h1p polarization propagator also satisfies a Bethe-Salpeter-like equation:

$$\begin{aligned} R_{\alpha\beta\gamma,\mu\nu\lambda}(\omega_1, \omega_2, \omega_3) = & [g_{\alpha\mu}(\omega_1)g_{\beta\nu}(\omega_2) - g_{\beta\mu}(\omega_2)g_{\alpha\nu}(\omega_1)]g_{\lambda\gamma}(-\omega_3) \\ & + \left(g_{\beta\beta_1}(\omega_2)g_{\gamma_1\gamma}(-\omega_3)V_{\beta_1\sigma,\gamma_1\rho} \int \frac{ds}{2\pi i} R_{\alpha\rho\sigma,\mu\nu\lambda}(\omega_1, s, \omega_2 + \omega_3 - s) \right. \\ & + g_{\alpha\alpha_1}(\omega_1)g_{\gamma_1\gamma}(-\omega_3)V_{\alpha_1\sigma,\gamma_1\rho} \int \frac{ds}{2\pi i} R_{\rho\beta\sigma,\mu\nu\lambda}(s, \omega_2, \omega_1 + \omega_3 - s) \\ & \left. + \frac{1}{2}g_{\alpha\alpha_1}(\omega_1)g_{\beta\beta_1}(\omega_2)V_{\alpha_1\beta_1,\rho\sigma} \int \frac{ds}{-2\pi i} R_{\rho\sigma\gamma,\mu\nu\lambda}(s, \omega_1 + \omega_2 - s, \omega_3) \right) \end{aligned}$$

However, this depends on 4-times (3 frequencies) and it is much more complicated than the p-h Bethe-Salpeter.

Faddeev RPA method

The full 2p1h/2h1p polarization propagator also satisfies a Bethe-Salpeter-like equation:



Strategy: solve each "pp" and "ph" channel separately, by solving the (simpler) DRPA equations. Then couple to a third line and mix the corresponding amplitudes \rightarrow Faddeev eqs.!!

Faddeev equations for the 2h1p motion

Strategy: solve each "pp" and "ph" channel separately, by solving the (simpler) DRPA equations. Then couple to a third line and mix the corresponding amplitudes \rightarrow Faddeev eqs.!!

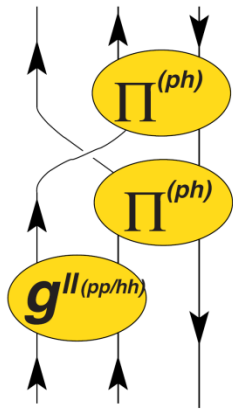
$$R^{2h1p}(\omega) = \begin{array}{c} \downarrow \downarrow \downarrow \\ \downarrow \downarrow \downarrow \\ \downarrow \downarrow \downarrow \end{array} - \begin{array}{c} \swarrow \swarrow \\ \swarrow \swarrow \\ \downarrow \downarrow \end{array} + R^1(\omega) + R^2(\omega) + R^3(\omega) \quad \text{Faddeev components}$$

Faddeev eqns.

$$\begin{pmatrix} R^1 \\ R^2 \\ R^3 \end{pmatrix} = \begin{pmatrix} \begin{array}{c} \downarrow \downarrow \downarrow \\ \downarrow \downarrow \downarrow \\ \downarrow \downarrow \downarrow \end{array} \\ \begin{array}{c} \downarrow \downarrow \downarrow \\ \downarrow \downarrow \downarrow \\ \downarrow \downarrow \downarrow \end{array} \\ \begin{array}{c} \downarrow \downarrow \downarrow \\ \downarrow \downarrow \downarrow \\ \downarrow \downarrow \downarrow \end{array} \end{pmatrix} + \begin{pmatrix} 0 & \begin{array}{c} \downarrow \downarrow \downarrow \\ \downarrow \downarrow \downarrow \\ \downarrow \downarrow \downarrow \end{array} & \begin{array}{c} \downarrow \downarrow \downarrow \\ \downarrow \downarrow \downarrow \\ \downarrow \downarrow \downarrow \end{array} \\ \begin{array}{c} \downarrow \downarrow \downarrow \\ \downarrow \downarrow \downarrow \\ \downarrow \downarrow \downarrow \end{array} & 0 & \begin{array}{c} \downarrow \downarrow \downarrow \\ \downarrow \downarrow \downarrow \\ \downarrow \downarrow \downarrow \end{array} \\ \begin{array}{c} \downarrow \downarrow \downarrow \\ \downarrow \downarrow \downarrow \\ \downarrow \downarrow \downarrow \end{array} & \begin{array}{c} \downarrow \downarrow \downarrow \\ \downarrow \downarrow \downarrow \\ \downarrow \downarrow \downarrow \end{array} & 0 \end{pmatrix} \begin{pmatrix} R^1 \\ R^2 \\ R^3 \end{pmatrix}$$

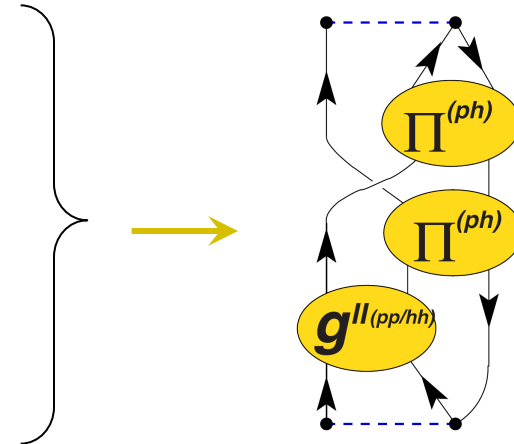
TDA/RPA phonons

FRPA: Faddeev summation of RPA propagators

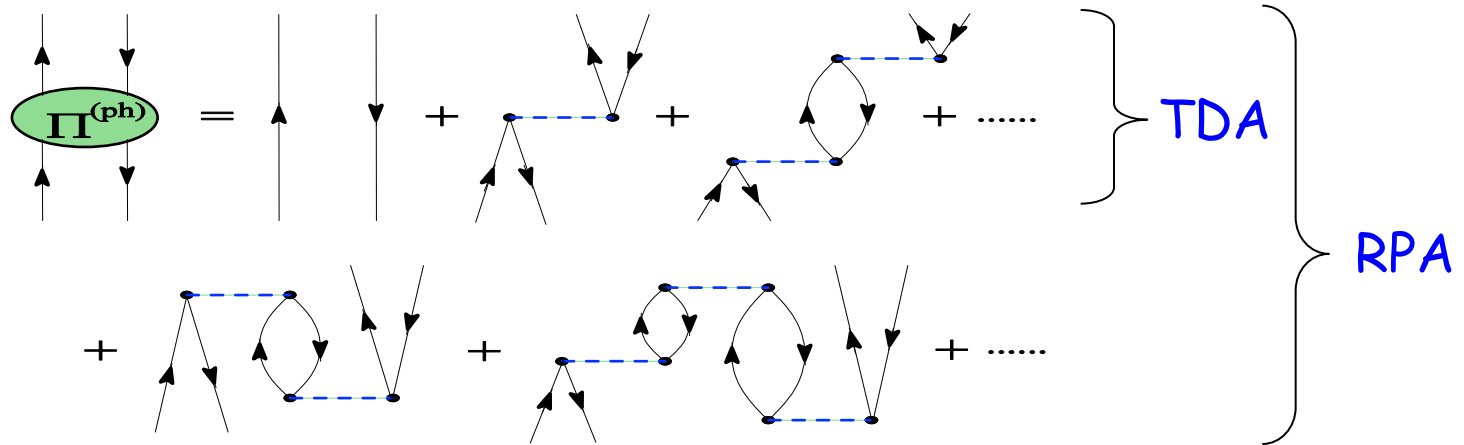


- Both pp/hh (ladder) and ph (ring) response included
- Pauli exchange at 2p1h/2h1p level

- All order summation through a set of Faddeev equations

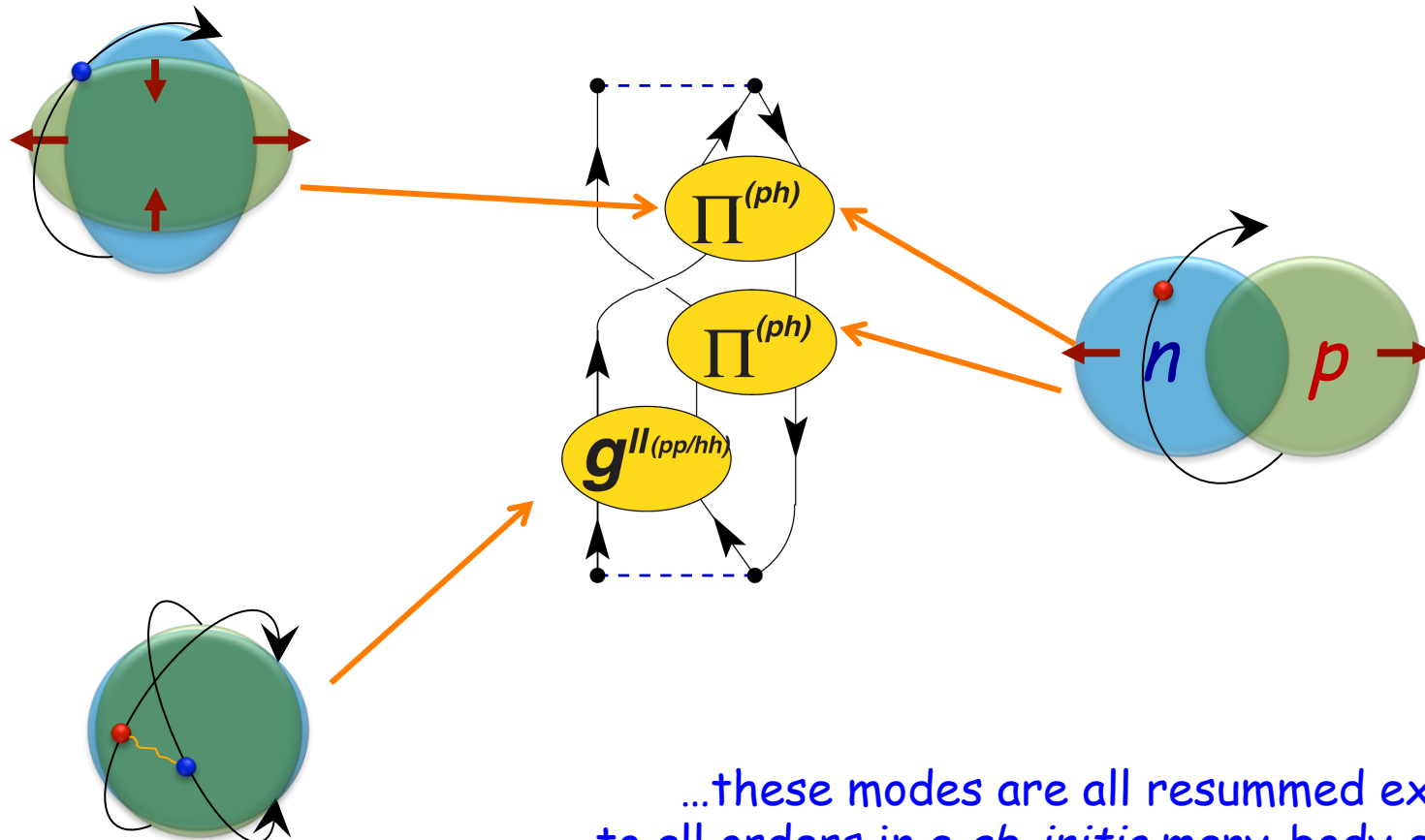
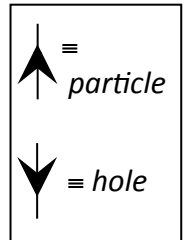


where:



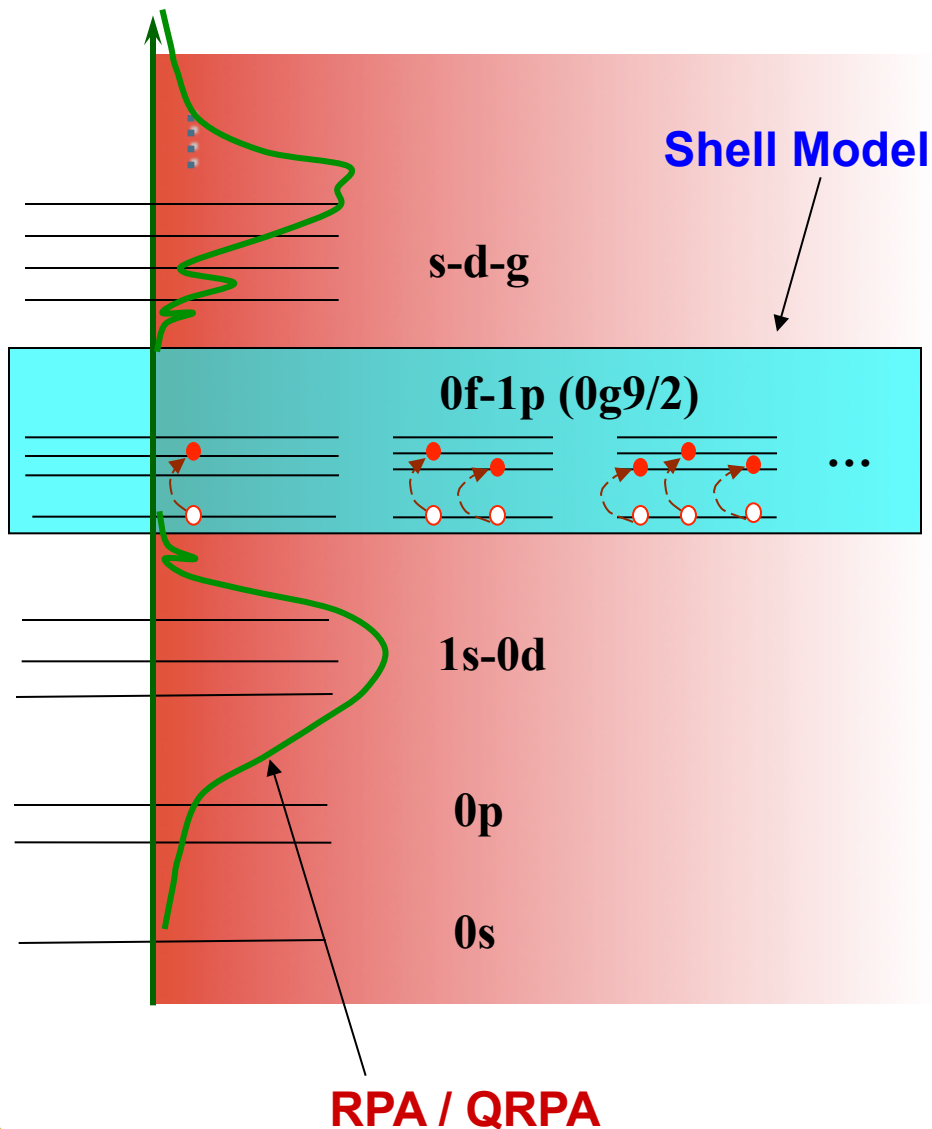
Faddeev-RPA in two words...

Particle vibration coupling is the main cause driving the distribution of particle strength—a least close to the Fermi surface...



...these modes are all resummed exactly and to all orders in a *ab-initio* many-body expansion.

Correlations & model space (RPA and SM)



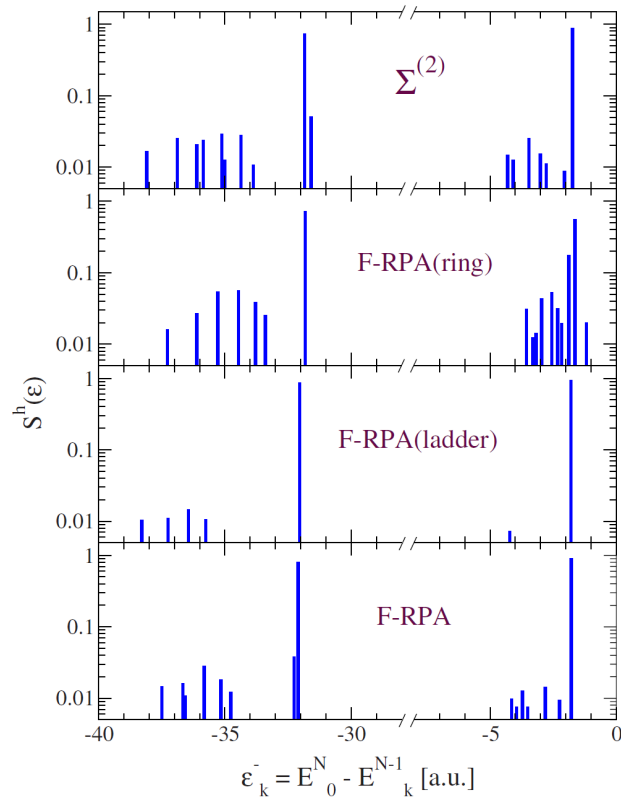
Open-shell nuclei require explicit configuration mixing: shell model

Faddeev-RPA describes well the coupling to collective modes—including those *outside* the reach of the shell model

→ apply at shell closures!!

Ladder vs rings interference

Example of sole "ladder" or "ring" and full mixing



Atom of Ne
(10 electrons
problem)

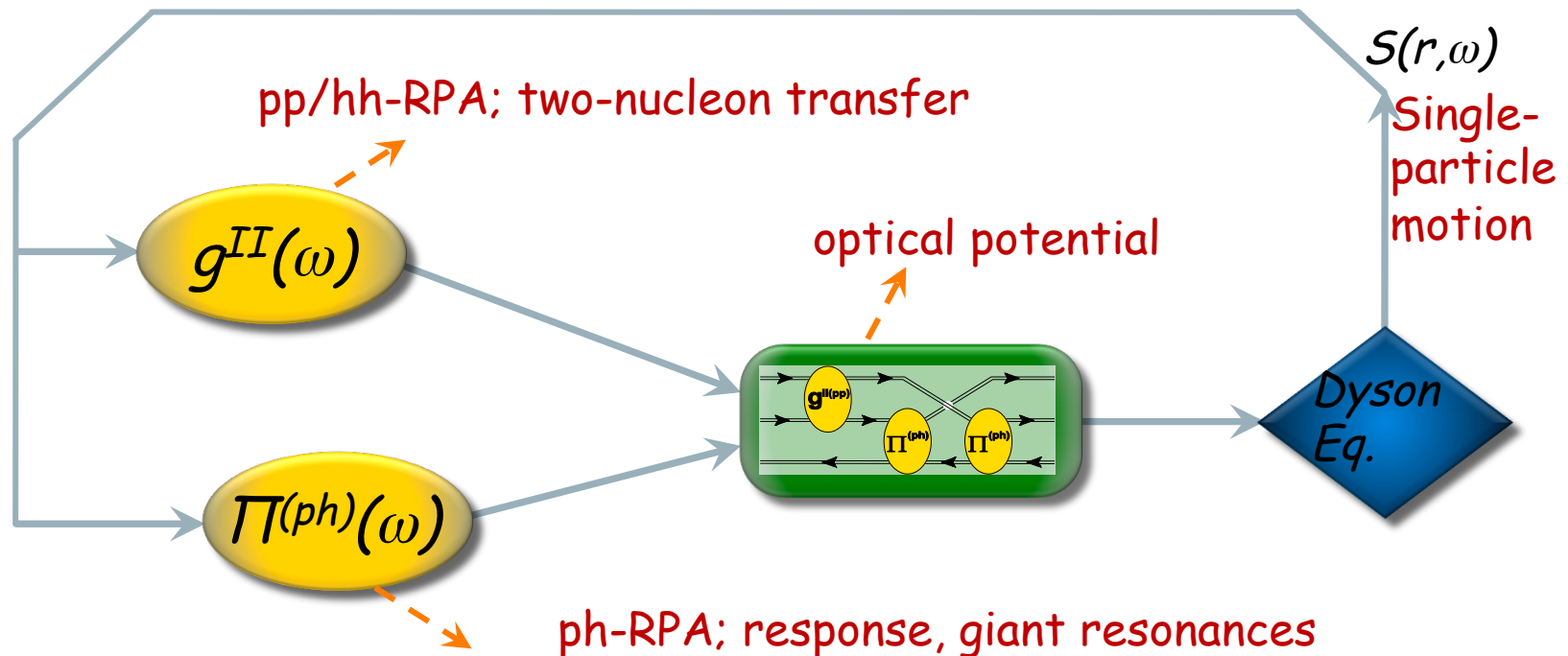
TABLE IV. Energy (in a.u.) and strength (numbers in parentheses) of the main fragments in the spectral function of neon, generated by different self-energies. Results for the HF+continuum basis. Consecutive rows refer to (1) HF; (2) second-order self-energy; (3) G_0W_0 results from Ref. [14]; (4) FRPA self-energy with only ph rings retained; (5) FRPA self-energy with only pp - hh ladders retained; (6) complete FRPA self-energy. In all FRPA results the self-energy was corrected at third order through Eq. (8). The static self-energy was pure HF (no partial self-consistency). The experimental values are taken from Refs. [32,33].

	1s	2s	2p
HF	-32.77 (1.00)	-1.931 (1.00)	-0.850 (1.00)
$\Sigma^{(2)}$	-31.84 (0.74)	-1.736 (0.88)	-0.747 (0.91)
G_0W_0	-31.14 (0.85)	-1.774 (0.91)	-0.801 (0.94)
FRPA (ring)	-31.82 (0.73)	-1.636 (0.56)	-0.730 (0.80)
FRPA (ladder)	-32.04 (0.87)	-1.802 (0.95)	-0.781 (0.96)
FRPA	-32.10 (0.81)	-1.792 (0.91)	-0.799 (0.94)
Expt.	-31.70	-1.782 (0.85)	-0.793 (0.92)

FIG. 4. (Color online) Spectral function for the s states in Ne obtained with various self-energy approximations. From the top down: the second-order ($\Sigma^{(2)}$), the FRPA (ring), the FRPA (ladder), and the full FRPA self-energies. The strength is given relative to the Hartree-Fock occupation of each shell. Only fragments with strength larger than $Z > 0.005$ are shown.

Self-Consistent Green's Function Approach

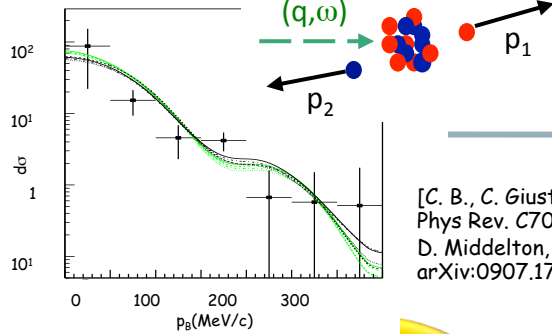
Why self-consistency ???



- Global picture of nuclear dynamics
- Reciprocal correlations among effective modes
- Guaranties *macroscopic conservation laws*

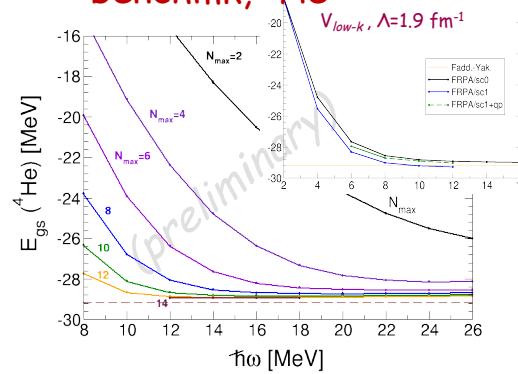
Self-Consistent Green's Function Approach

$^{16}\text{O}(e,e'pn)^{14}\text{N}$ @ MAINZ



[C. B., C. Giusti, et al. Phys Rev. C70, 014606 (2004)
D. Middleton, et al. arXiv:0907.1758; EPJA in print]

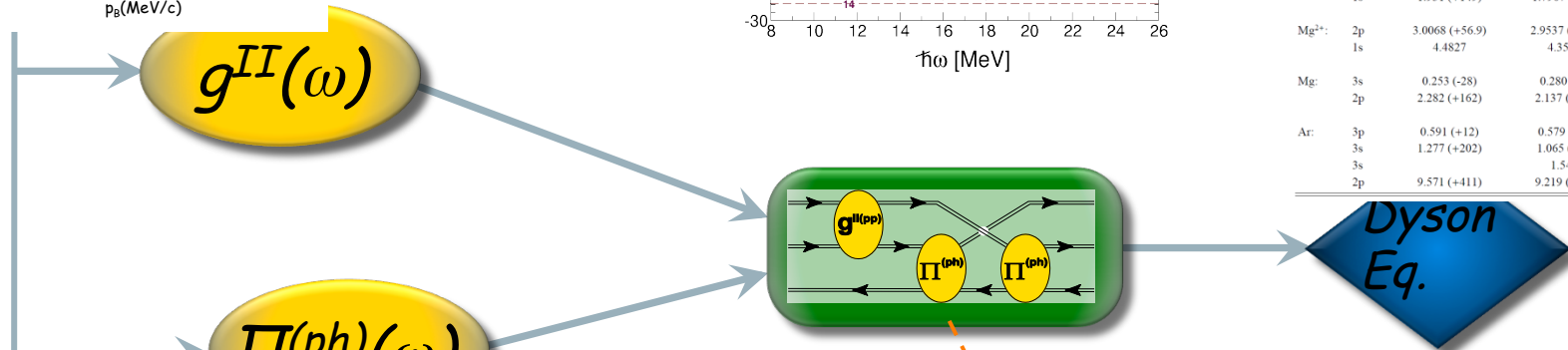
Binding energy benchmk, ^4He [C. B., arXiv:0909.0336]



Ionization energies/affinities, in atoms

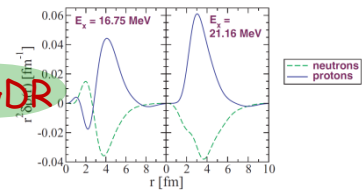
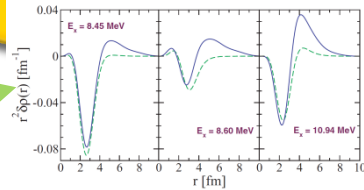
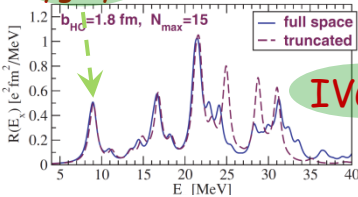
[CB, D. Van Neck, AIP Conf.Proc.1120,104 ('09) & in prep]

	Hartree-Fock	FRPAc	Experiment [16, 17]
He: 1s	0.918 (+14)	0.9008 (-2.9)	0.9037
Be ²⁺ : 1s	5.6672 (+116)	5.6551 (-0.5)	5.6556
Be: 2s	0.3093 (-34)	0.3224 (-20.2)	0.3426
1s	4.733 (+200)	4.5405 (+8)	4.533
Ne: 2p	0.852 (+57)	0.8037 (+11)	0.793
1s	1.931 (+149)	1.7967 (+15)	1.782
Mg ²⁺ : 2p	3.0068 (+56.9)	2.9537 (+3.8)	2.9499
1s	4.4827	4.3589	
Mg: 3s	0.253 (-28)	0.280 (-1)	0.281
2p	2.282 (+162)	2.137 (+17)	2.12
Ar: 3p	0.591 (+12)	0.579 (±0)	0.579
3s	1.277 (+202)	1.065 (-10)	1.075
3s		1.544	
2p	9.571 (+411)	9.219 (+59)	9.160



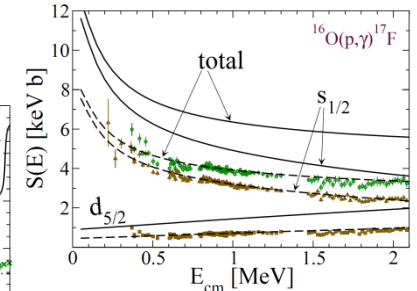
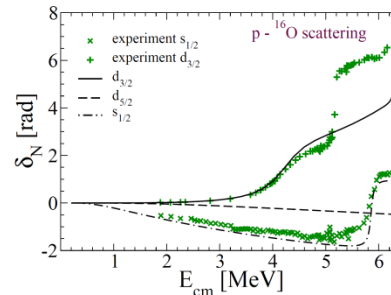
Isovector response for ^{32}Ar , ^{34}Ar

Proton Pygmy



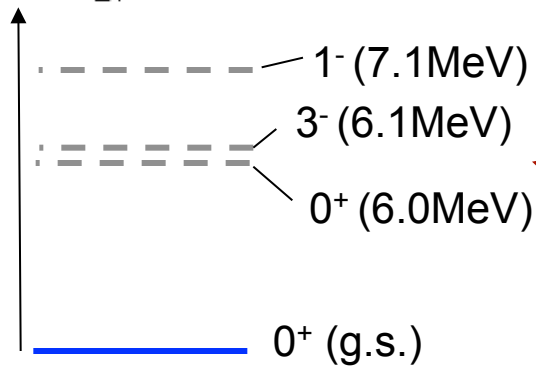
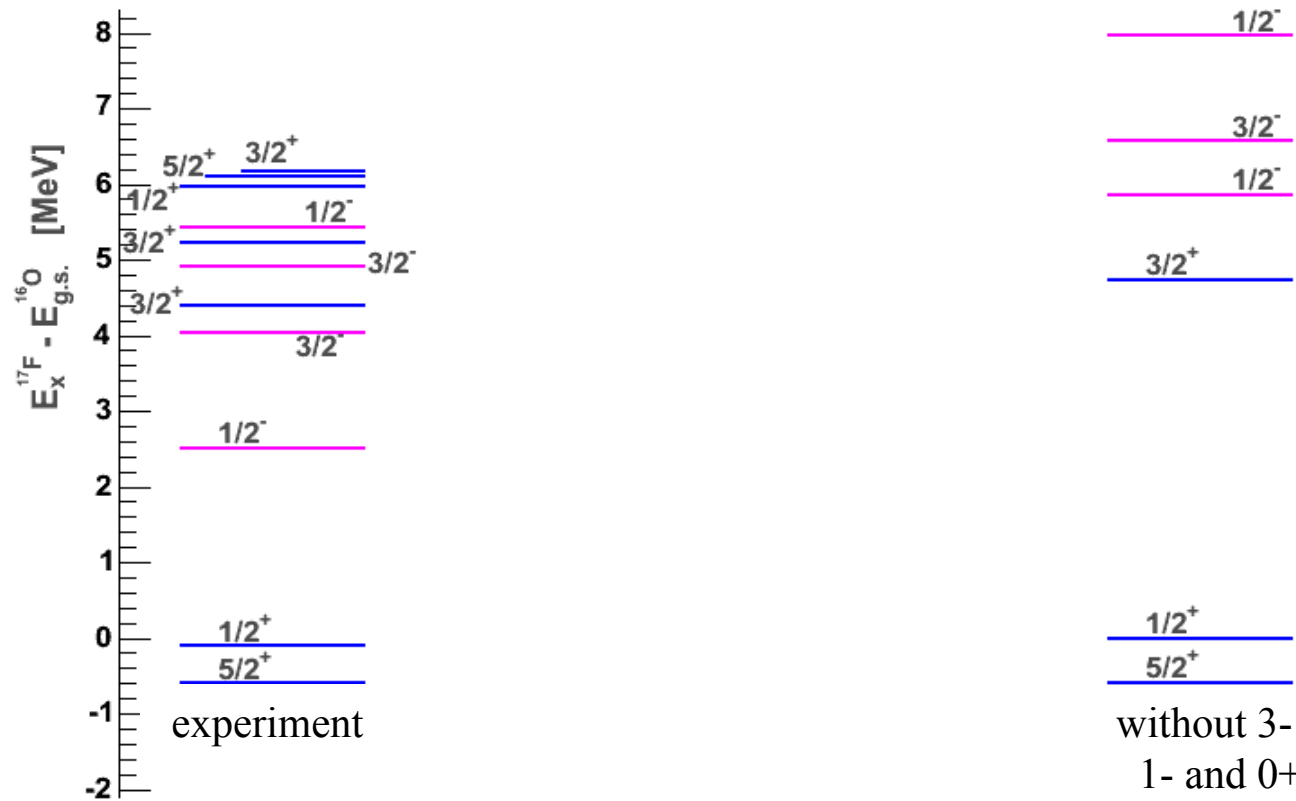
IVGDR

$^{16}\text{O}(p,\gamma)$

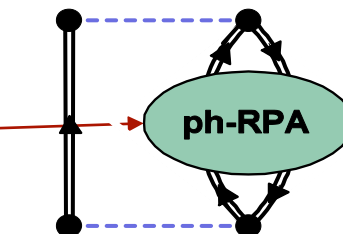


[C. B., B. K. Jennings Nucl. Phys A758, 395c (2005)
Phys Rev. C72, 014613 (2005)]

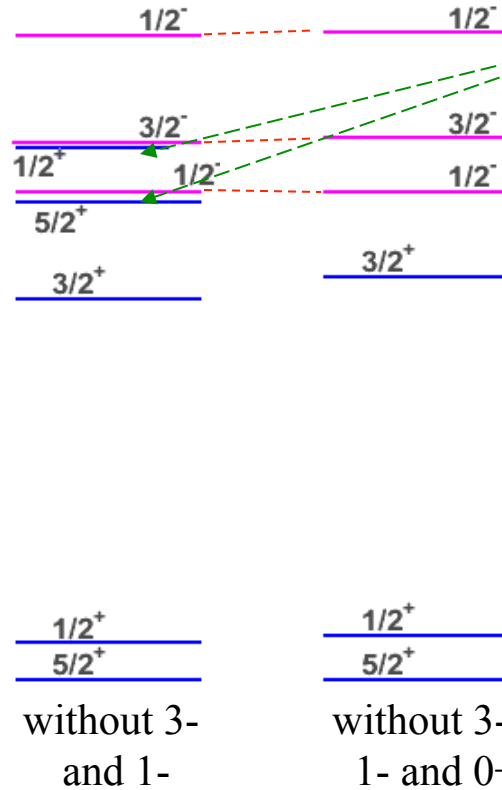
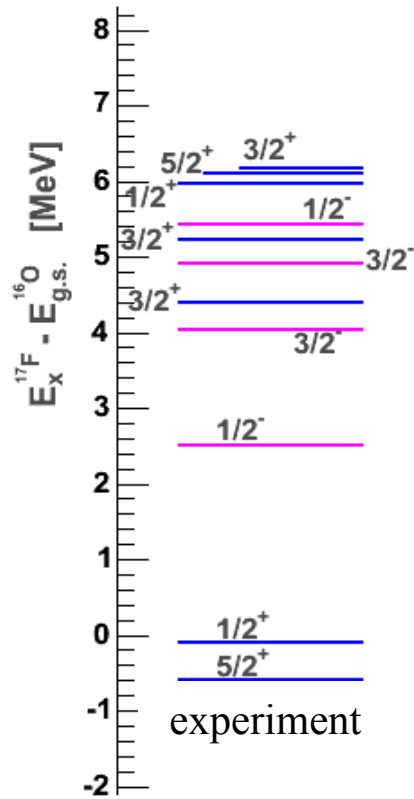
Quasiparticle spectrum of ^{16}O (i.e. ^{17}F)



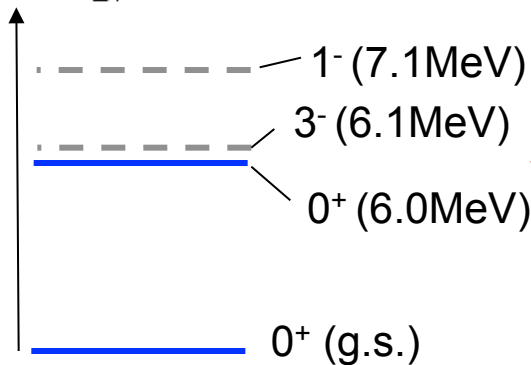
spectrum of ^{16}O



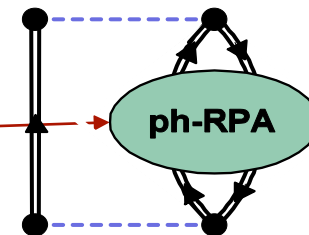
Quasiparticle spectrum of ^{16}O (i.e. ^{17}F)



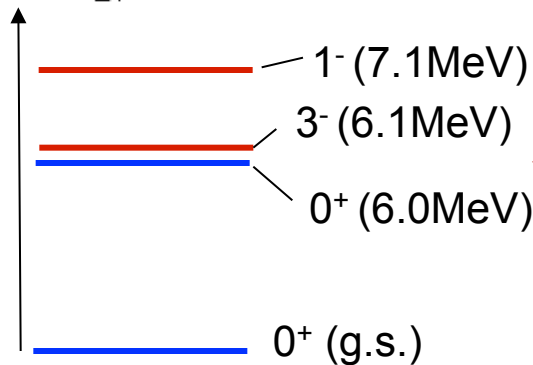
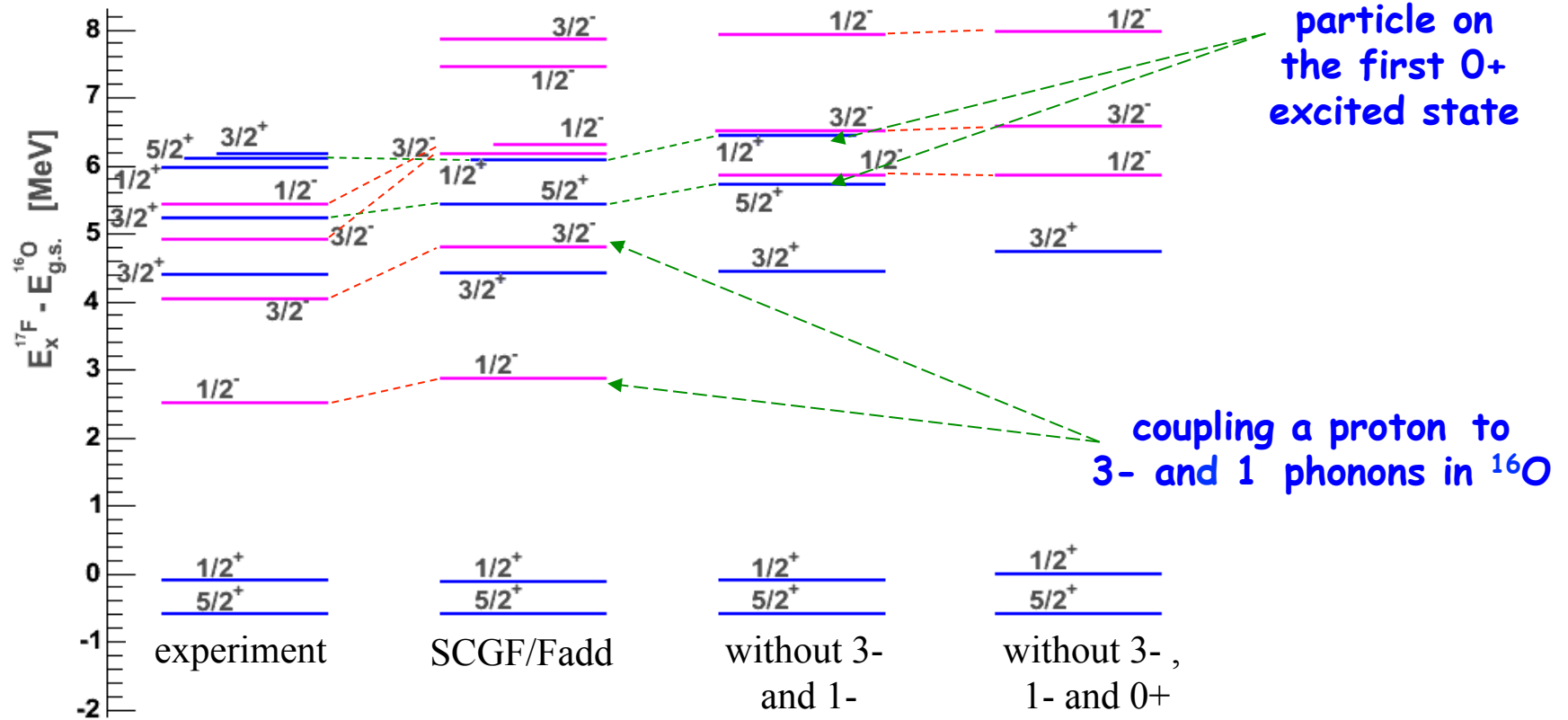
particle on the first 0^+ excited state



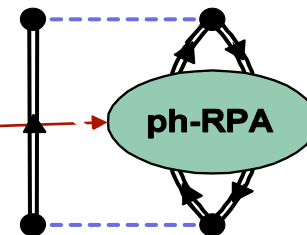
spectrum of ^{16}O



Quasiparticle spectrum of ^{16}O (i.e. ^{17}F)

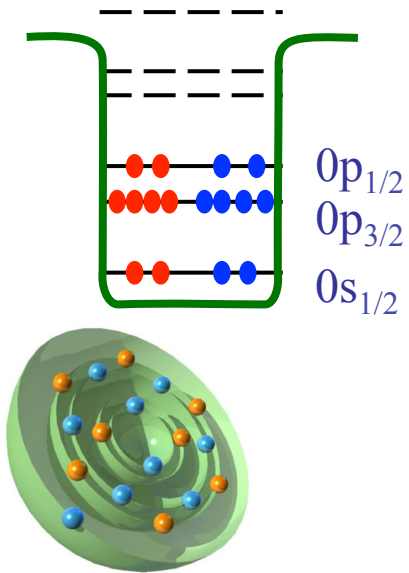


spectrum of ^{16}O

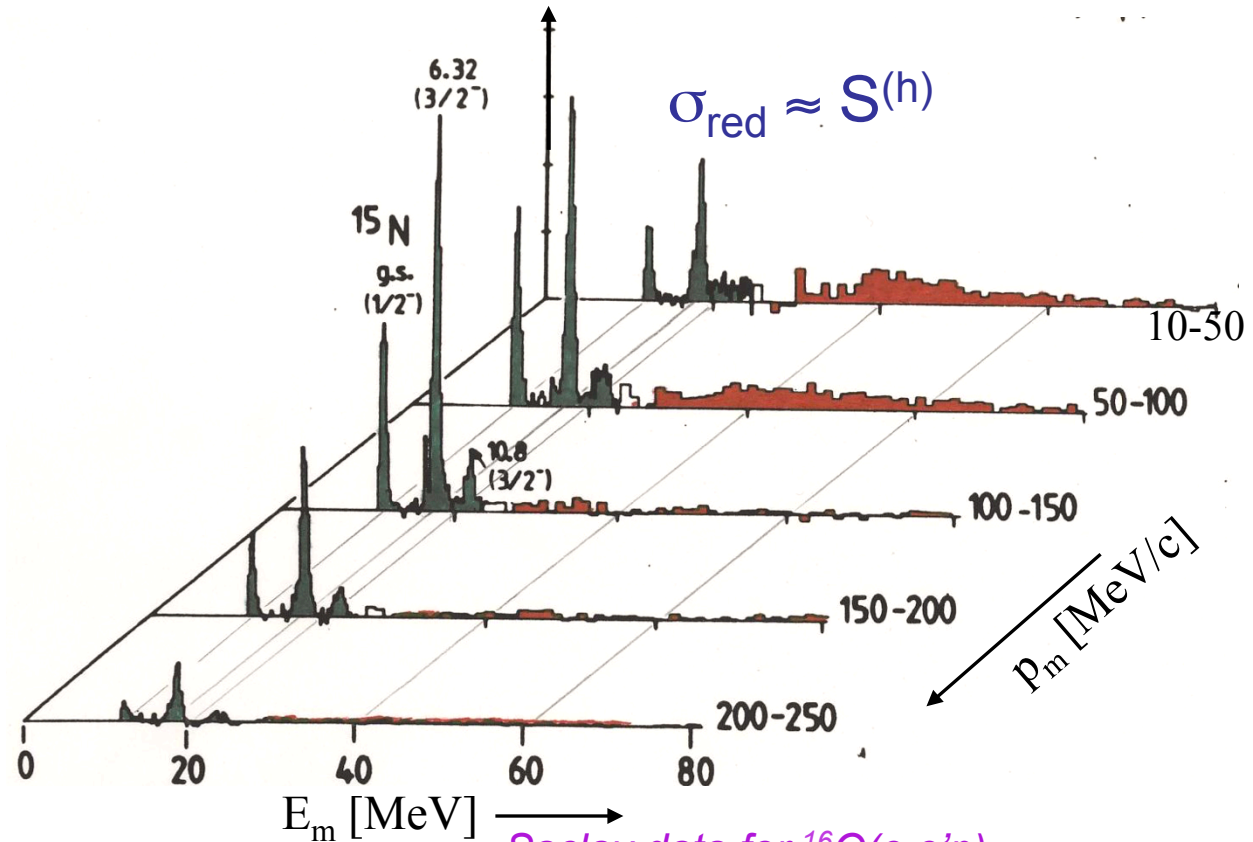


Concept of correlations

independent
particle picture



Spectral function: distribution of
momentum (p_m) and energies (E_m)



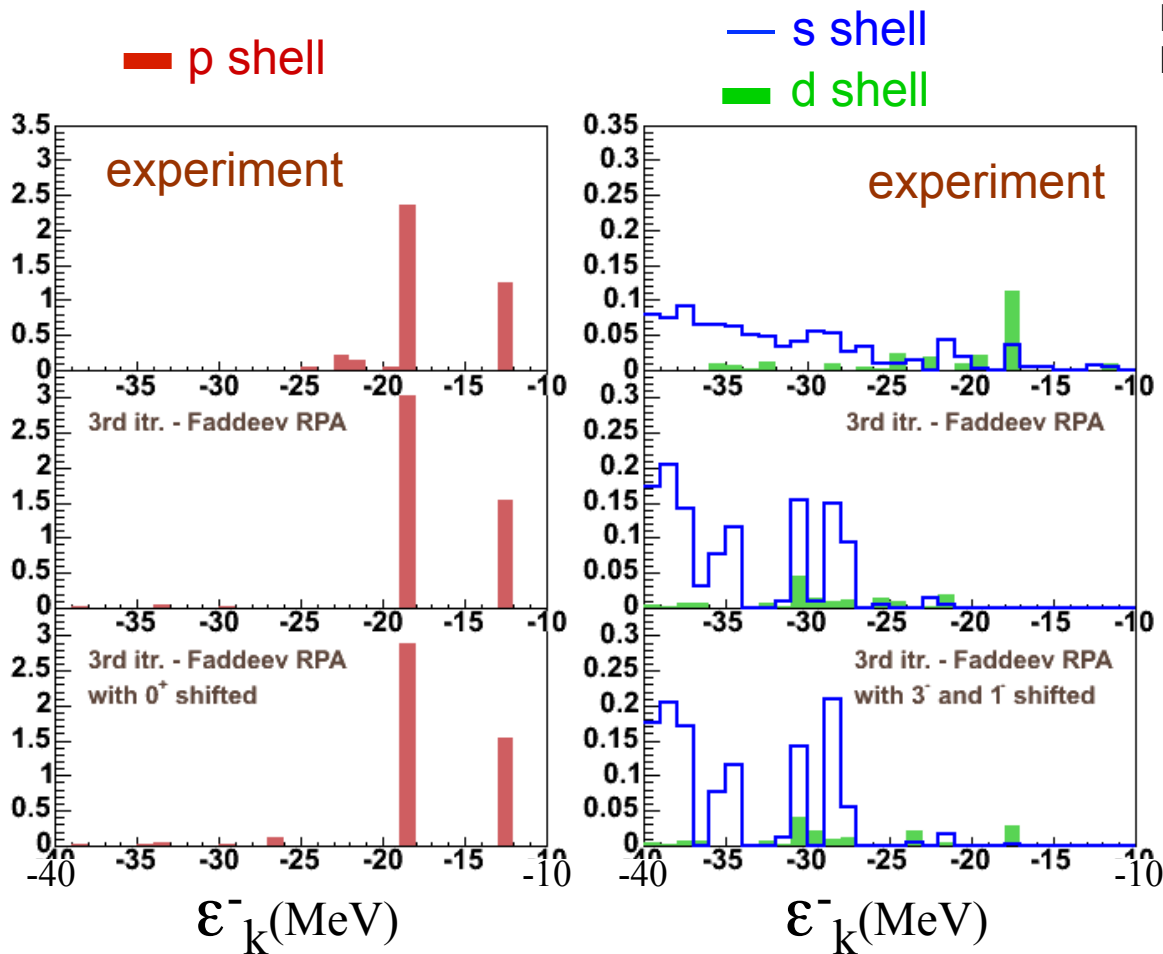
Saclay data for $^{16}\text{O}(e, e'p)$

[Mougey et al., Nucl. Phys. A335, 35 (1980)]

$$S^{(h)}(p_m, E_m) = \sum_n \left| \langle \Psi_n^{A-1} | c_{p_m}^- | \Psi_0^A \rangle \right|^2 \delta(E_m - (E_0^A - E_n^{A-1}))$$

Hole spectral function of ^{16}O

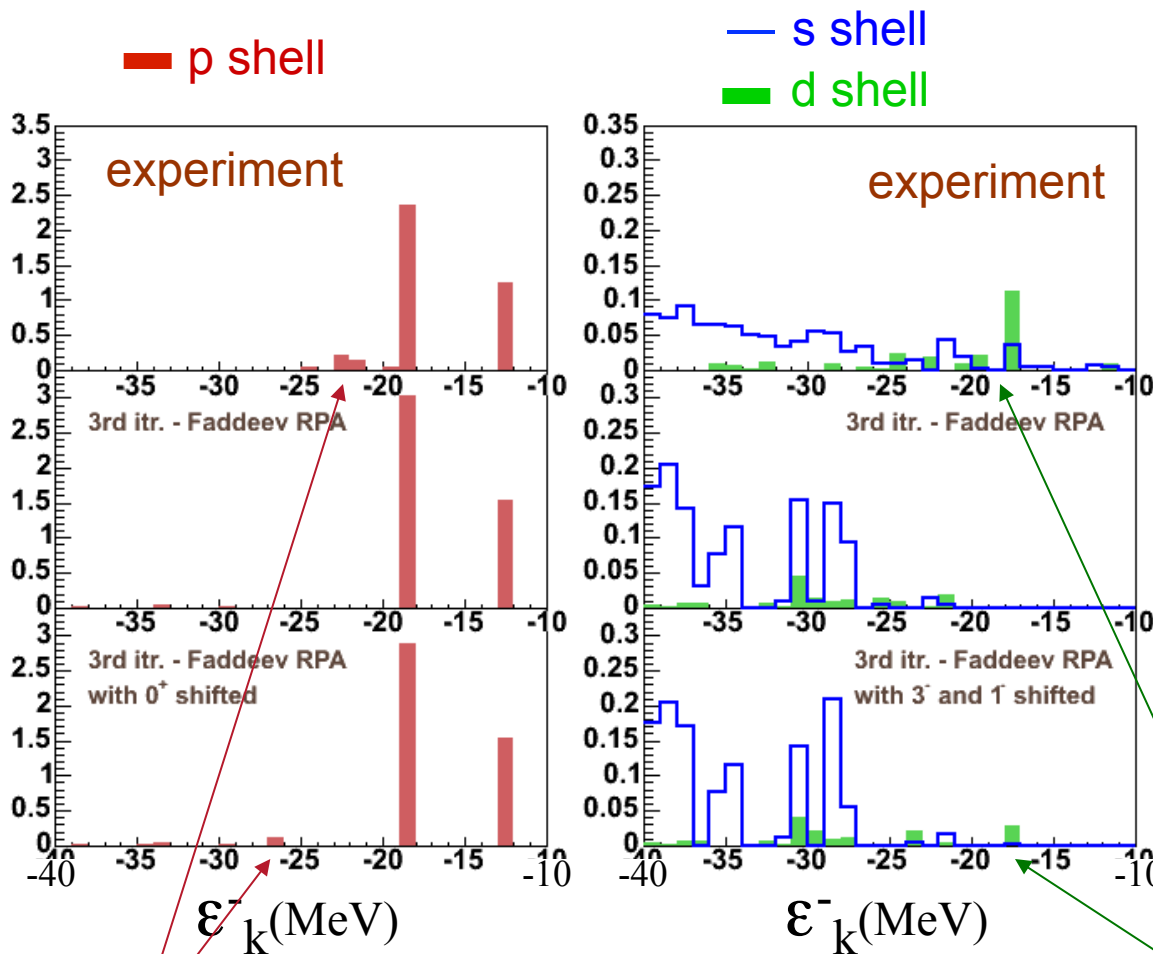
NIKHEF data,
Leuschner et. al., PRC59, 655 (94)



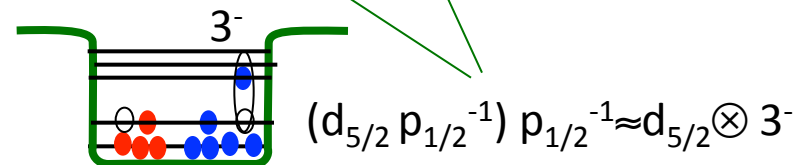
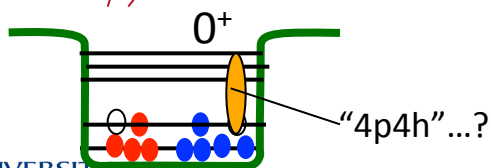
Results from
Faddeev
expansion and
SCGF

Hole spectral function of ^{16}O

NIKHEF data,
Leuschner et. al., PRC59, 655 (94)



Results from
FRPA expansion
of SCGF





High momentum components - where are they?

Momentum distribution:

$$n(k) = \int_{-\infty}^{\varepsilon_F^-} d\omega S^{(h)}(k, \omega)$$

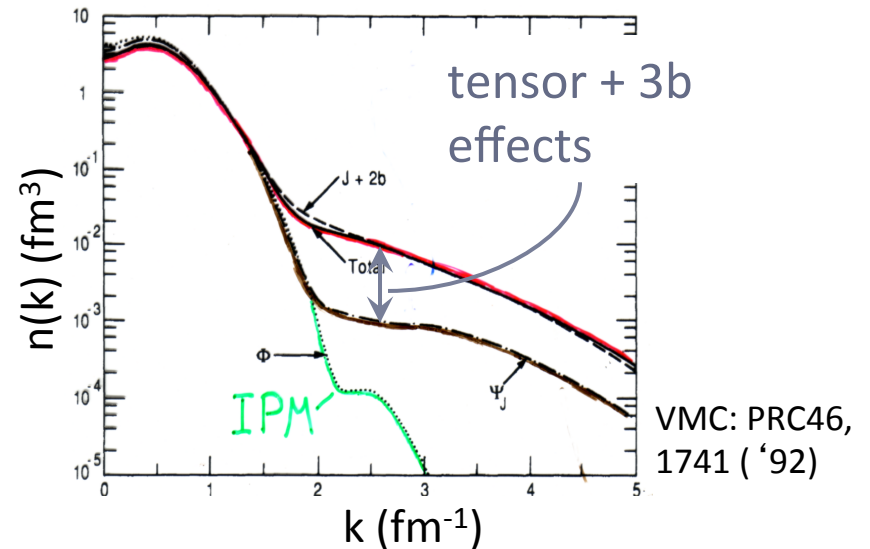
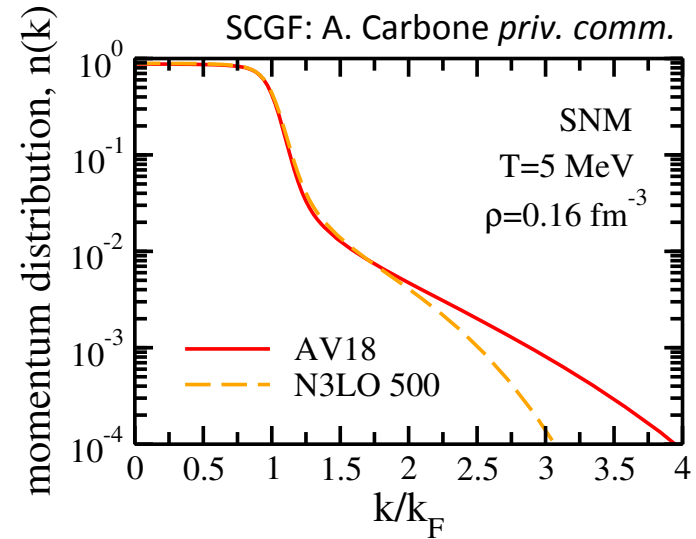
- High k components are found at high missing energies

- Short-range repulsion in r -space
 \leftrightarrow strong potential at large momenta

- A complication: the nuclear interaction includes also a tensor term (from Yukawa's meson meson exchange):

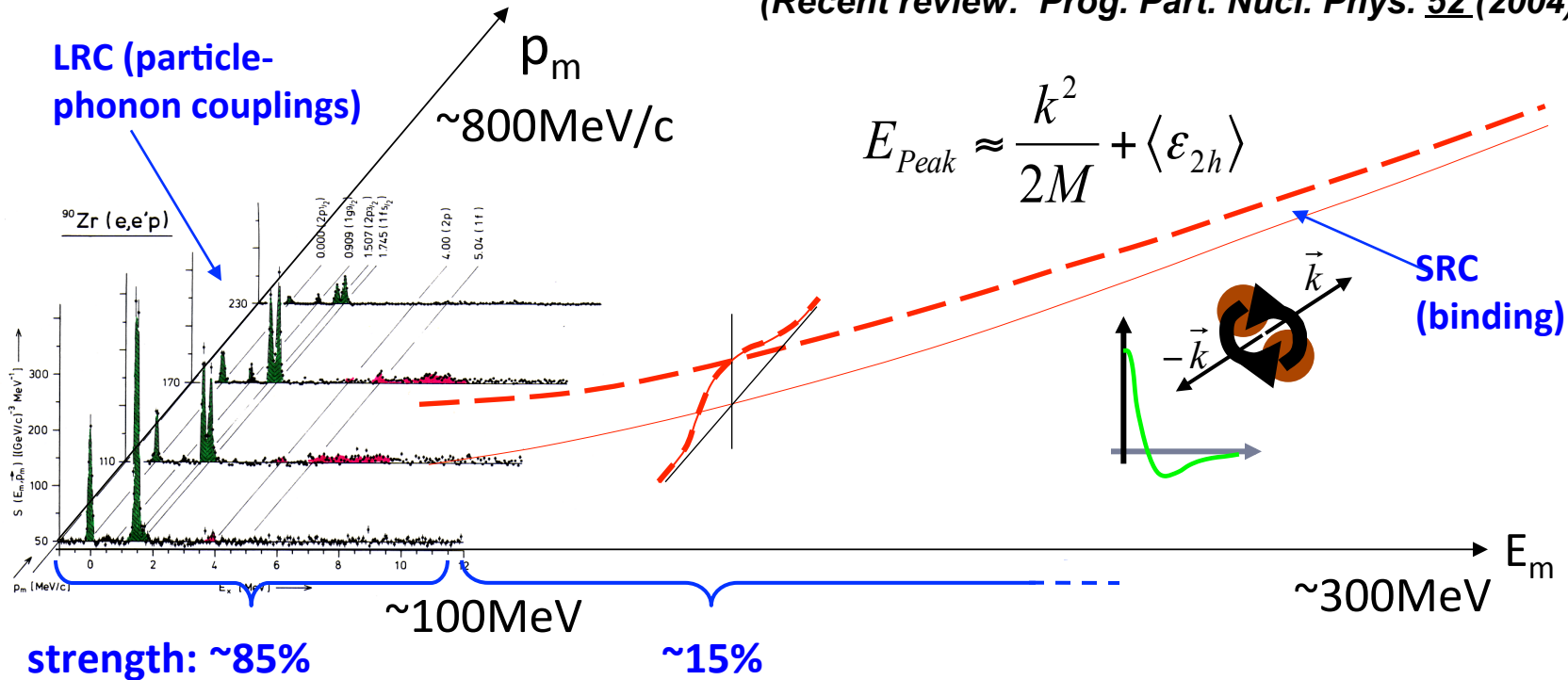
$$S_{12} = 3(\vec{\sigma}_1 \cdot \hat{r})(\vec{\sigma}_2 \cdot \hat{r}) - 1$$

\rightarrow interaction among 2 dipoles!!!!!!



Distribution of (All) the Nuclear Strength

(Recent review: *Prog. Part. Nucl. Phys.* **52** (2004) 337.)



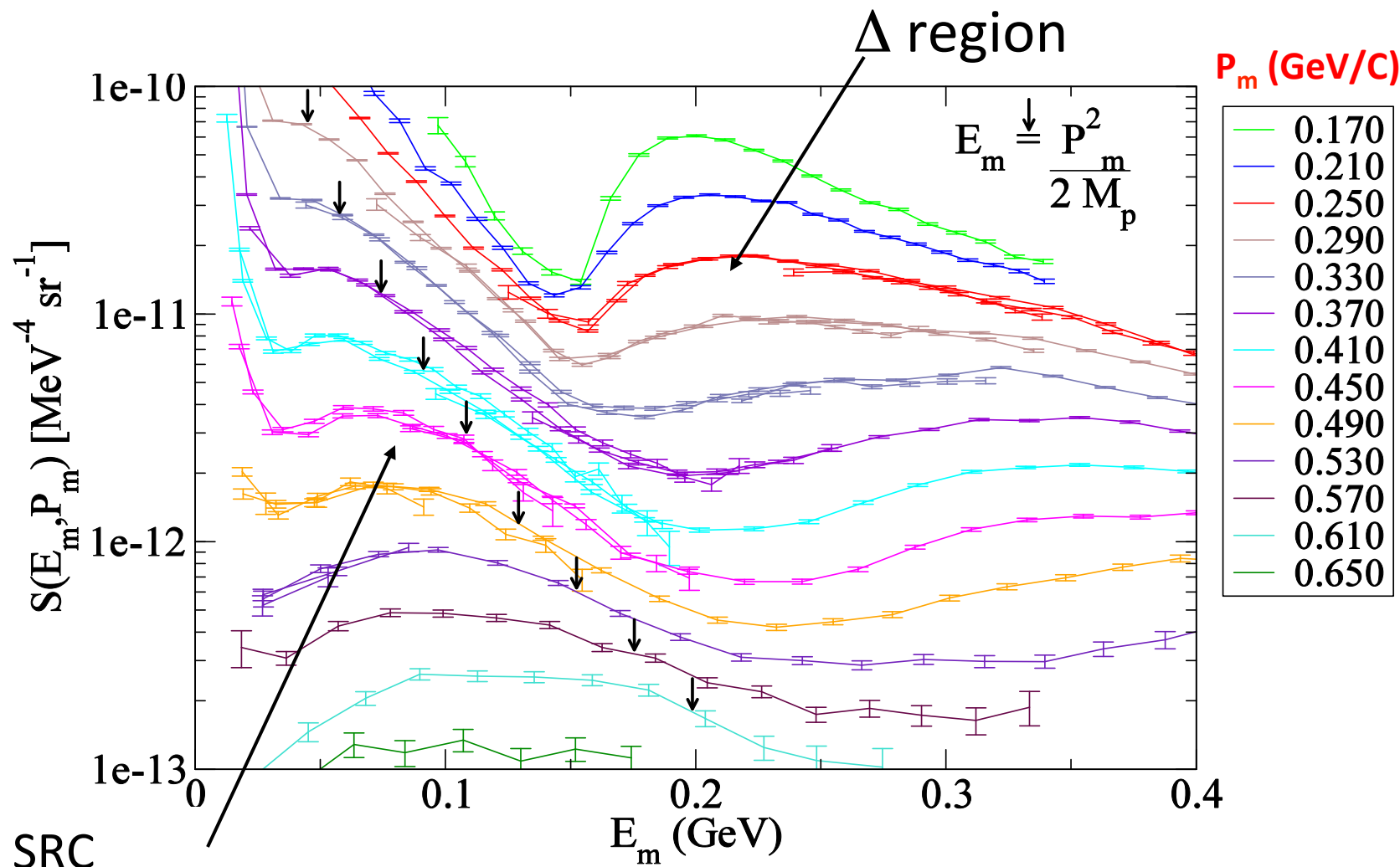
strength: ~85%

~15%

Interest in short range correlations:

- a fraction of the total number of nucleons:
 - ~10% in light nuclei (VMC, FHNC, Green's function)
 - 15-20% in heavy systems (CBF, Green's function)
- can explain up to **2/3 of the binding energy** [see ex. PRC51, 3040 ('95) for ^{16}O]
- influence NM saturation properties [see ex. PRL90, 152501 ('03)]

Spectral strength of ^{12}C from exp. E97-006



SRC
correlations

D.Rohe, et. al, Eur. Phys. J. A17, 349 (2003),
Phys Rev. Lett. 93 182501 (2004).

Theory vs. measured strength - I

- About 0.6 protons are found in the correlated region:

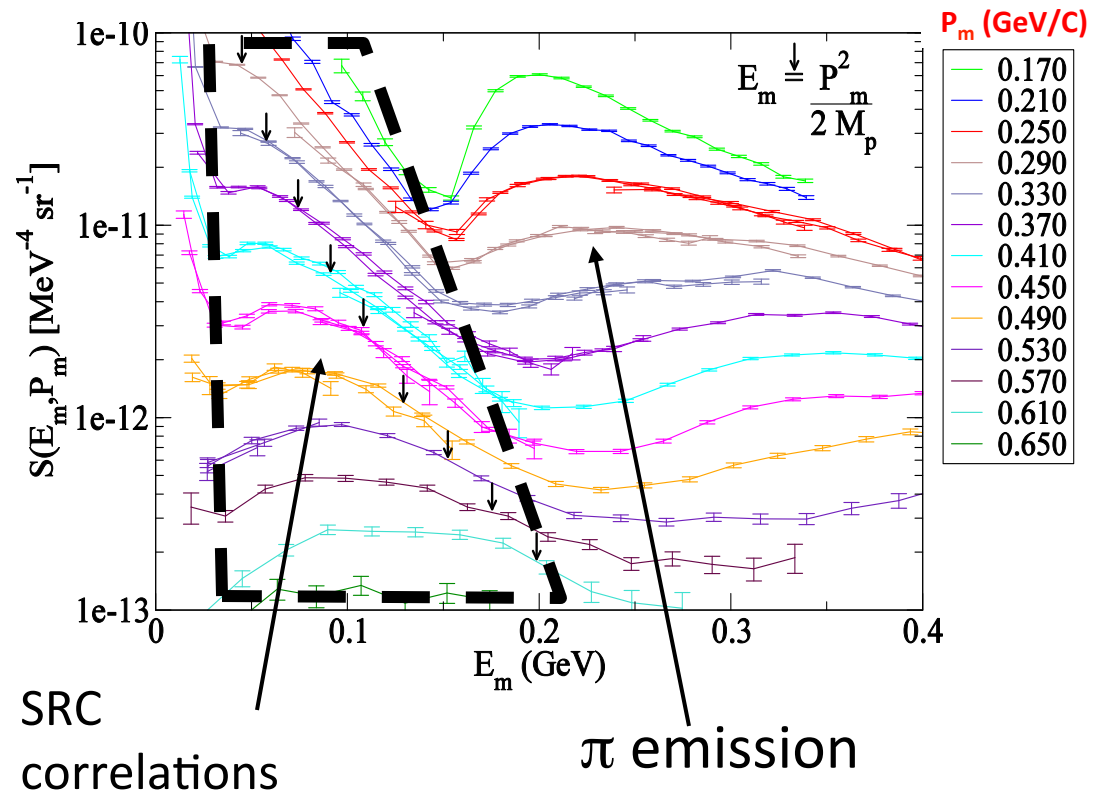
TABLE I. Correlated strength, integrated over shaded area of Fig. 2 (quoted in terms of the number of protons in ^{12}C .)

Experiment	0.61 ± 0.06
Greens Function Theory [28]	0.46
CBF Theory [3]	0.64

D.Rohe, et. Al,
Eur. Phys. J.
A17, 349 (2003)
PRL93 182501 (2004)

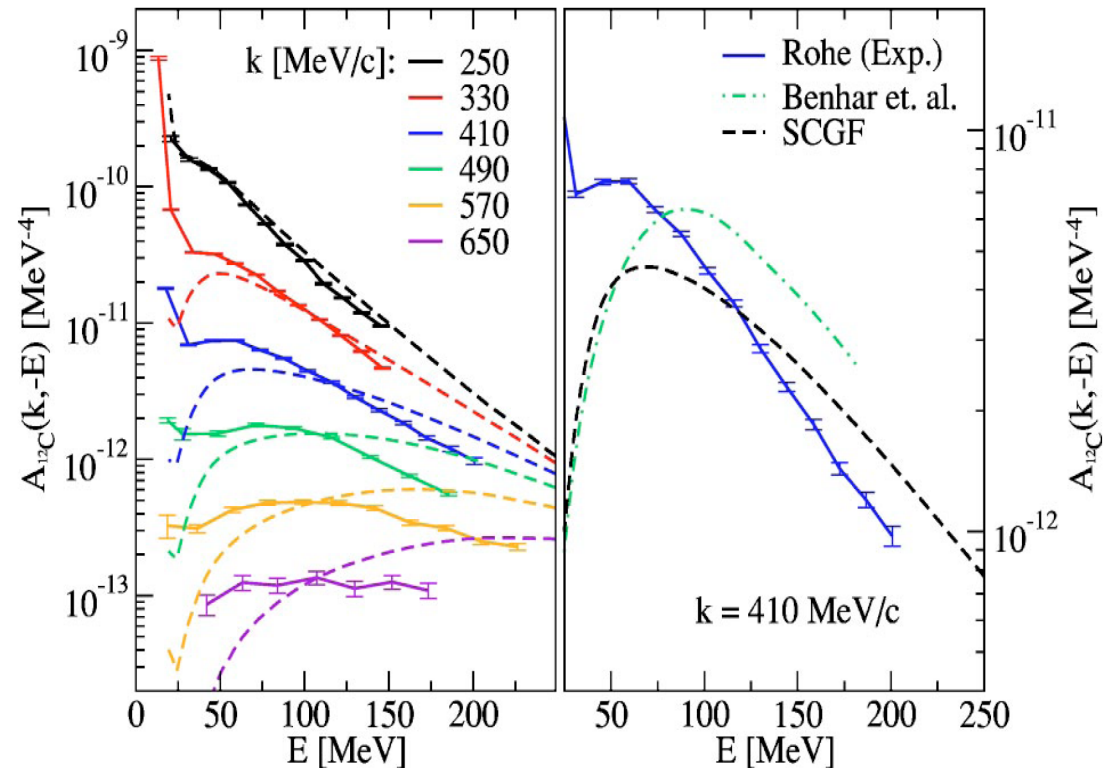
→ in good agreement with early theoretical predictions!

- what about the position of the peak?



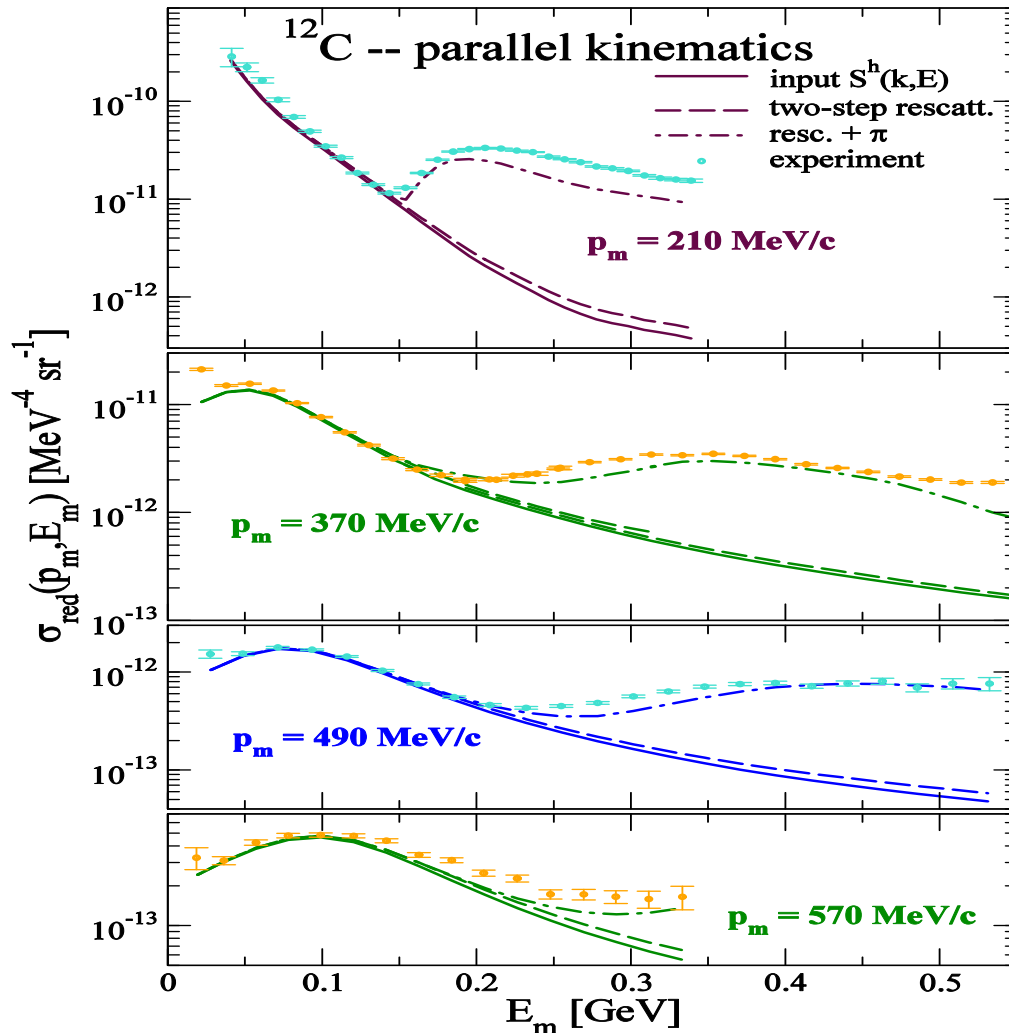
Theory vs. measured strength - II

- Theory reproduces the total amount of correlated strength and its shape
- The exact position of the correlated peak depends on the particular many-body approach and (NN interaction?) used.



Phys. Rev. C70, 0243909 (2004)

Comparison to Experiment in Parallel Kinematics – ^{12}C



Pion production
at very high
missing energies

$Q^2 = 0.4 (\text{GeV}/c)^2$
 beam: 3.3 GeV
 $p_f = 1 - 2 \text{ GeV}$

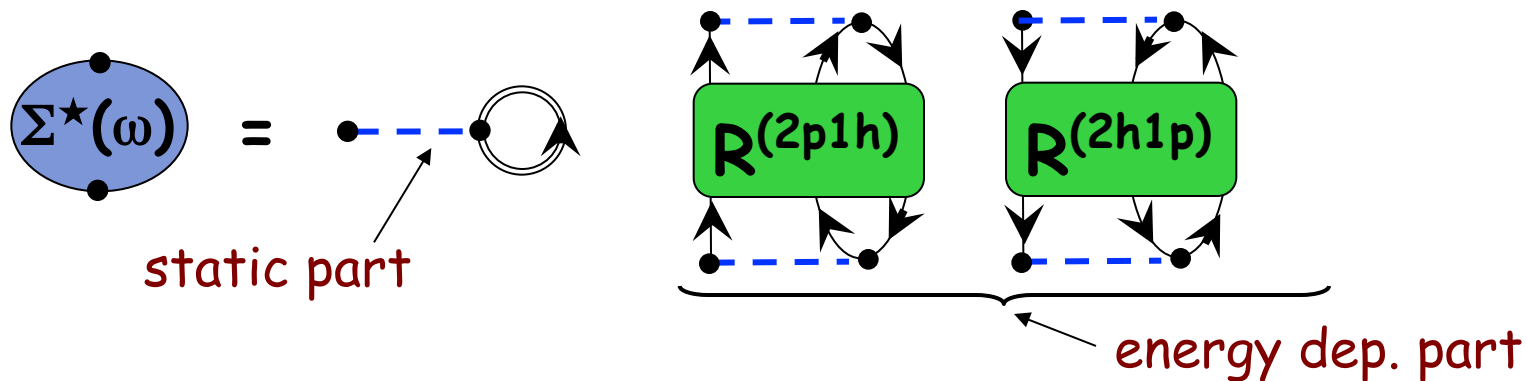
CB et. al. Phys. Lett. B608 47 (2005)

Using the G -matrix for renormalizing SRC

- Strong short-range cores require “renormalizing” the interaction:
 - G -matrix, SRG, Lee Suzuki, Bloch-Horowitz, ...
- Long-range correlations \rightarrow *FRPA/ADC(3)!!*

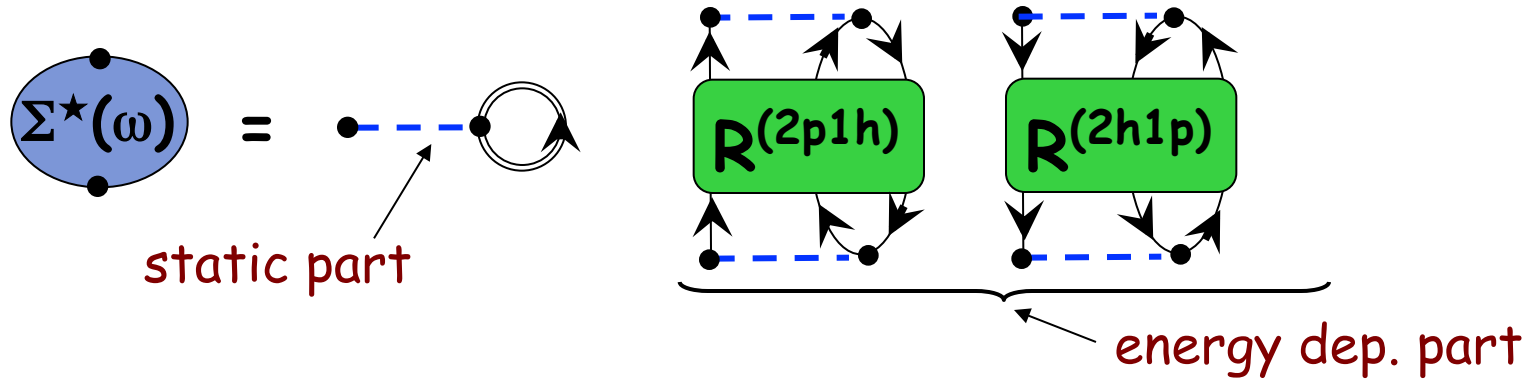
Treating short-range correlations directly...

- Non perturbative expansion of the self-energy:



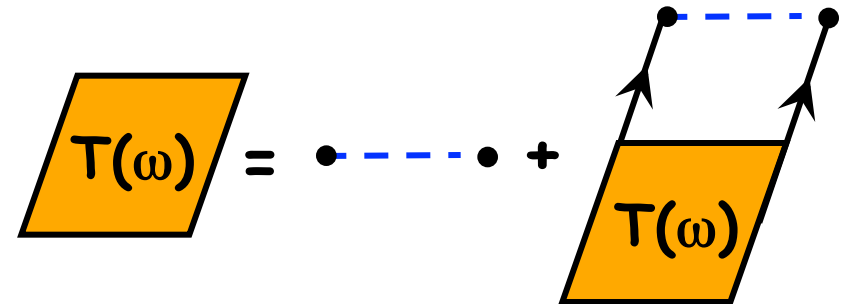
Treating short-range correlations directly...

- Non perturbative expansion of the self-energy:



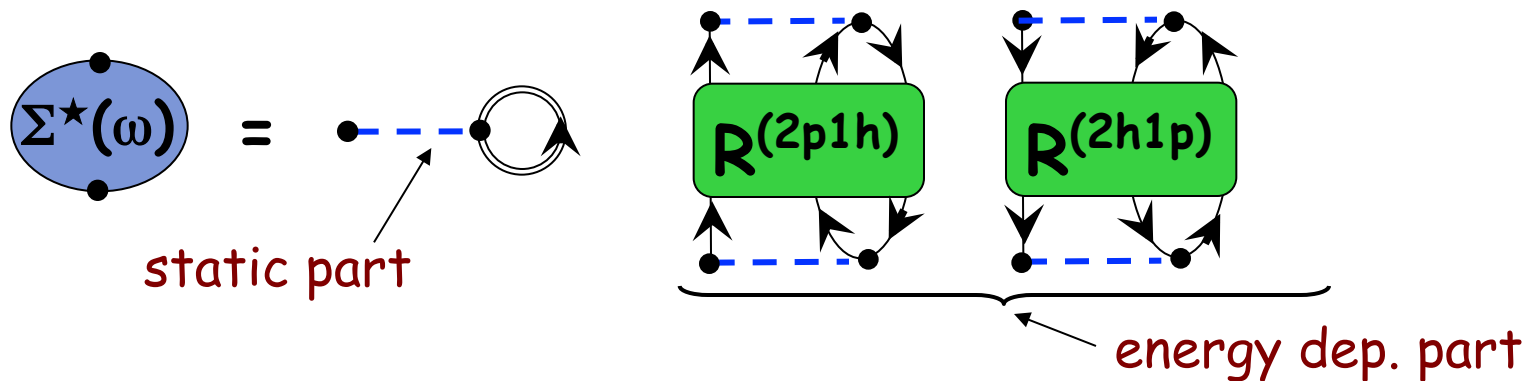
- 2 nucleons in free space: \rightarrow solve for the scatt. matrix...

$$T(\omega) = V + V \frac{1}{\omega - (k_a^2 + k_b^2)/2m + i\eta} T(\omega)$$



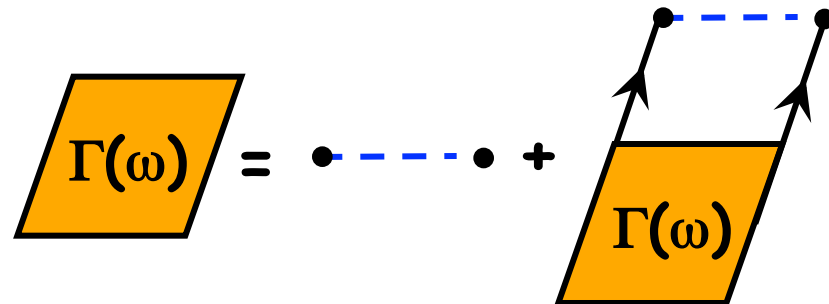
Treating short-range correlations directly...

- Non perturbative expansion of the self-energy:



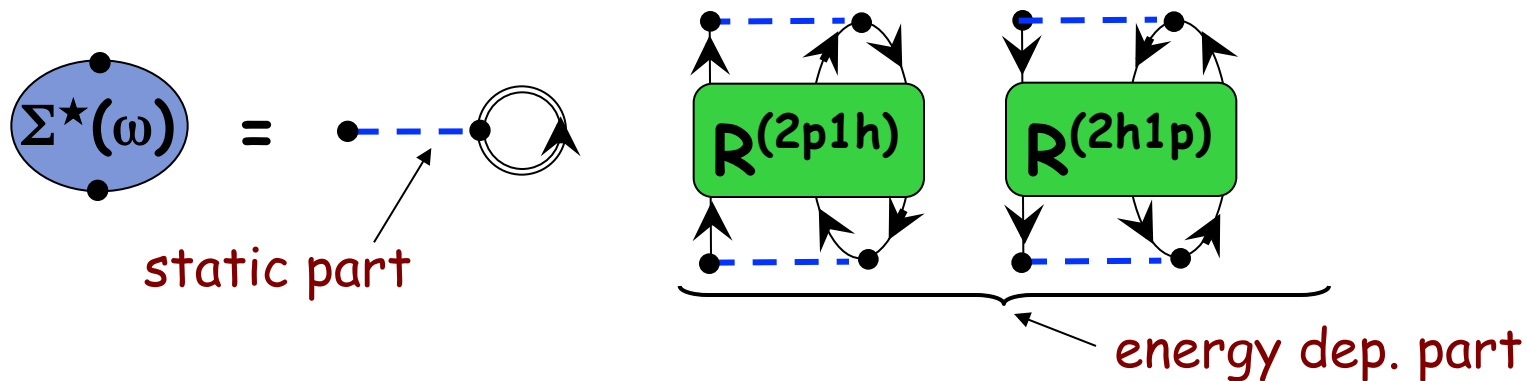
- 2 nucleons in medium: \rightarrow resum pp ladders...

$$\Gamma(\omega) \approx V + V \frac{[1 - n(k_a)][1 - n(k_b)]}{\omega - (k_a^2 + k_b^2)/2m + i\eta} \Gamma(\omega)$$

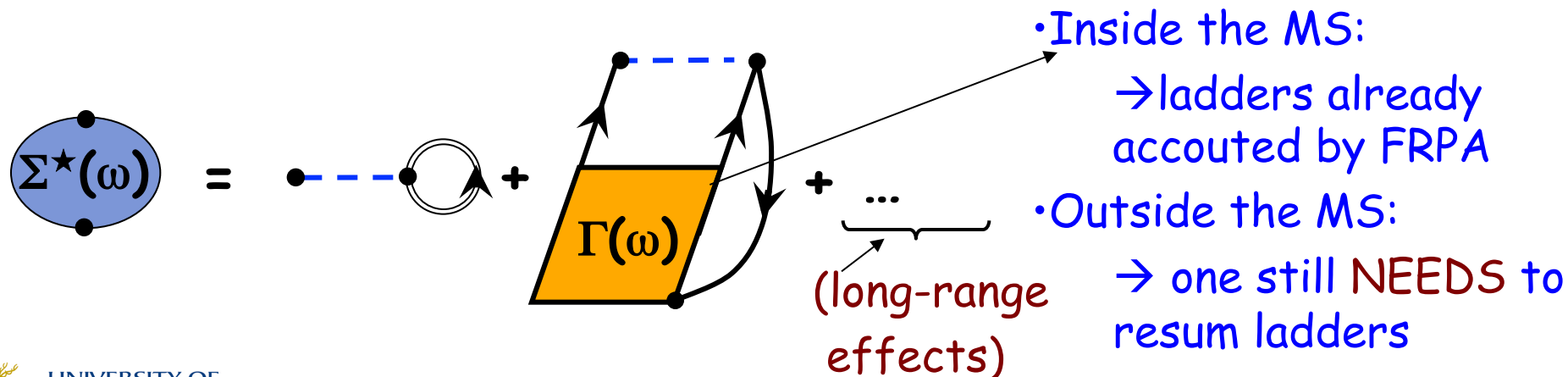


Treating short-range correlations directly...

- Non-perturbative expansion of the self-energy:



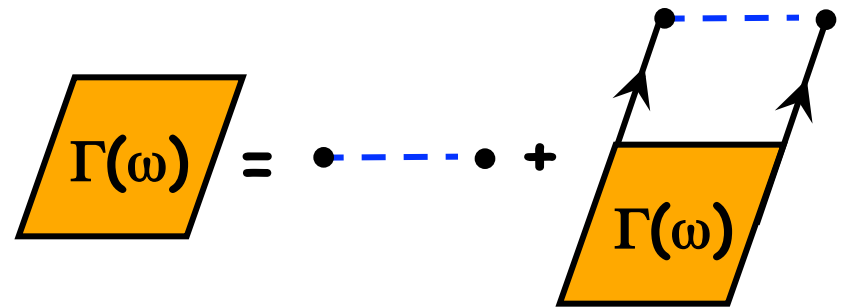
- Identify the pp resummations (which account for short range correlations) in the expansion of $R(\omega)$:



Treating short-range corr. with a G-matrix

- The short-range core can be treated by resumming ladders outside the model space:

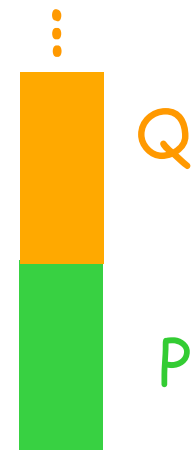
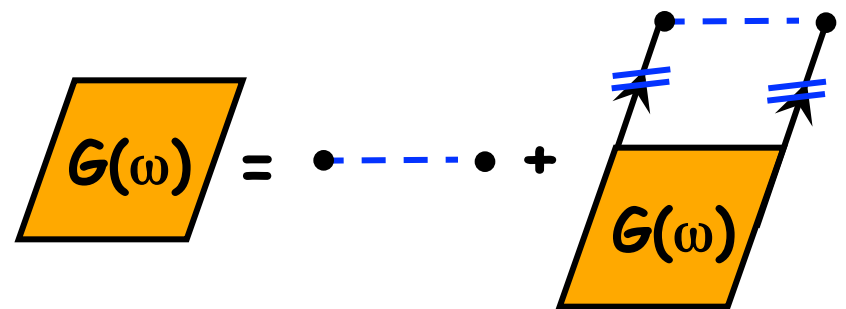
$$\Gamma(\omega) \approx V + V \frac{[1-n(k_a)][1-n(k_b)]}{\omega - (k_a^2 + k_b^2)/2m + i\eta} \Gamma(\omega)$$



Treating short-range corr. with a G-matrix

- The short-range core can be treated by resumming ladders outside the model space:

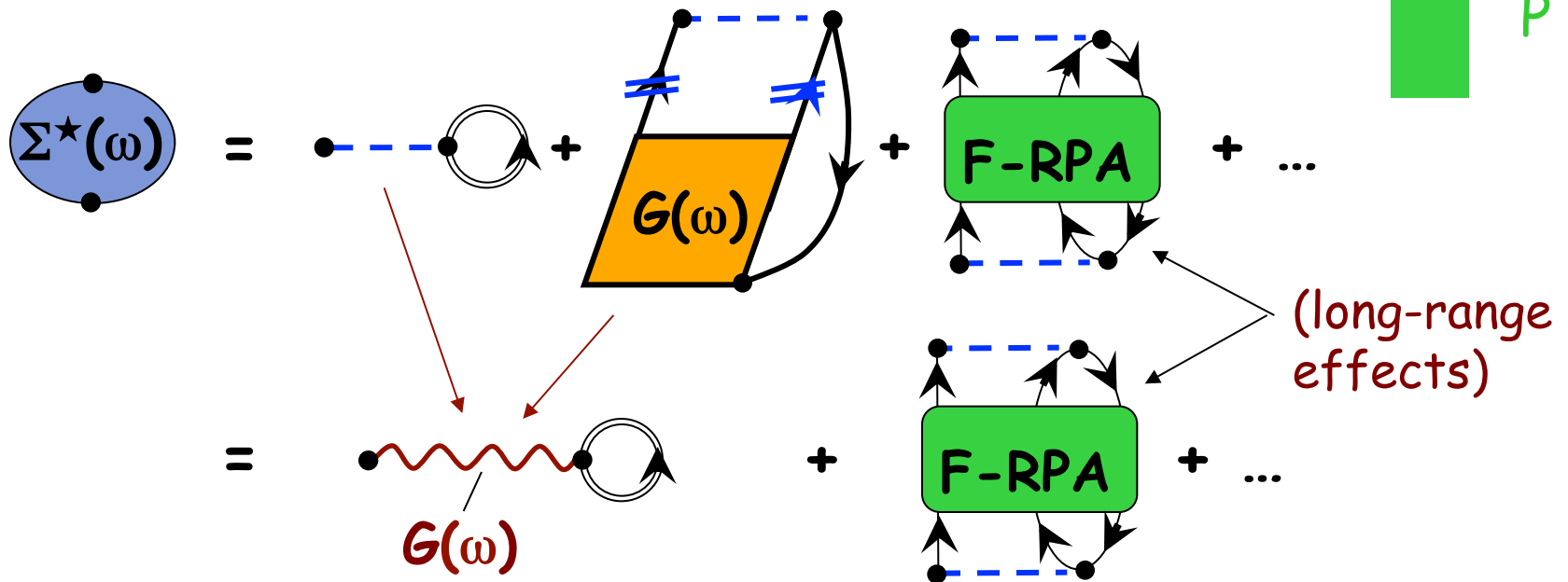
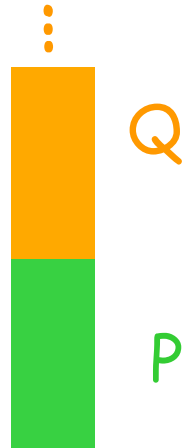
$$G(\omega) = V + V \frac{\hat{Q}}{\omega - (k_a^2 + k_b^2)/2m + i\eta} G(\omega)$$



Treating short-range corr. with a G-matrix

- The short-range core can be treated by summing ladders outside the model space:

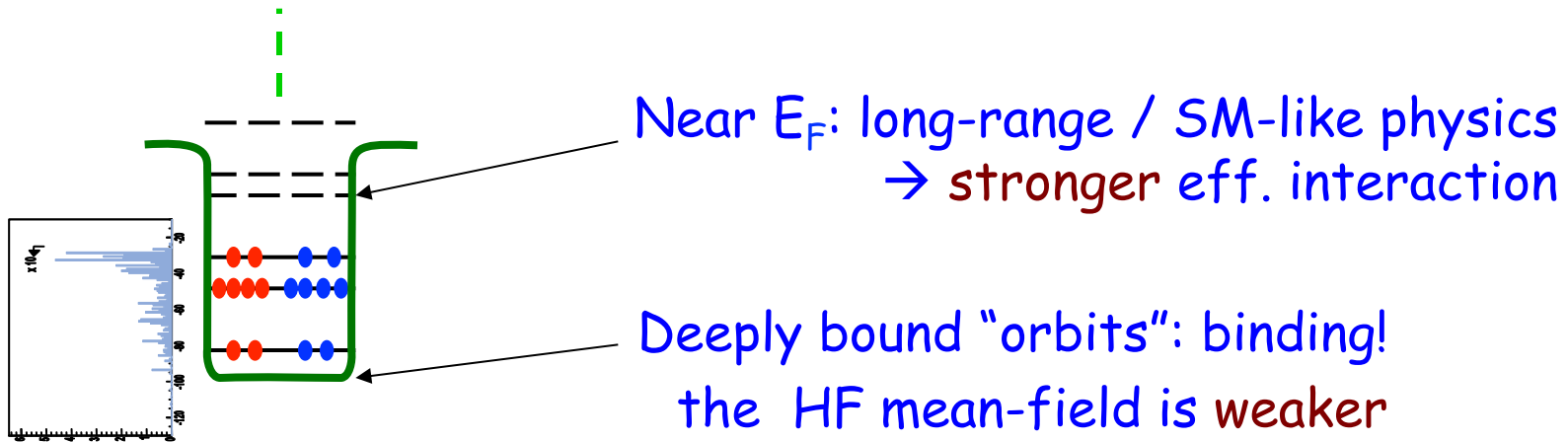
$$G(\omega) = V + V \frac{\hat{Q}}{\omega - (k_a^2 + k_b^2)/2m + i\eta} G(\omega)$$



Treating short-range corr. with a G -matrix

- The short-range core can be treated by summing ladders outside the model space:

$$\Sigma_{\alpha\beta}^{\text{BHF}}(\omega) = i \sum_{\gamma\delta} \int \frac{d\omega'}{2\pi} G_{\alpha\gamma, \delta\beta}(\omega + \omega') g_{\delta\gamma}(\omega') = \text{Diagram}$$



\rightarrow It is **NOT** optimal to fix the starting energy in $G(\omega)$ at the HF/mean field level !!

Treating short-range corr. with a G-matrix

- The short-range core can be treated by summing ladders outside the model space:

$$\Sigma_{\alpha\beta}^{MF}(\omega) = i \sum_{\gamma\delta} \int \frac{d\omega'}{2\pi} G_{\alpha\gamma, \delta\beta}(\omega + \omega') g_{\delta\gamma}(\omega') = \text{Diagram}$$

The diagram shows a red wavy line labeled $G(\omega)$ connecting two black dots. The right dot is part of a self-energy loop diagram with two arrows.

$$\Sigma^*(\mathbf{r}, \mathbf{r}'; \omega) = \Sigma^{MF}(\mathbf{r}, \mathbf{r}'; \omega) + \tilde{\Sigma}(\mathbf{r}, \mathbf{r}'; \omega).$$

$$Z_\alpha = \int d\mathbf{r} |\psi_\alpha^{A\pm 1}(\mathbf{r})|^2 = \frac{1}{1 - \frac{\partial \Sigma_{\hat{a}\hat{a}}^*(\omega)}{\partial \omega}} \Bigg|_{\omega = \pm(E_\alpha^{A\pm 1} - E_0^A)}$$

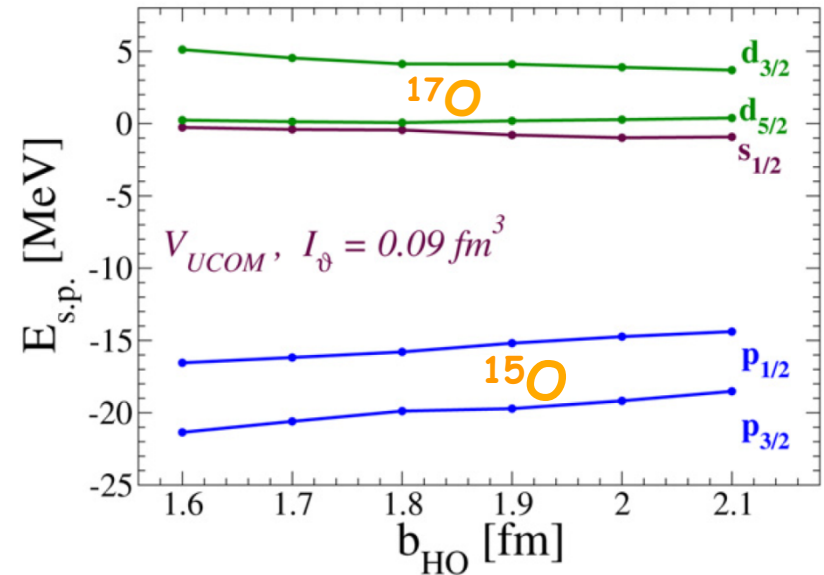
Two contributions to the derivative:

- $\Sigma_{\alpha\beta}^{MF}(\omega)$ is due to scattering to (high-k) states in the Q space
- $\Sigma(\mathbf{r}, \mathbf{r}'; \omega)$ accounts for low-energy (long range) correlations

G-matrix based applications

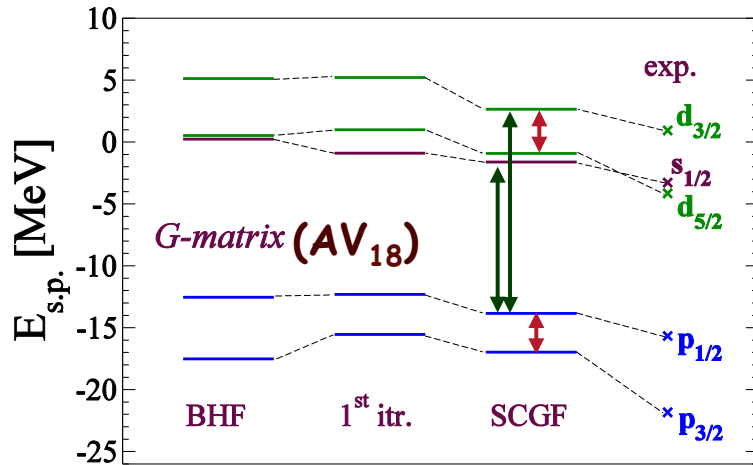
Some details of calculations

- ^{16}O →
- 8 major oscillator shells (see also R. Roth's talk)
 - G -matrix derived from Argonne v18
 - Full self-consistency
- [CB, Phys. Lett. B643, 268 (2006)]



- $^{48}\text{Ca}, ^{56}\text{Ni},$
etc... →
- Up to 10 major oscillator shells
 - G -matrix derived from N3LO + Coulomb
 - *Monopole correction* to mock 3NF
 - Partial self-consistency only for the mean-field

Single neutron levels around ^{16}O with FRPA



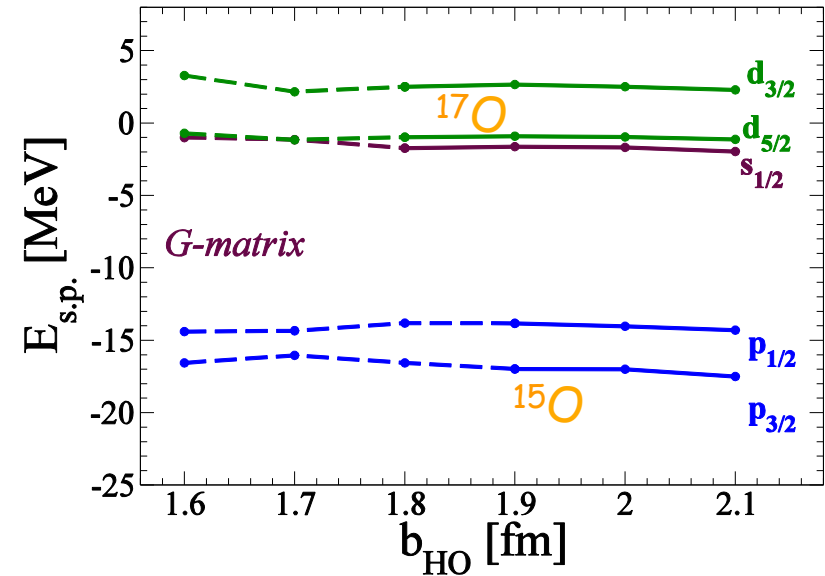
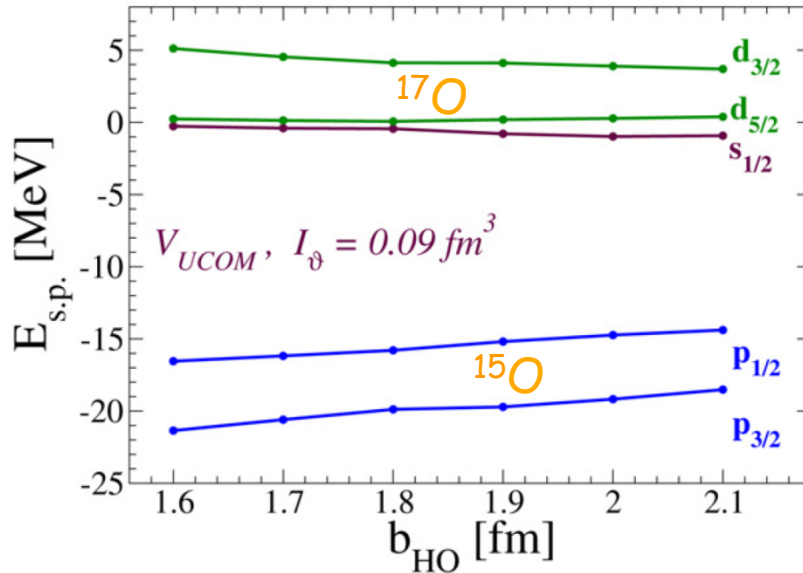
[CB, Phys. Lett. B643, 268 (2006)]

	V_{UCOM}	Argonne v18 (G -matrix)	Exp.[MeV]
spin-orbit:			
$E_{d_{3/2}} - E_{d_{5/2}}$	3.9	3.5	5.08
$E_{p_{1/2}} - E_{p_{3/2}}$	4.5	3.1	6.18
p-h gap:			
$E_{d_{3/2}} - E_{p_{1/2}}$	19.3	16.5	16.6
$E_{s_{1/2}} - E_{p_{1/2}}$	14.6	12.2	12.4
$E_{d_{5/2}} - E_{p_{1/2}}$	15.4	13.0	11.5

- particle-hole gap accurate with a G -matrix with w -dependence
- $p_{3/2} - p_{1/2}$ spin-orbit splitting agrees with $\approx 3.4\text{MeV}$ from variational Monte Carlo (VMC) [S. Pieper et al. Phys. Rev. Lett. 70 ('93) 2541, using AV_{14}]

Single neutron levels around ^{16}O with FRPA

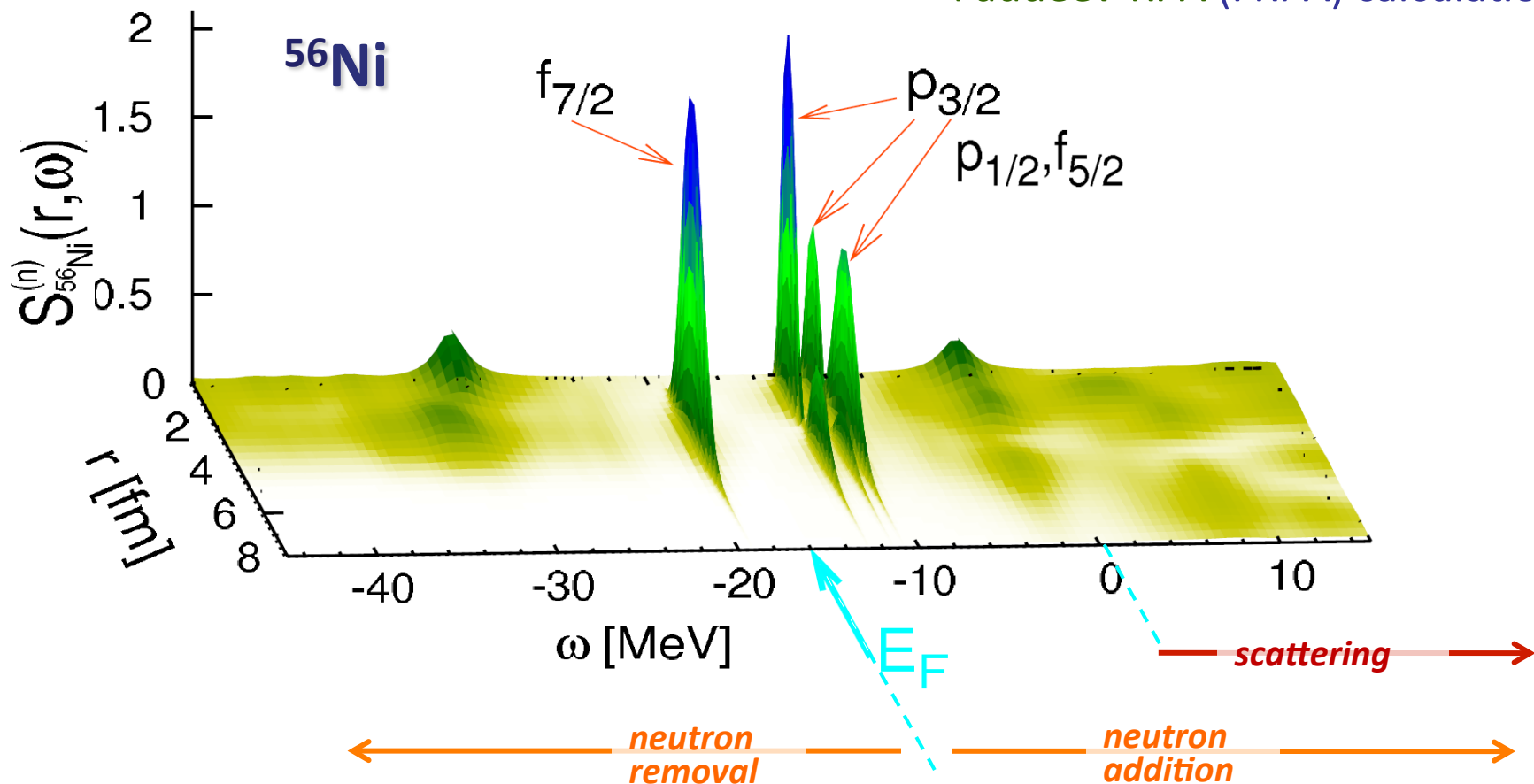
[CB, Phys. Lett. B643, 268 (2006)]



- particle-hole gap accurate with a G -matrix with w -dependence
- $p_{3/2}$ - $p_{1/2}$ spin-orbit splitting agrees with $\approx 3.4 \text{ MeV}$ from variational Monte Carlo (VMC) [S. Pieper et al. Phys. Rev. Lett. 70 ('93) 2541, using AV_{14}]

Spectral Function of ^{56}Ni

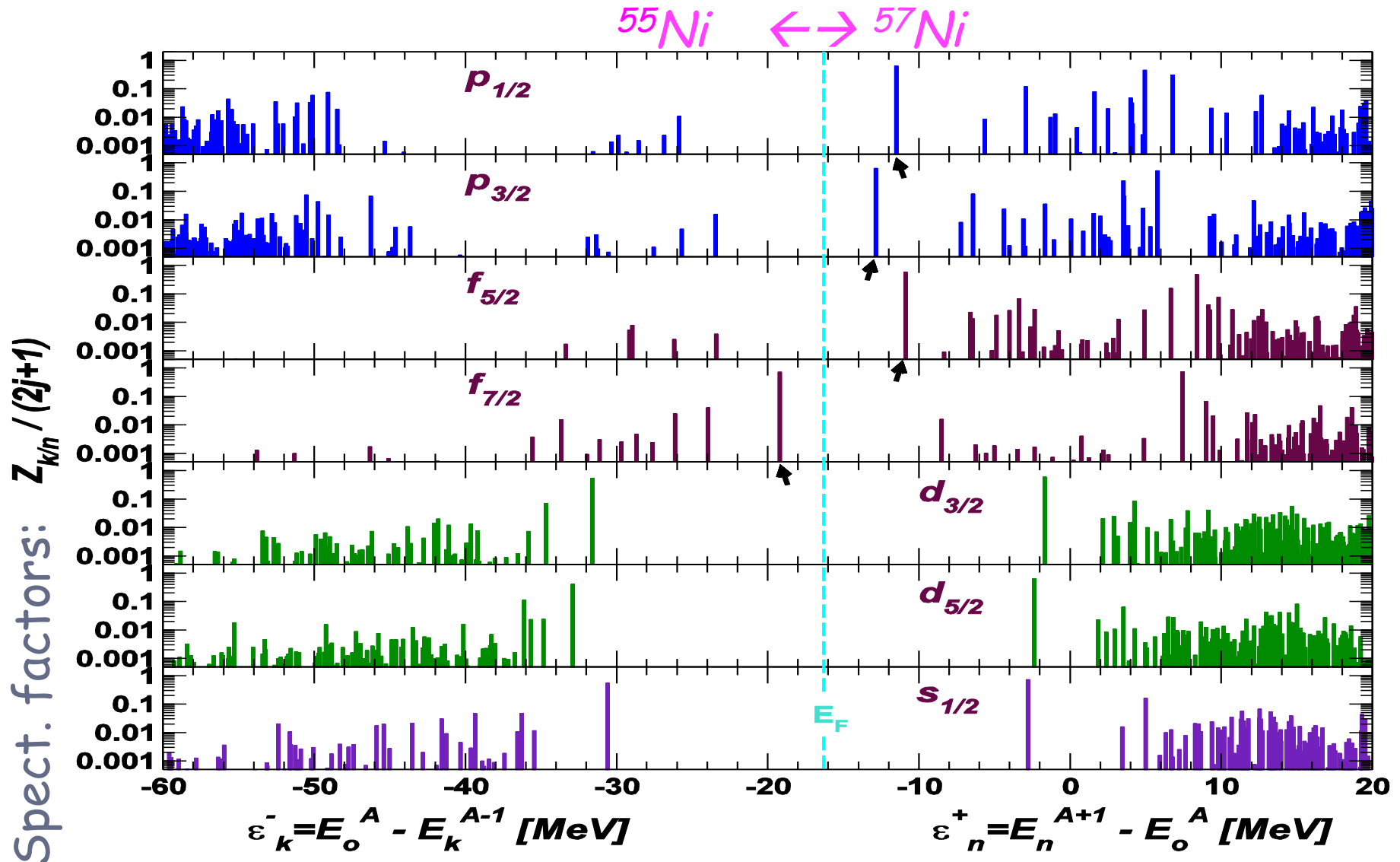
Faddeev-RPA (FRPA) calculations



[CB, M.Hjorth-Jensen, Pys. Rev. **C79**, 064313 (2009)]

CB, Phys. Rev. Lett. **103**, 202502 (2009)]

Neutron spectral distribution of ^{56}Ni



Spectroscopic Factors

Quenching of absolute spectroscopic factors

[CB, Phys. Rev. Lett. **103**, 202520 (2009)]

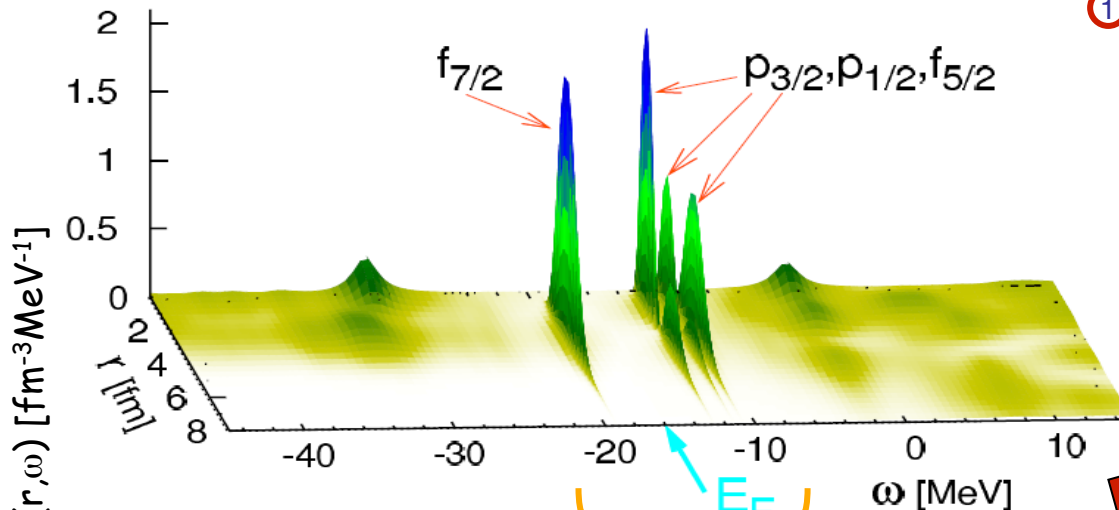
...with analogous conclusions for ^{48}Ca

Overall quenching of *spectroscopic factors* is driven by:

- SRC* → ~10%
- part-vibr. coupling* → dominant
- "shell-model"* → in open shell

	10 osc. shells		Exp. [30]	1p0f space		
	FRPA (SRC)	full FRPA		FRPA SM	ΔZ_α	

^{57}Ni	$\nu 1p_{1/2}$	0.96	0.63	0.61		0.79	0.77	-0.02
	$\nu 0f_{5/2}$	0.95	0.59	0.55		0.79	0.75	-0.04
	$\nu 1p_{3/2}$	0.95	0.65	0.62	0.58(11)	0.82	0.79	-0.03
^{55}Ni	$\nu 0f_{7/2}$	0.95	0.72	0.69		0.89	0.86	-0.03



$$Z_\alpha = \int d^3r |\psi_\alpha^{overlap}(\mathbf{r})|^2 = \frac{1}{1 - \left. \frac{\partial \Sigma_{\hat{\alpha}\hat{\alpha}}(\omega)}{\partial \omega} \right|_{\omega=\epsilon_\alpha}}$$

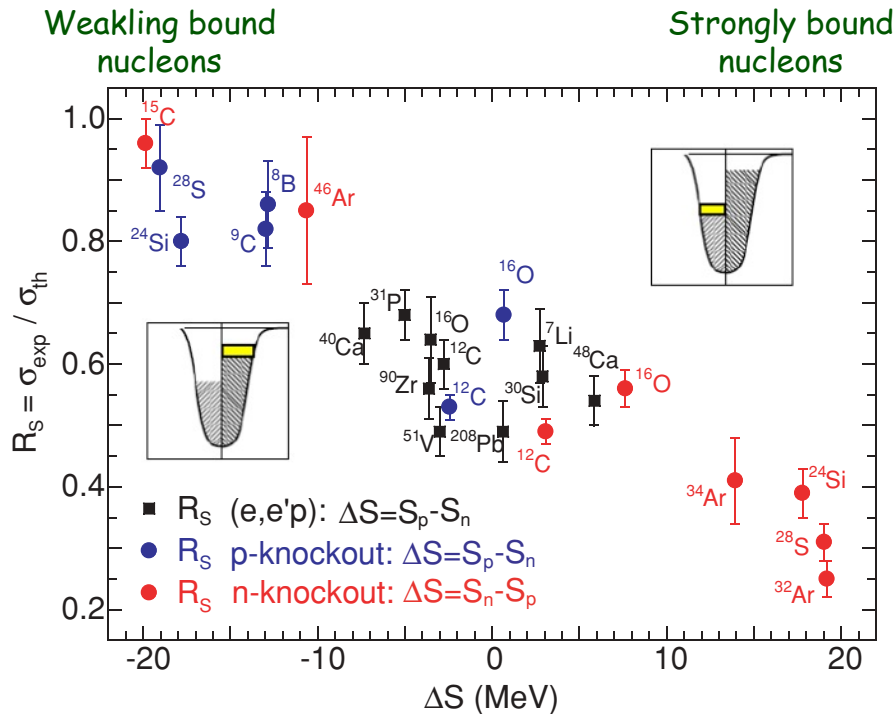
① SHORT RANGE CORRELATIONS

② PARTICLE-VIBRATION COUPLING

③ SHELL MODEL

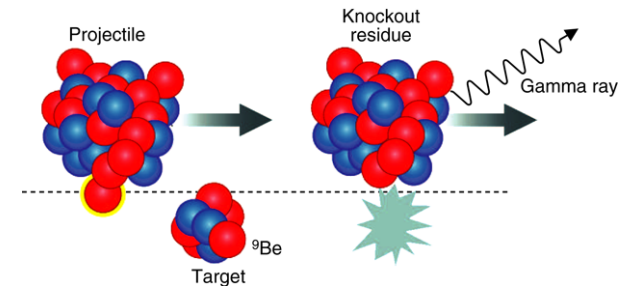
^{56}Ni
NN-N3LO(500)

Spectroscopic factors @ limits of stability



[Phys. Rev. C77, 044306 (2008)]

High energy knock-out in inverse kinematics



? ORIGIN ?
UNCLEAR
?

- Challenged by recent experiments

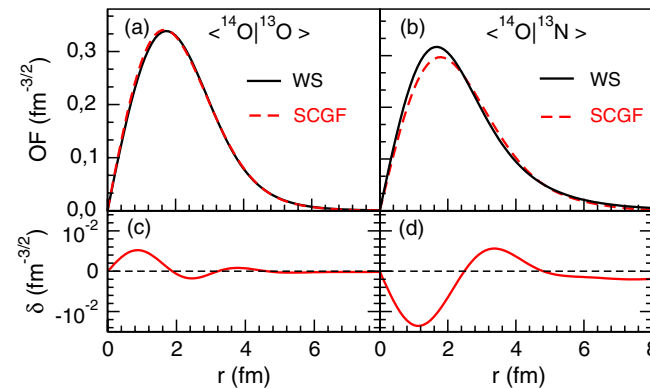
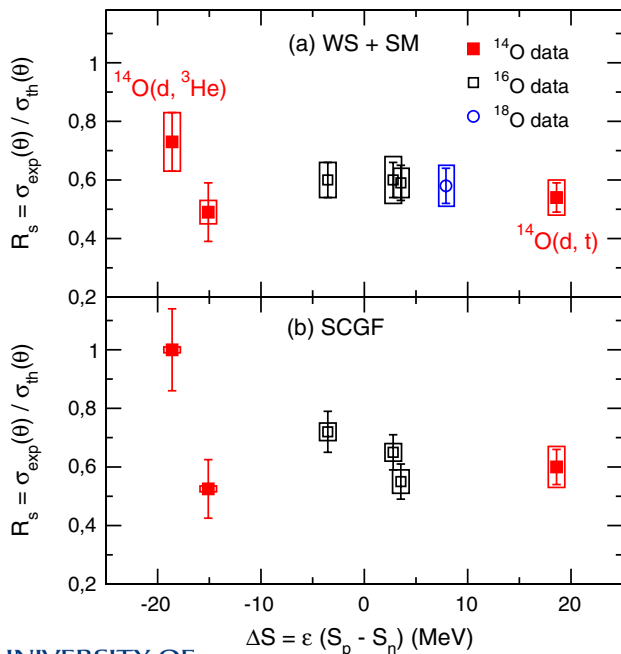
- May be correlations or scattering analysis

Single nucleon transfer in the oxygen chain

[F. Flavigny et al, PRL110, 122503 (2013)]

→ Analysis of $^{14}\text{O}(d,t)^{13}\text{O}$ and $^{14}\text{O}(d,^3\text{He})^{13}\text{N}$ transfer reactions @ SPIRAL

Reaction	E^* (MeV)	J^π	$R_{\text{rms}}^{\text{HFB}}$ (fm)	r_0 (fm)	C^2S_{exp} (WS)	C^2S_{th} $0p + 2\hbar\omega$	R_s (WS)	C^2S_{exp} (SCGF)	C^2S_{th} (SCGF)	R_s (SCGF)
$^{14}\text{O}(d,t)^{13}\text{O}$	0.00	$3/2^-$	2.69	1.40	1.69 (17)(20)	3.15	0.54(5)(6)	1.89(19)(22)	3.17	0.60(6)(7)
$^{14}\text{O}(d,^3\text{He})^{13}\text{N}$	0.00	$1/2^-$	3.03	1.23	1.14(16)(15)	1.55	0.73(10)(10)	1.58(22)(2)	1.58	1.00(14)(1)
	3.50	$3/2^-$	2.77	1.12	0.94(19)(7)	1.90	0.49(10)(4)	1.00(20)(1)	1.90	0.53(10)(1)
$^{16}\text{O}(d,t)^{15}\text{O}$	0.00	$1/2^-$	2.91	1.46	0.91(9)(8)	1.54	0.59(6)(5)	0.96(10)(7)	1.73	0.55(6)(4)
$^{16}\text{O}(d,^3\text{He})^{15}\text{N}$ [19,20]	0.00	$1/2^-$	2.95	1.46	0.93(9)(9)	1.54	0.60(6)(6)	1.25(12)(5)	1.74	0.72(7)(3)
	6.32	$3/2^-$	2.80	1.31	1.83(18)(24)	3.07	0.60(6)(8)	2.24(22)(10)	3.45	0.65(6)(3)
$^{18}\text{O}(d,^3\text{He})^{17}\text{N}$ [21]	0.00	$1/2^-$	2.91	1.46	0.92(9)(12)	1.58	0.58(6)(10)			

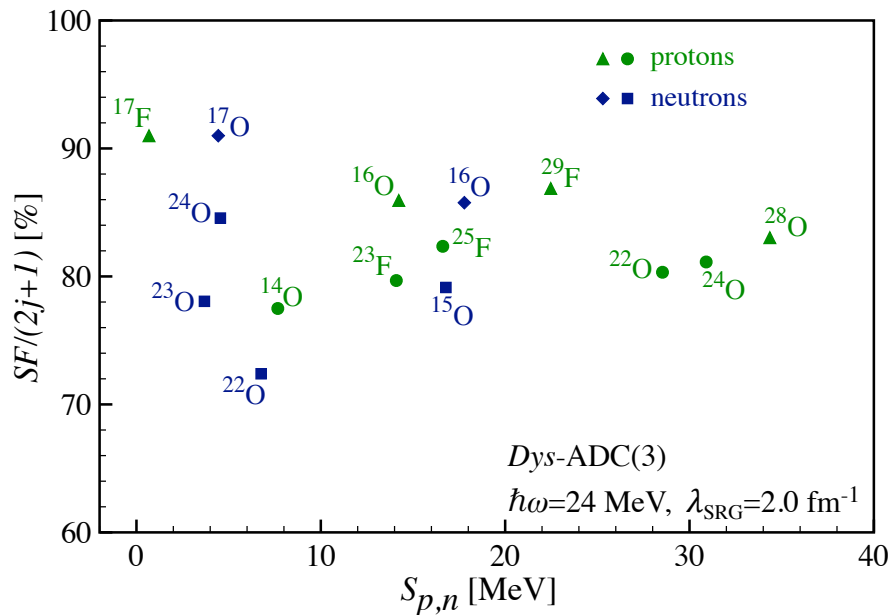


- Overlap functions and strengths from GF
- R_s independent of asymmetry

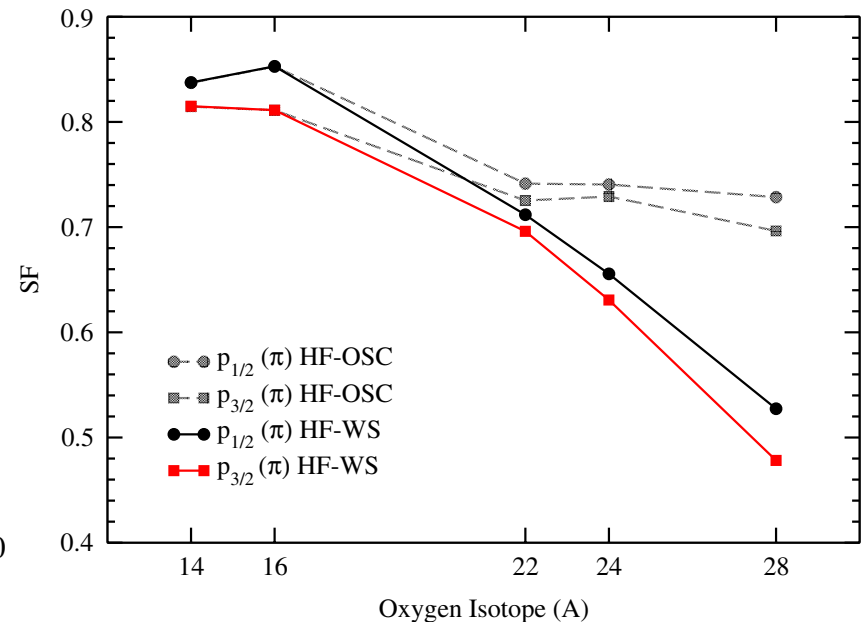
Z/N asymmetry dependence of SFs - Theory

Ab-initio calculations explain the Z/N dependence but the effect is much lower than observed

Effects of continuum become important at the driplines



[Cipollone, et al.
Phys. Rev. C92 014306 (2015)]

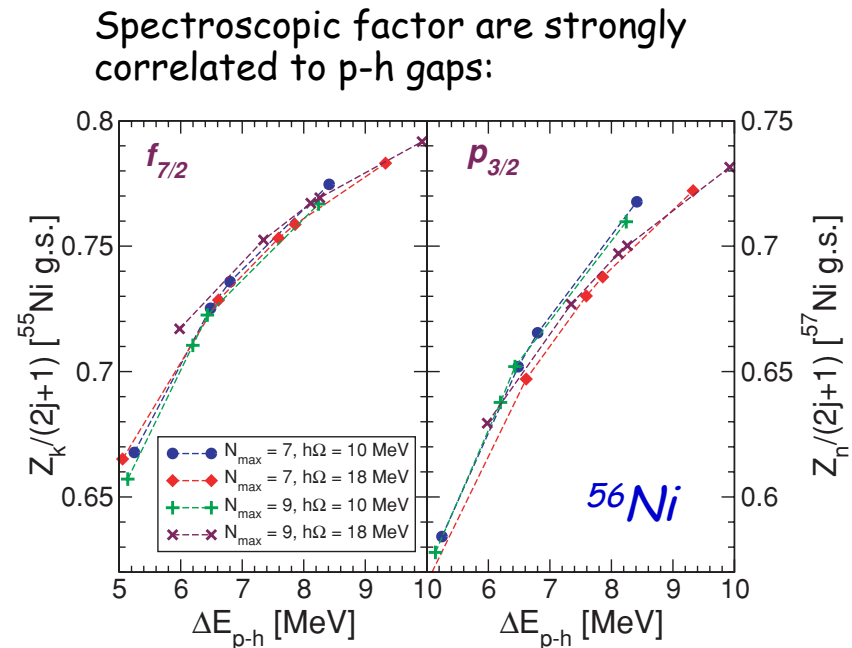
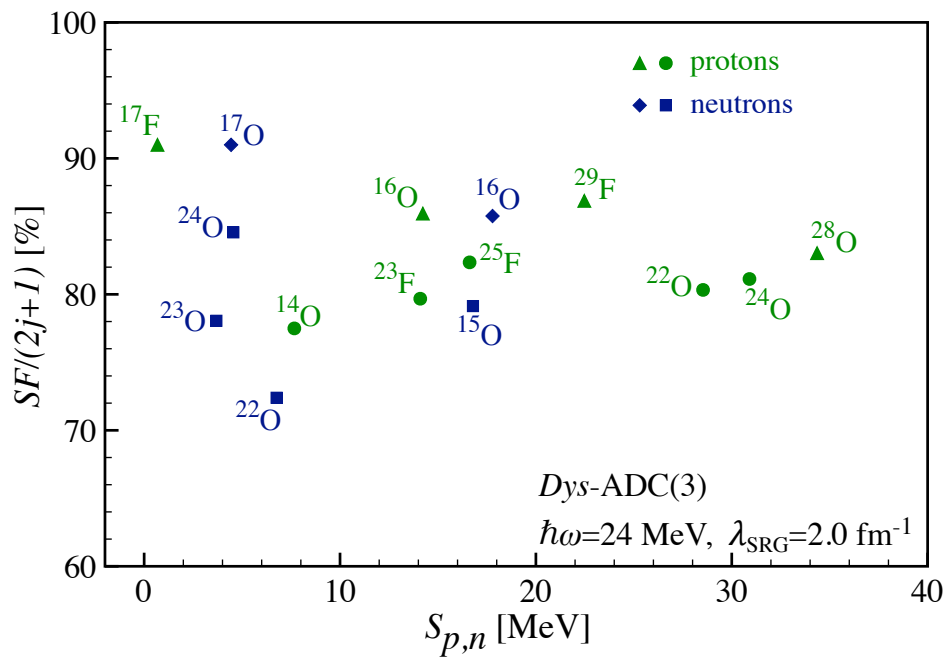


[Hagen et al.
Phys. Rev. Lett. 107, 032501 (2011)]

Z/N asymmetry dependence of SFs - Theory

Ab-initio calculations explain the Z/N dependence but the effect is much lower than suggested by direct knockout

Effects of continuum become important at the driplines



Knockout & transfer experiments

✱ Neutron removal from proton- and neutron- Ar isotopes @ NSCL:

Isotopes	lj^π	Sn(MeV)	ΔS (MeV)	(theo.)	(expt.)		(expt.)	
				SF(LB-SM)	SF(JLM + HF)	R_s (JLM + HF)	SF(CH89)	R_s (CH89)
^{34}Ar	$s1/2^+$	17.07	12.41	1.31	0.85 ± 0.09	0.65 ± 0.07	1.10 ± 0.11	0.84 ± 0.08
^{36}Ar	$d3/2^+$	15.25	6.75	2.10	1.60 ± 0.16	0.76 ± 0.08	2.29 ± 0.23	1.09 ± 0.11
^{46}Ar	$f7/2^-$	8.07	-10.03	5.16	3.93 ± 0.39	0.76 ± 0.08	5.29 ± 0.53	1.02 ± 0.10

[Lee *et al.* 2010]

	Sn (MeV)	ΔS (MeV)	SF
^{34}Ar	33.0	18.6	1.46
^{36}Ar	27.7	7.5	1.46
^{46}Ar	16.0	-22.3	5.88

$$\Delta S = S_n - S_p$$

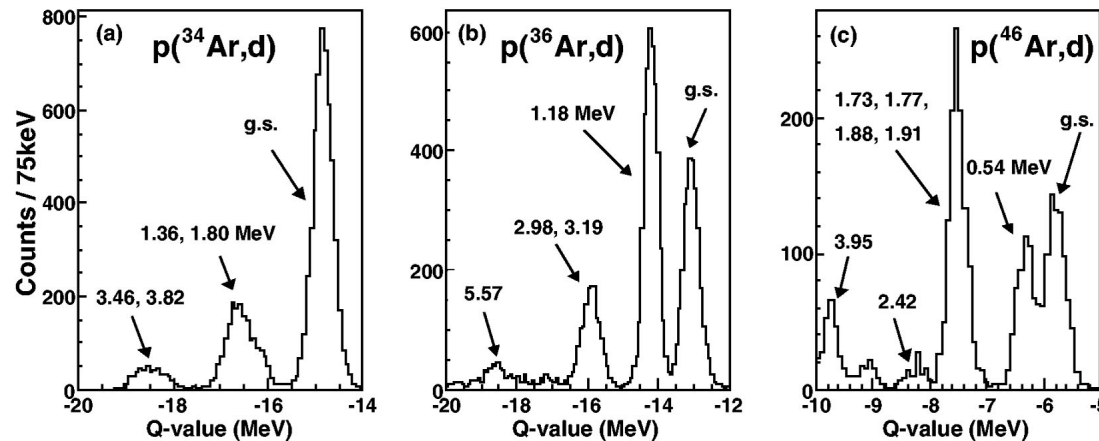
Gorkov GF NN

^{34}Ar	22.4	15.5	1.56
^{36}Ar	15.3	7.2	1.54
^{46}Ar	6.5	-15.7	6.64

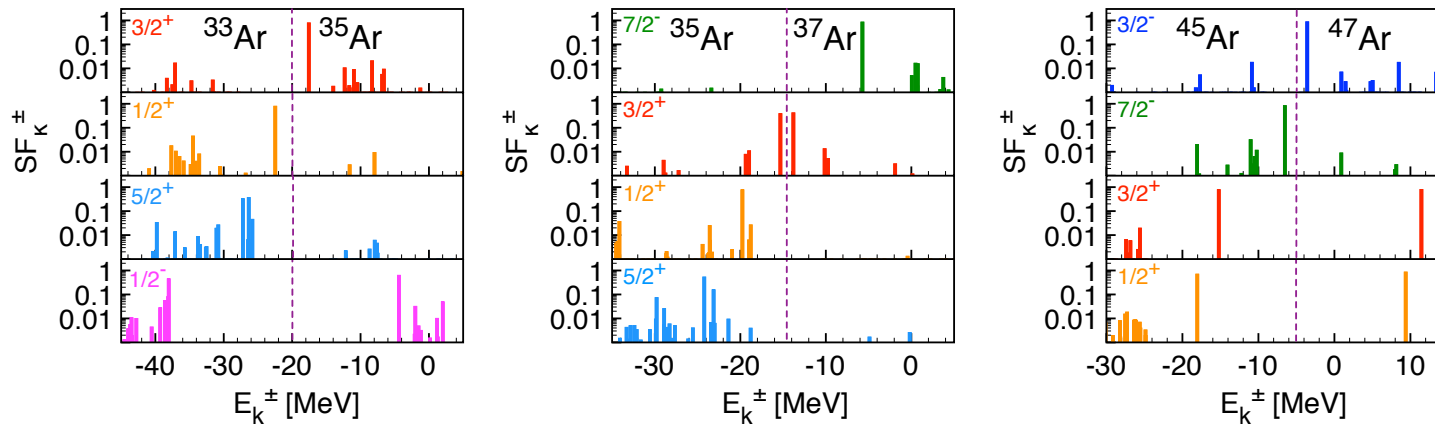
Gorkov GF NN + 3N

Knockout & transfer experiments

✱ Neutron removal from proton- and neutron- Ar isotopes @ NSCL:



[Lee *et al.* 2010]



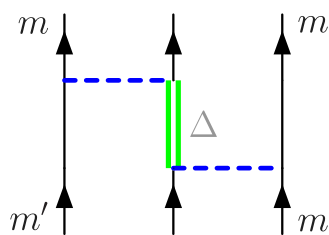


Adding 3-nucleon forces

What are three-body forces?

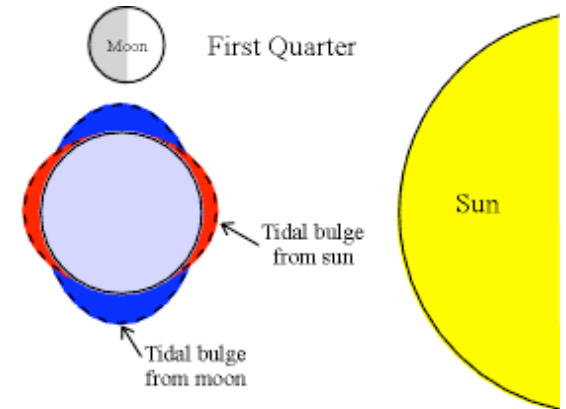
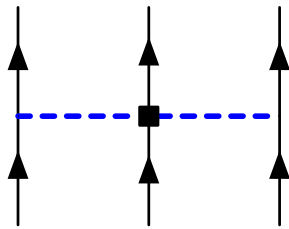
Nucleons are composite particle, they can be excited to resonances

- Main contributions is $\Delta(1232 \text{ MeV})$

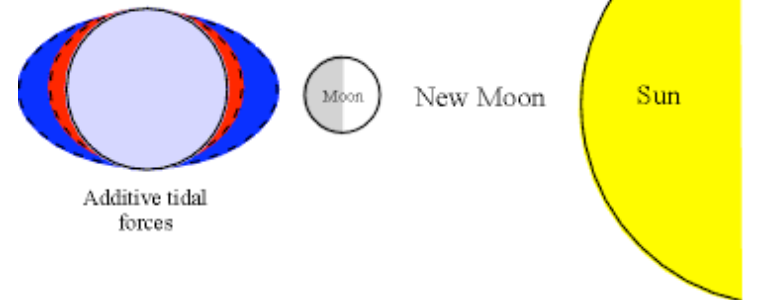


+ short range parts

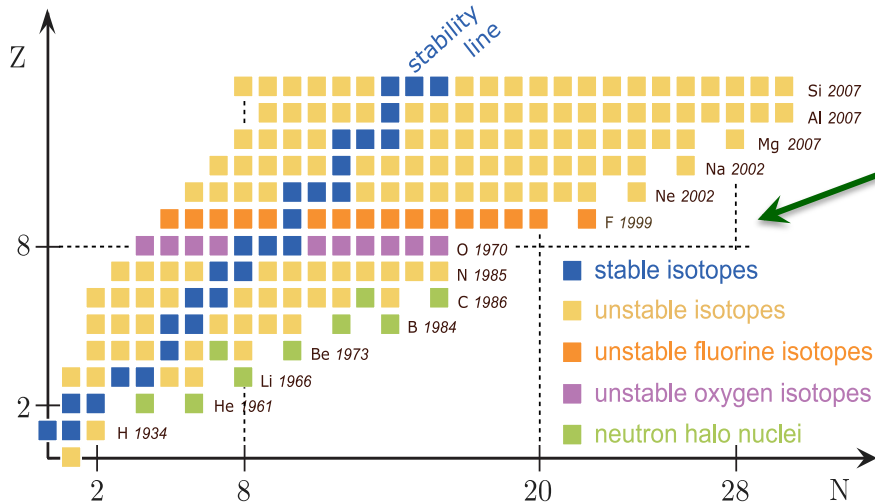
For Δ -less effectiv theories



tidal effects lead to 3-body forces in earth-sun-moon system



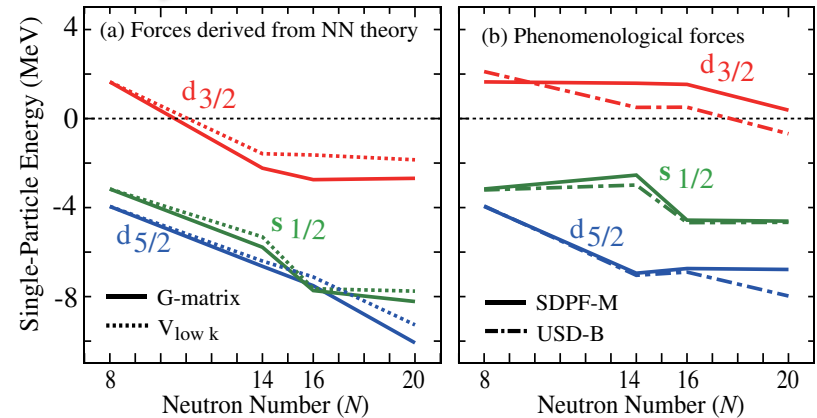
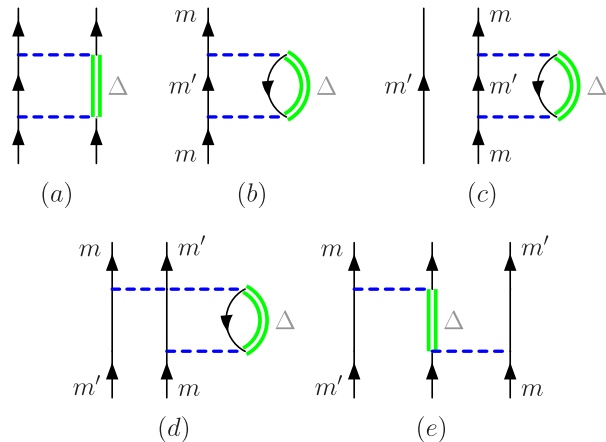
Oxygen puzzle...



The oxygen dripline is at ^{24}O , at odds with other neighbor isotope chains.

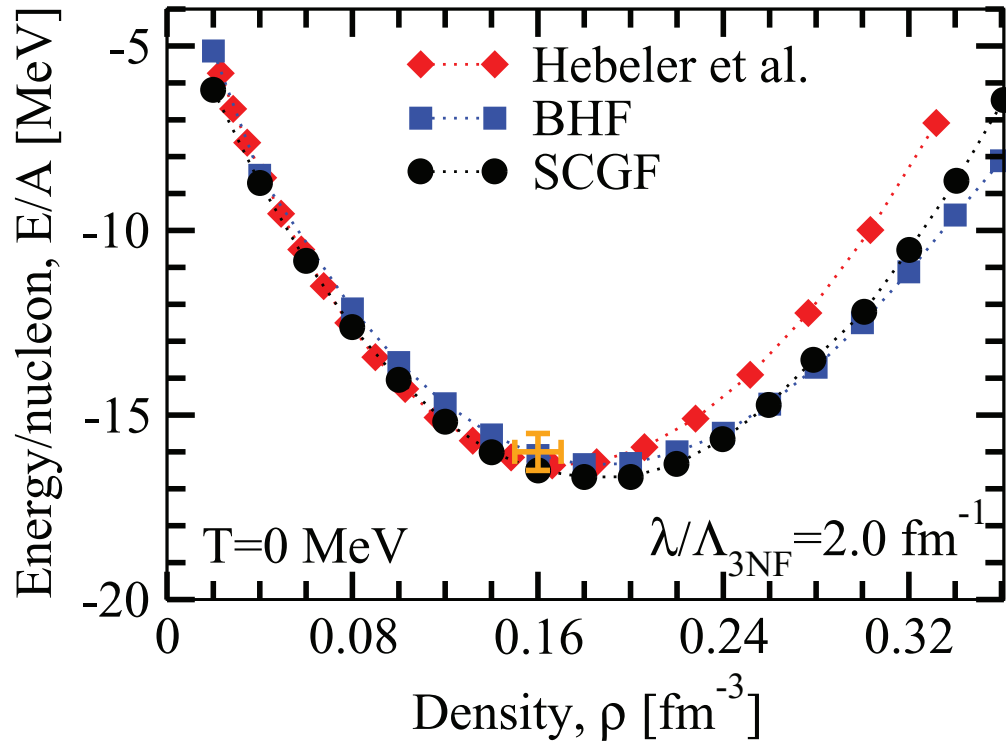
Phenomenological shell model interaction reflect this in the s.p. energies but no realistic NN interaction alone is capable of reproducing this...

The fujita-Miyazawa 3NF provides repulsion through Pauli screening of other 2NF terms:



[T. Otsuka et al., Phys Rev. Lett **105**, 32501 (2010)]

Saturation of nuclear matter:

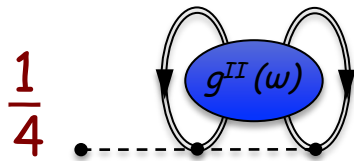


[A. Carbone et al.,
Phys. Rev. C **88**, 044302 (2013)]

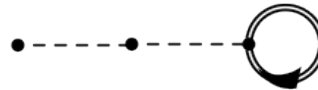
Inclusion of NNN forces

A. Carbone, CB, et al., Phys. Rev. C88, 054326 (2013)

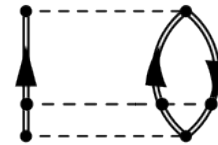
* NNN forces can enter diagrams in three different ways:



Correction to external
1-Body interaction



Correction to
non-contracted
2-Body interaction



pure 3-Body
contribution

- Contractions are with fully correlated density matrices (BEYOND a normal ordering...)

Inclusion of NNN forces

A. Carbone, CB, et al., Phys. Rev. C88, 054326 (2013)

* NNN forces can enter diagrams in three different ways:

→ Define new 1- and 2-body interactions and use only interaction-irreducible diagrams

$$\tilde{U} = \sum_{\alpha\beta} \left[-U_{\alpha\beta} - i\hbar \sum_{\delta\gamma} v_{\alpha\gamma,\beta\delta} g_{\delta\gamma}(\tau = 0^-) + \frac{i\hbar}{4} \sum_{\gamma\delta\mu\nu} g_{\mu\nu,\gamma\delta}^{II}(\tau = 0^-) w_{\alpha\gamma\delta,\beta\mu\nu} \right] a_{\alpha}^{\dagger} a_{\beta}$$

$$\tilde{V} = \sum_{\alpha\beta} \frac{1}{4} \left[v_{\alpha\beta,\gamma\delta} - i\hbar \sum_{\mu\nu} w_{\alpha\beta\mu,\gamma\delta\nu} g_{\nu\mu}(\tau = 0^-) \right] a_{\alpha}^{\dagger} a_{\beta}^{\dagger} a_{\delta} a_{\gamma}$$

$$W = \bullet \text{---} \bullet \text{---} \bullet \quad \equiv \quad W_{\alpha\beta\gamma,\mu\nu\lambda} a_{\alpha}^{\dagger} a_{\beta}^{\dagger} a_{\gamma}^{\dagger} a_{\lambda} a_{\nu} a_{\mu}$$

- Contractions are with fully correlated density matrices (BEYOND a normal ordering...)

Inclusion of NNN forces

A. Carbone, CB, et al., Phys. Rev. C88, 054326 (2013)

- Second order PT
diagrams with 3BFs:

effectively:

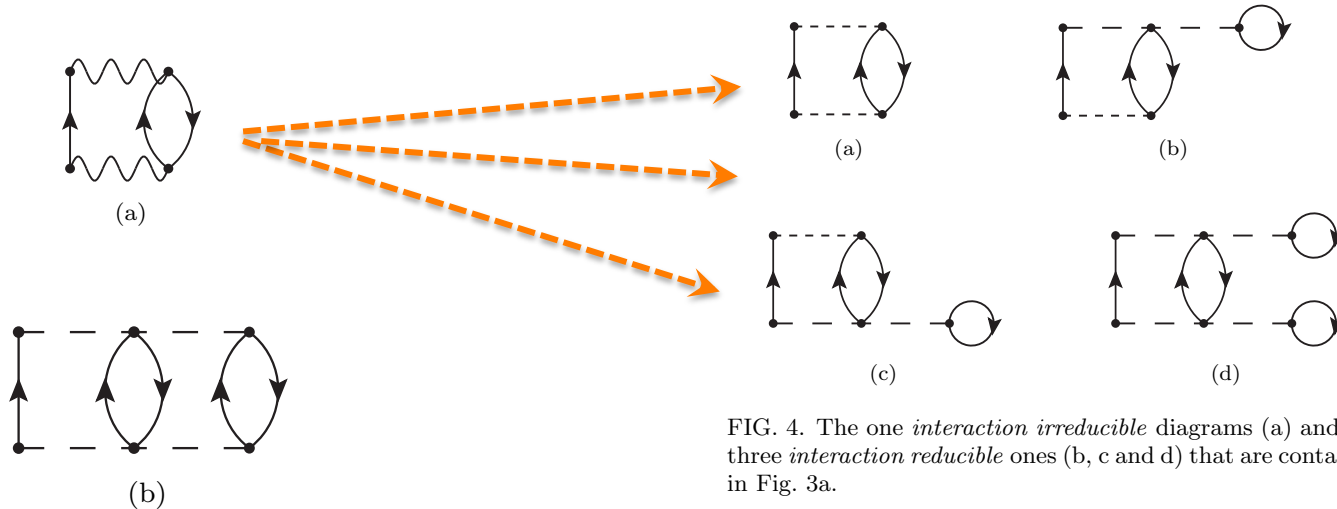
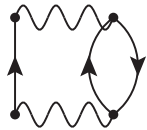


FIG. 4. The one *interaction irreducible* diagrams (a) and the three *interaction reducible* ones (b, c and d) that are contained in Fig. 3a.

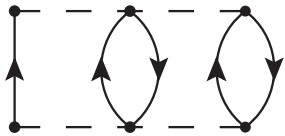
Inclusion of NNN forces

A. Carbone, CB, et al., Phys. Rev. C88, 054326 (2013)

- Second order PT diagrams with 3BFs:

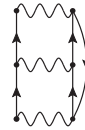


(a)

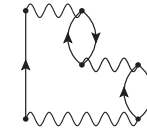


(b)

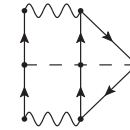
- Third order PT diagrams with 3BFs:



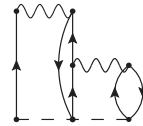
(a)



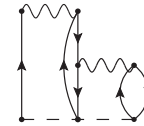
(b)



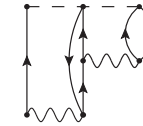
(c)



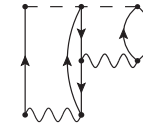
(d)



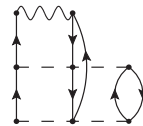
(e)



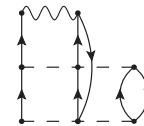
(f)



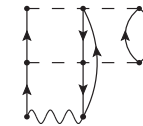
(g)



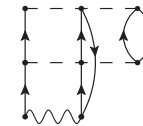
(h)



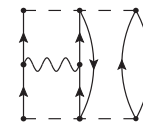
(i)



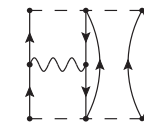
(j)



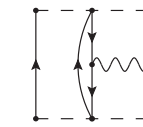
(k)



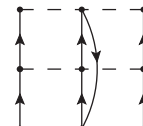
(l)



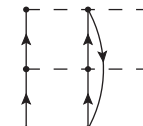
(m)



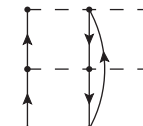
(n)



(o)



(p)



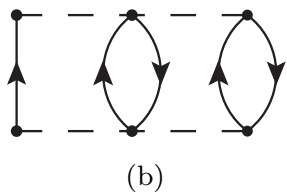
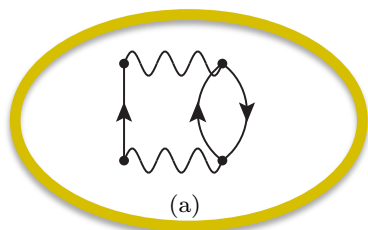
(q)

FIG. 5. 1PI, skeleton and interaction irreducible self-energy diagrams appearing at 3^{rd} -order in perturbative expansion (7), making use of the effective hamiltonian of Eq. (9).

Inclusion of NNN forces

A. Carbone, CB, et al., Phys. Rev. C88, 054326 (2013)

- Second order PT diagrams with 3BFs:



- Third order PT diagrams with 3BFs:

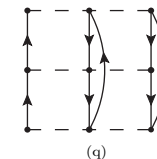
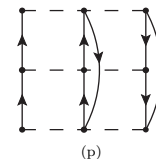
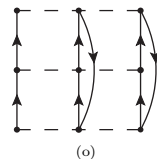
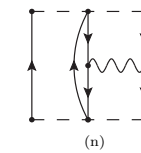
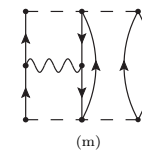
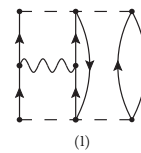
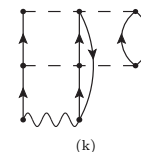
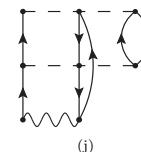
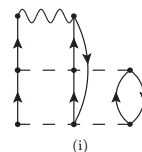
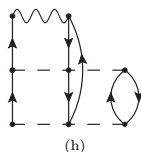
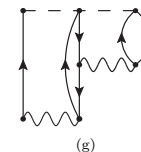
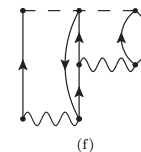
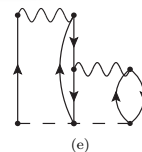
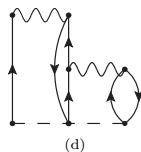
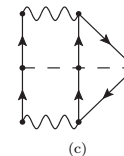
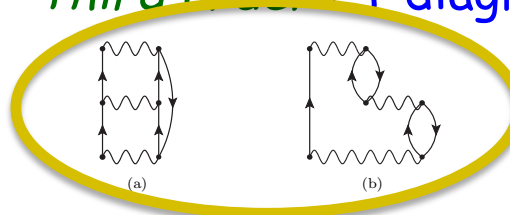
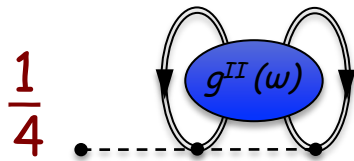


FIG. 5. 1PI, skeleton and interaction irreducible self-energy diagrams appearing at 3^{rd} -order in perturbative expansion (7), making use of the effective hamiltonian of Eq. (9).

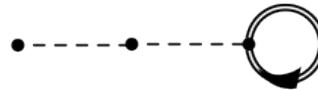
Inclusion of NNN forces

A. Carbone, CB, et al., Phys. Rev. C88, 054326 (2013)

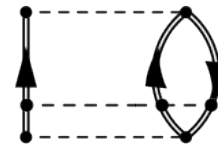
* NNN forces can enter diagrams in three different ways:



Correction to external
1-Body interaction



Correction to
non-contracted
2-Body interaction



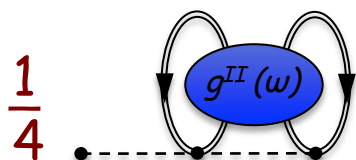
pure 3-Body
contribution

- Contractions are with fully correlated density matrices (BEYOND a normal ordering...)

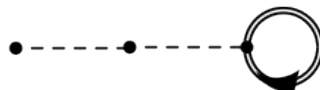
Inclusion of NNN forces

A. Carbone, CB, et al., Phys. Rev. C88, 054326 (2013)

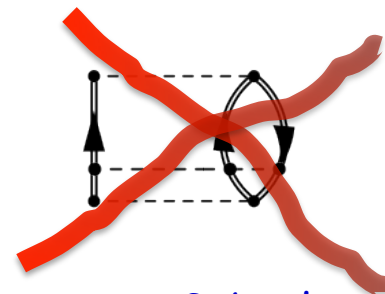
* NNN forces can enter diagrams in three different ways:



Correction to external
1-Body interaction

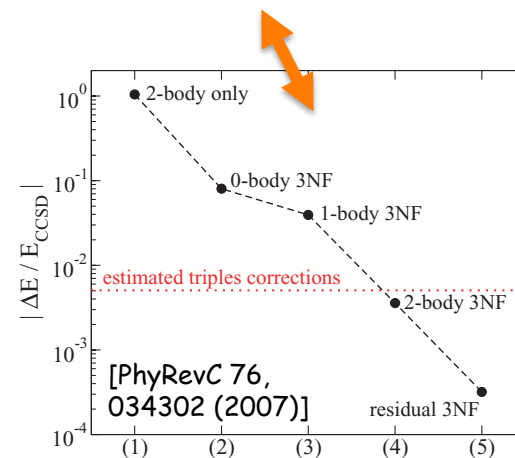


Correction to
non-contracted
2-Body interaction



pure 3-body
contribution (small)

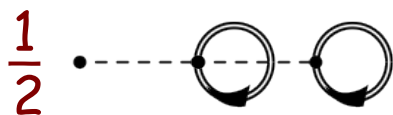
- Contractions are with fully correlated density matrices (BEYOND a normal ordering...)



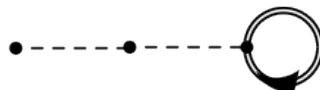
Inclusion of NNN forces

A. Carbone, CB, et al., Phys. Rev. C88, 054326 (2013)

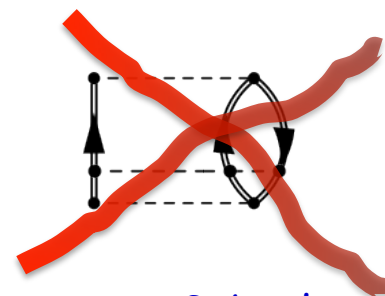
* NNN forces can enter diagrams in three different ways:



Correction to external
1-Body interaction

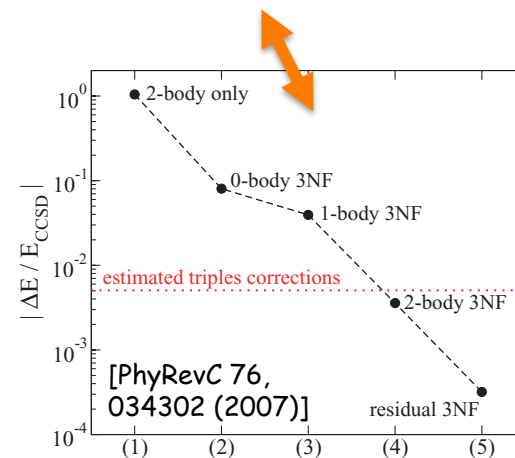


Correction to
non-contracted
2-Body interaction



pure 3-body
contribution (small)

- Contractions are with fully correlated density matrices (BEYOND a normal ordering...)



Inclusion of NNN forces

A. Carbone, CB, et al., Phys. Rev. C88, 054326 (2013)

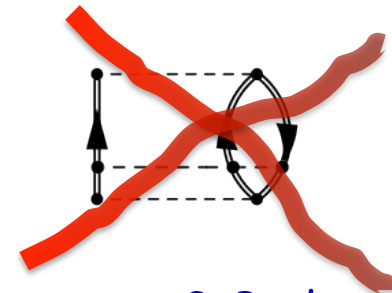
* NNN forces can enter diagrams in three different ways:



Correction to external
1-Body interaction

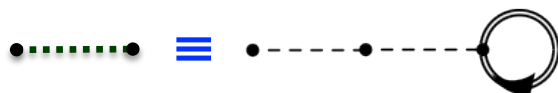


Correction to
non-contracted
2-Body interaction



pure 3-Body
contribution

BEWARE that defining:



and then:



would double count the 1-body term.

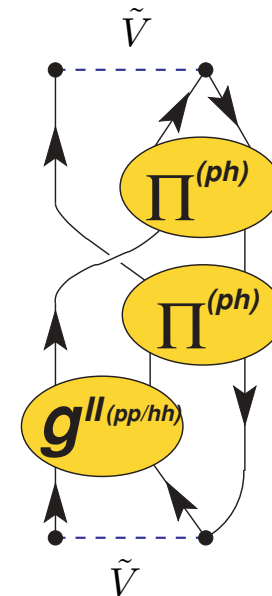
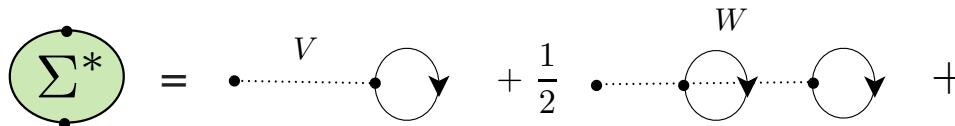
NNN forces in FRPA/FTDA formalism

A. Cipollone, CB, P. Navrátil, Phys. Rev. Lett. **111**, 062501 (2013)

Use: $\dots \tilde{V} \dots = \dots V \dots + \dots W \dots$ as 2-body potential in all V-irred. RPA/TDA summations



Then:



...approximations and some improvements still being assessed - this is all work in progress

(Galitskii-Migdal-Boffi-) Koltun sumrule

✱ Koltun sum rule (with NNN interactions):

$$\sum_{\alpha} \frac{1}{\pi} \int_{-\infty}^{\epsilon_F^-} d\omega \omega \operatorname{Im} G_{\alpha\alpha}(\omega) = \langle \Psi_0^N | \hat{T} | \Psi_0^N \rangle + 2 \langle \Psi_0^N | \hat{V} | \Psi_0^N \rangle + 3 \langle \Psi_0^N | \hat{W} | \Psi_0^N \rangle$$

two-body
three-body

✱ Thus, need an extra correction:

$$E_0^N = \frac{1}{3\pi} \int_{-\infty}^{\epsilon_F^-} d\omega \sum_{\alpha\beta} (2T_{\alpha\beta} + \omega\delta_{\alpha\beta}) \operatorname{Im} G_{\beta\alpha}(\omega) + \frac{1}{3} \langle \Psi_0^N | \hat{V} | \Psi_0^N \rangle$$

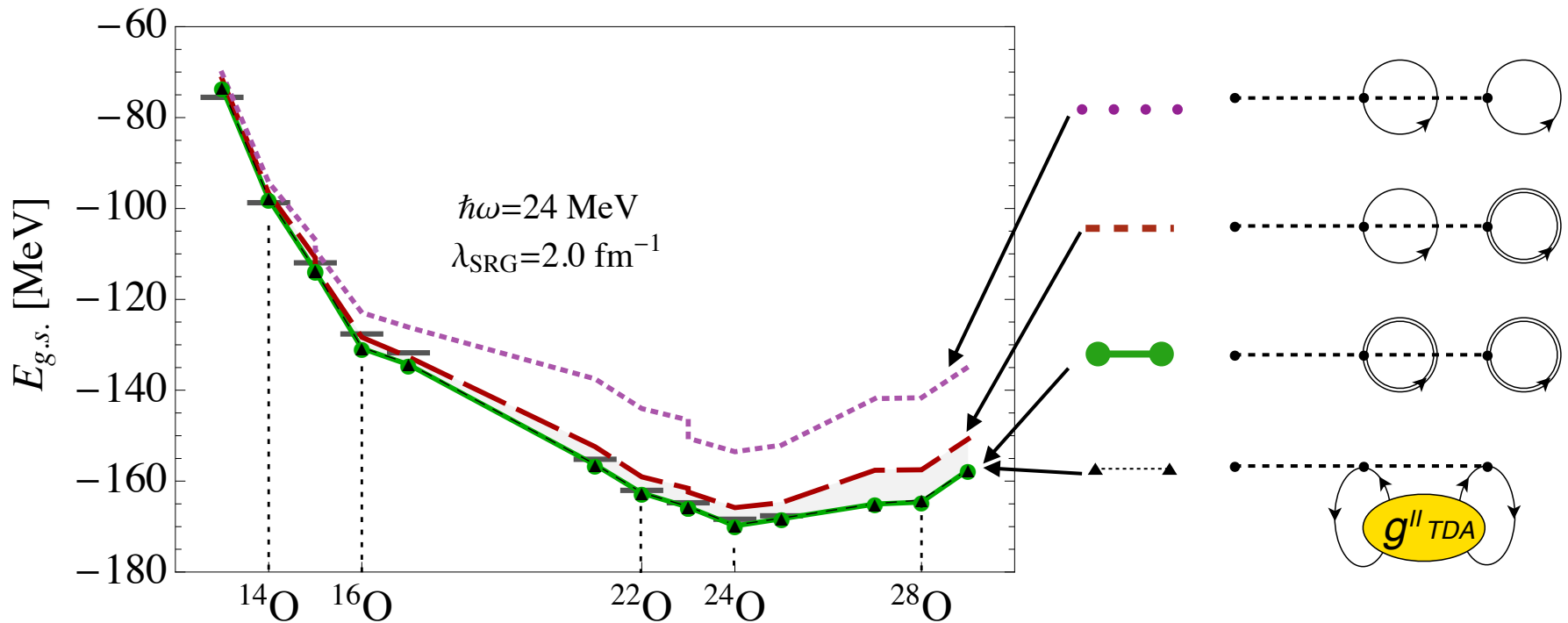
or

$$E_0^N = \frac{1}{2\pi} \int_{-\infty}^{\epsilon_F^-} d\omega \sum_{\alpha\beta} (T_{\alpha\beta} + \omega\delta_{\alpha\beta}) \operatorname{Im} G_{\beta\alpha}(\omega) - \frac{1}{2} \langle \Psi_0^N | \hat{W} | \Psi_0^N \rangle$$

$$\langle \Psi_0^N | \hat{W} | \Psi_0^N \rangle \approx \frac{1}{6} \text{---} \text{---} \text{---}$$

3N forces in FRPA/FTDA formalism

→ Ladder contributions to static self-energy are negligible (in oxygen)



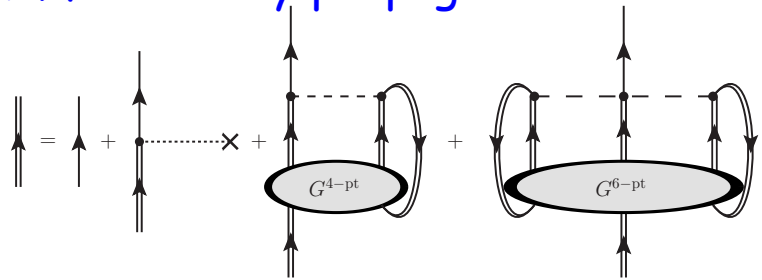
Equation of motion and SC diagrams including 3NFs

A. Carbone, CB, et al., Phys. Rev. C88, 054326 (2013)

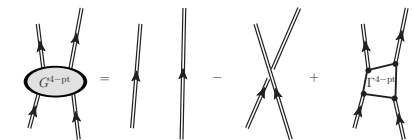
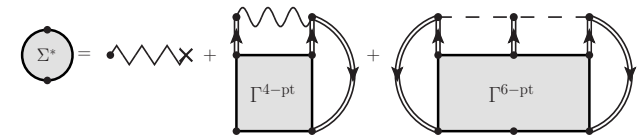
Equations of Motions with 3NF

A. Carbone, CB, et al., *Phys. Rev. C* **88**, 054326 (2013)

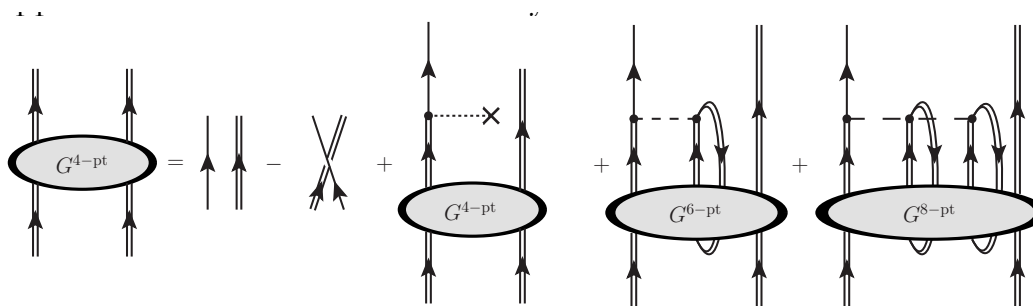
- EOM for 1-body propagator:



irred. self-energy:



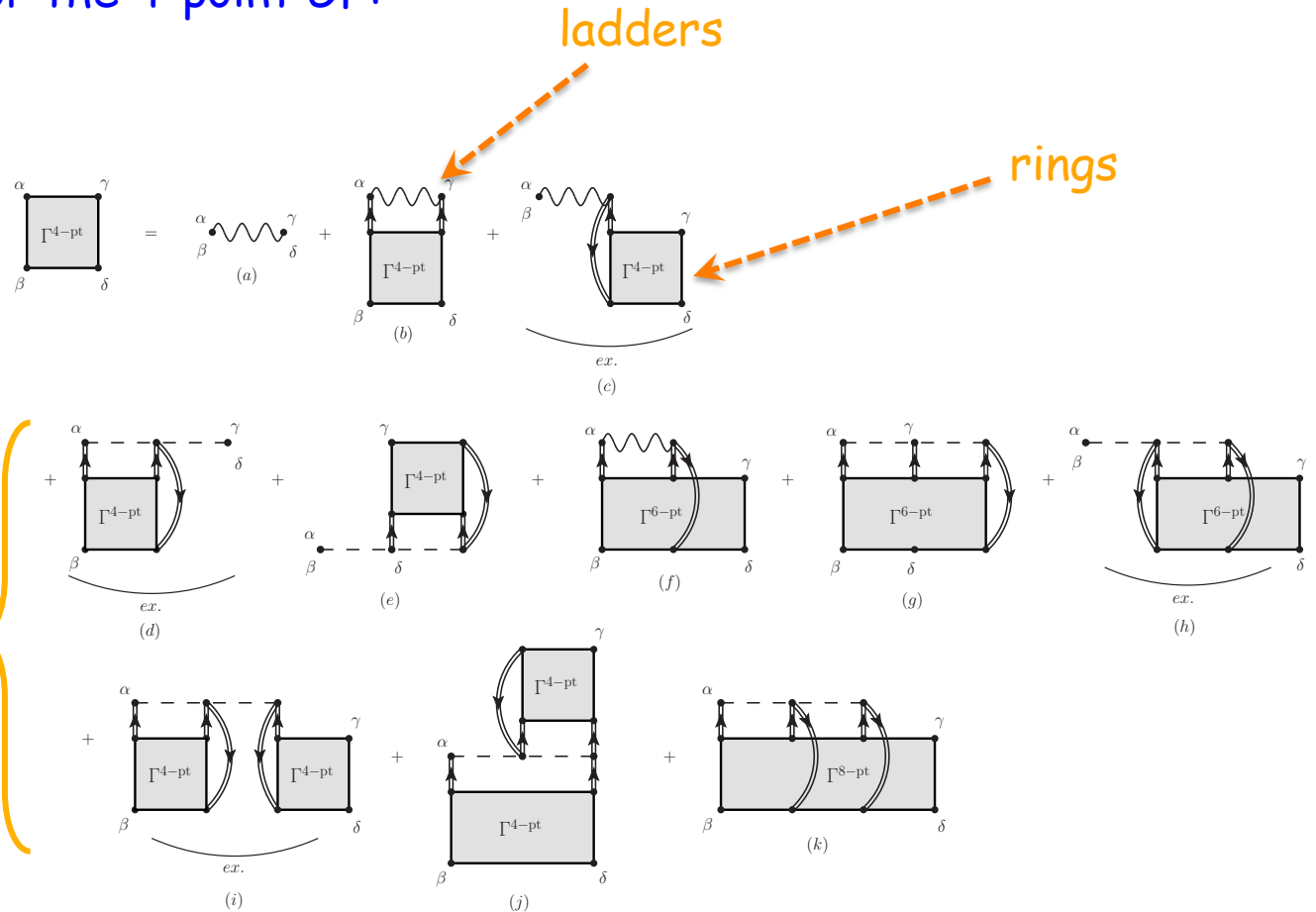
- EOM for 2-body propagator:



Equations of Motions with 3NF

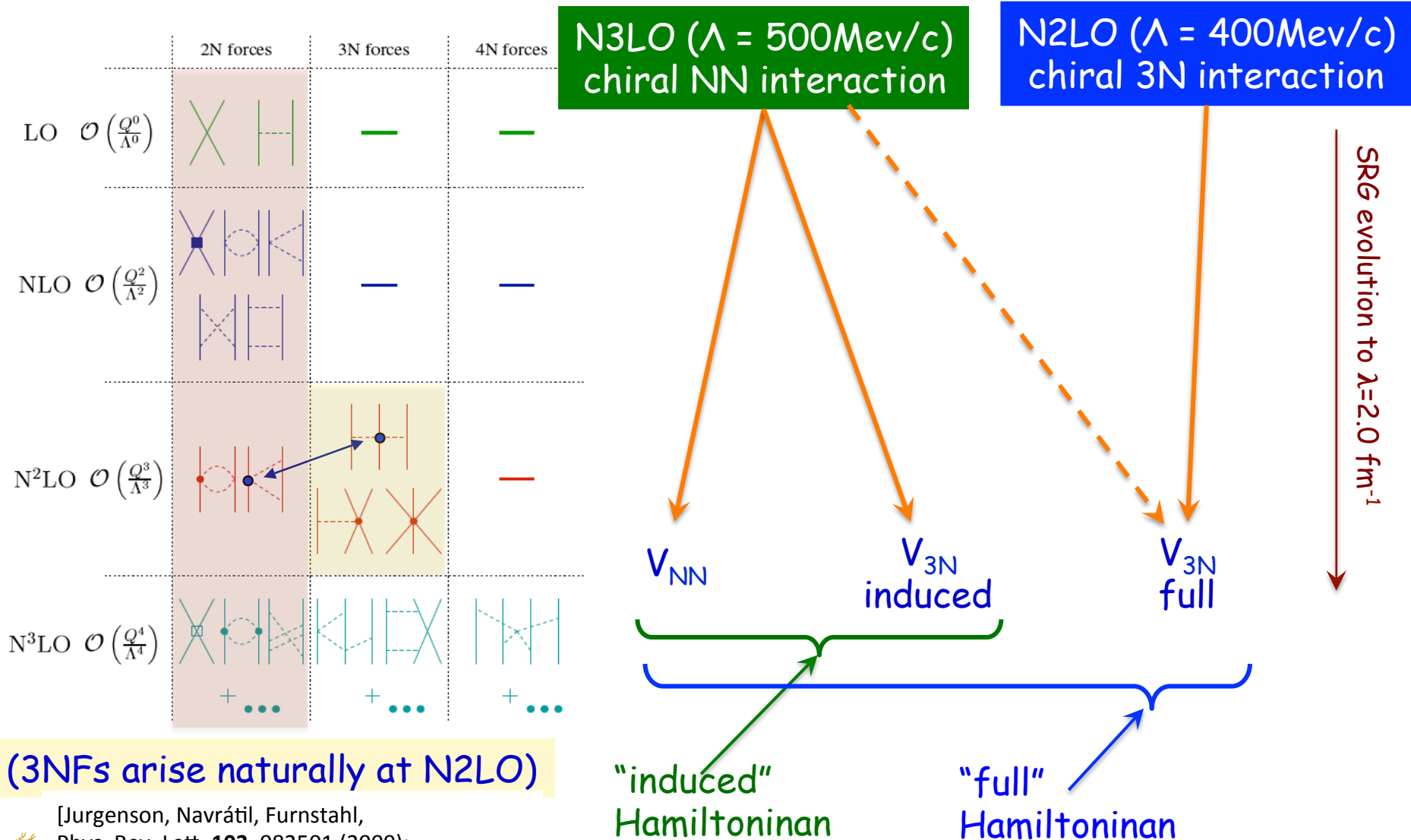
A. Carbone, CB, et al., Phys. Rev. C88, 054326 (2013)

- SC equations for the 4-point GF:





Chiral Nuclear forces - SRG evolved

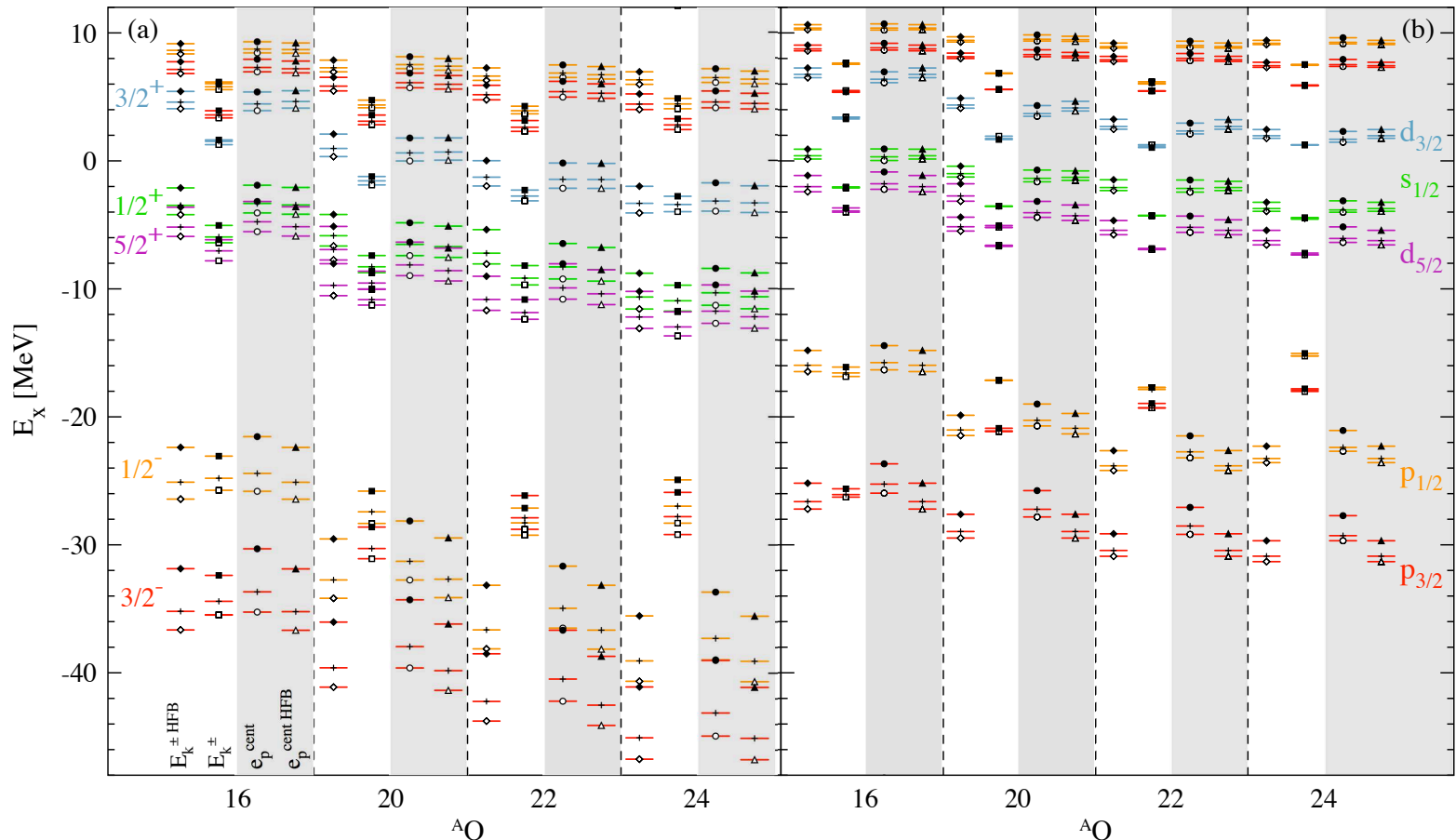


Convergence of s.p. spectra w.r.t. SRG

Cutoff dependence is reduced, indicating good convergence of many-body truncation and many-body forces

arXiv:1411.1237 (2014)

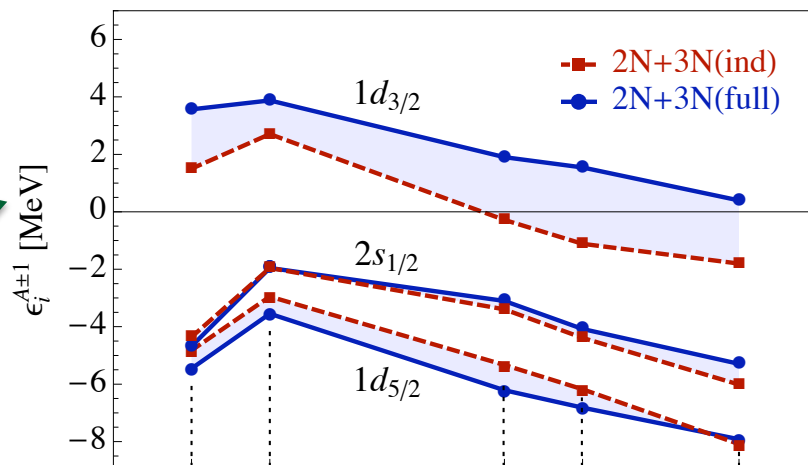
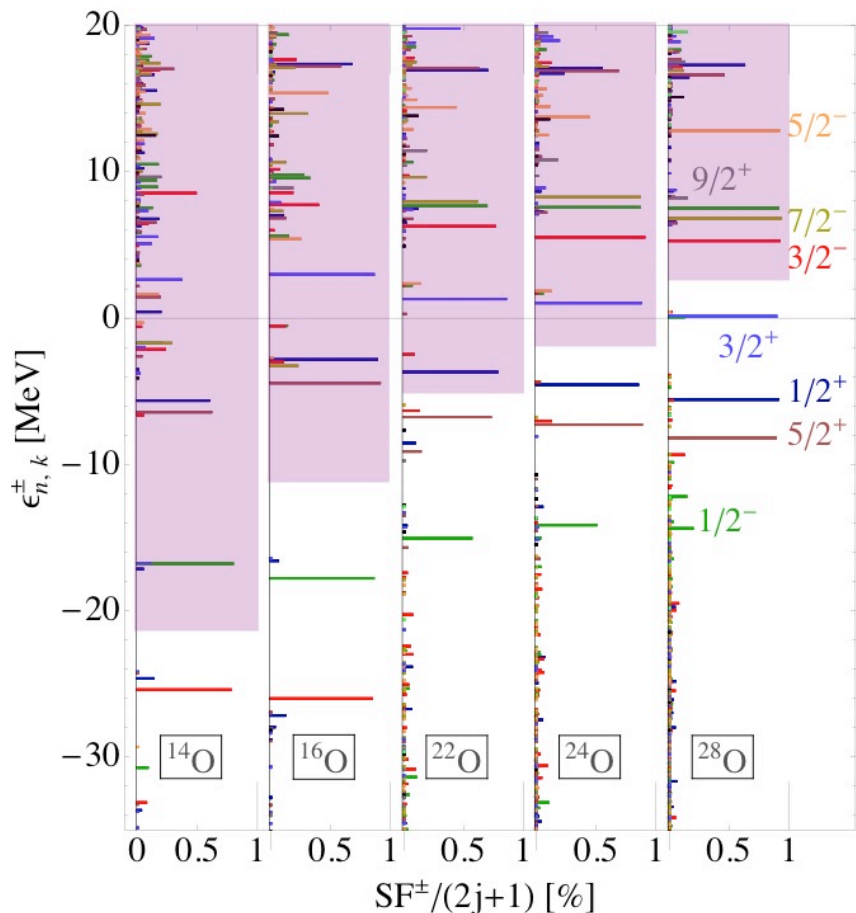
✓ only dominant s.p. states shown



NN terms (no induced 3NF) \leftrightarrow NN+3NF fully included

Results for the N-O-F chains

A. Cipollone, CB, P. Navrátil, Phys. Rev. Lett. **111**, 062501 (2013)
and arXiv:1412.3002 [nucl-th] (2014)

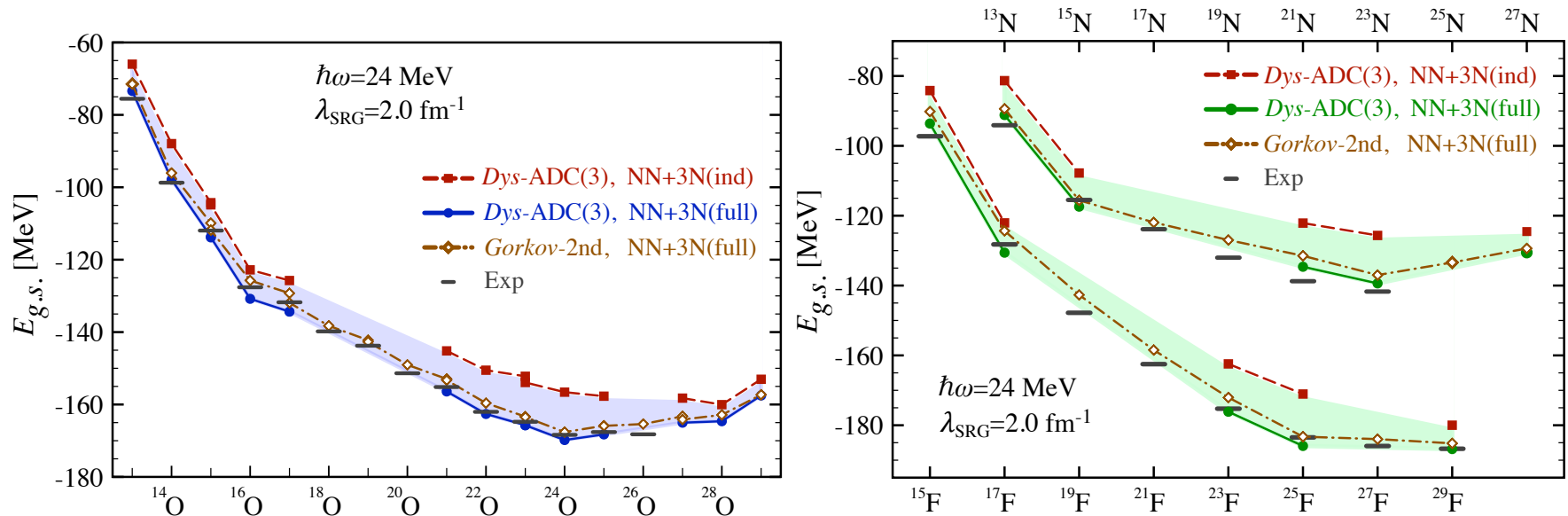


→ $d_{3/2}$ raised by genuine 3NF

→ cf. microscopic shell model [Otsuka et al, PRL**105**, 032501 (2010).]

Results for the N-O-F chains

A. Cipollone, CB, P. Navrátil, Phys. Rev. Lett. **111**, 062501 (2013)
and arXiv:1412.3002 [nucl-th] (2014)

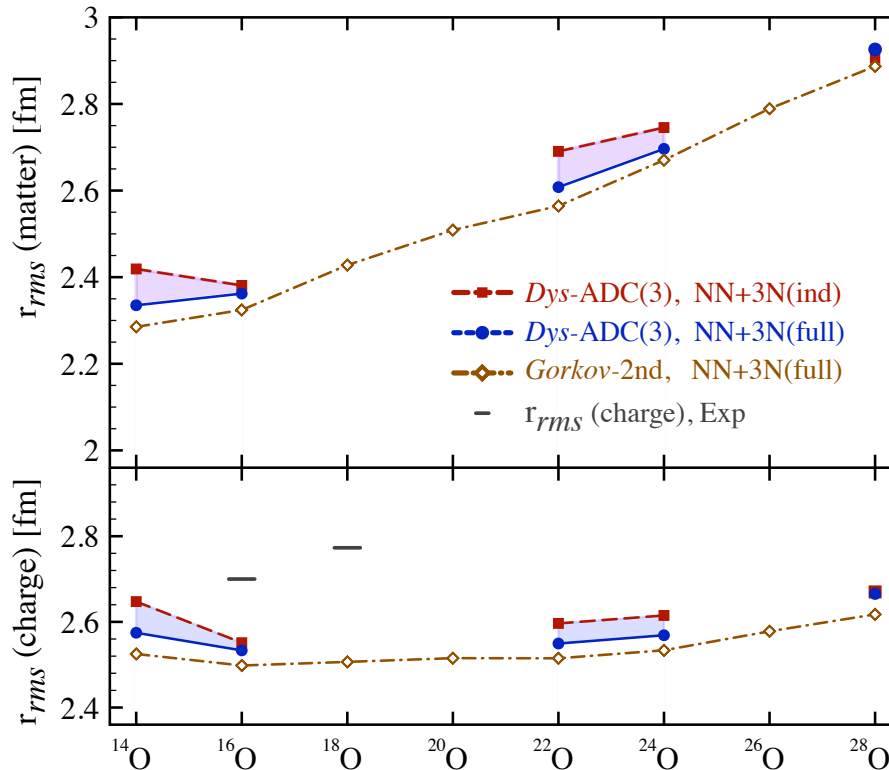


→ 3NF crucial for reproducing binding energies and driplines around oxygen

→ cf. microscopic shell model [Otsuka et al, PRL**105**, 032501 (2010).]

Results for the oxygen chain

A. Cipollone, CB, P. Navrátil, arXiv:1412.3002 [nucl-th] (2014)



→ Single particle spectra slightly to spread and

→ systematic underestimation of radii

Neutron spectral function of Oxygens

A. Cipollone, CB P. Navrátil, *PRC submitted* (2014)

